NEUTRON STARS AND GRAVITATIONAL WAVES

NIKOLAOS STERGIOULAS

DEPARTMENT OF PHYSICS
ARISTOTLE UNIVERSITY OF THESSALONIKI

9th Aegean Summer School, September 20, 2017

Neutron Stars

First neutron star detected almost 50 years ago.

Still, the fundamental properties of matter in the core of neutron stars remain largely uncertain.

No accurate radius determination.

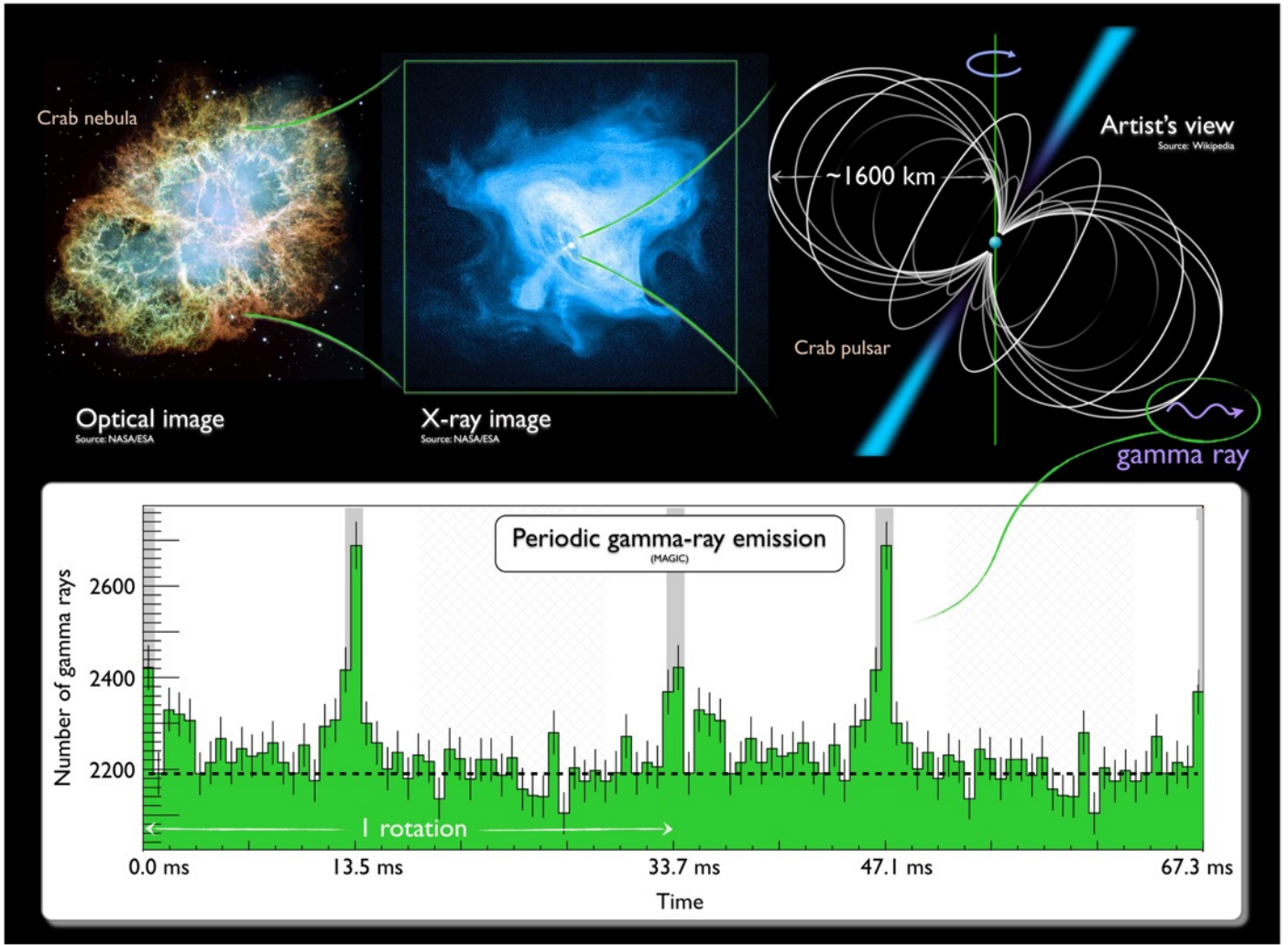

Image credit: MAGIC collaboration

Constraints on Neutron Star Radii or M/R

Main methods in EM spectrum:

- Thermonuclear X-ray bursts (*photospheric radius expansion*)

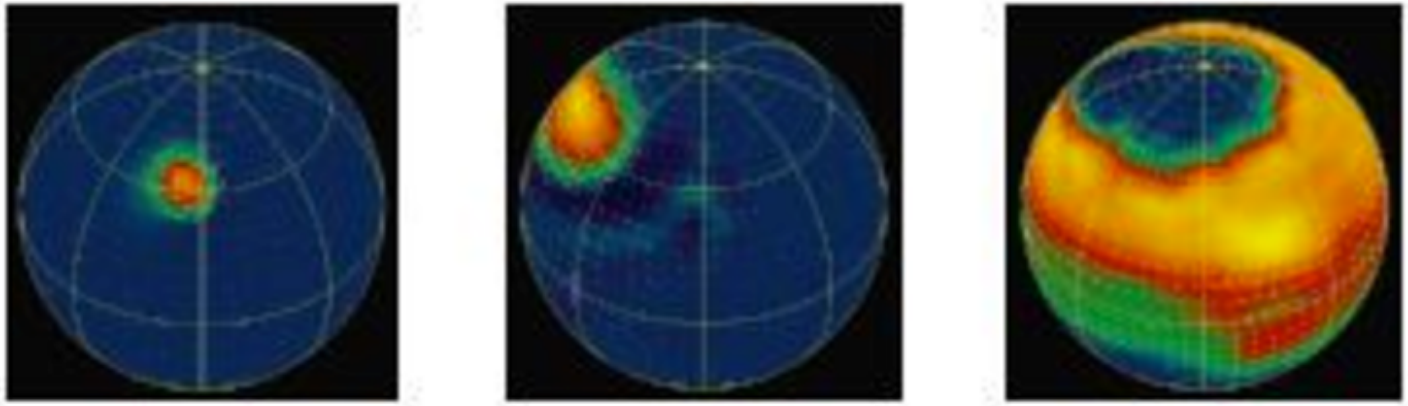

- Burst oscillations (*rotationally modulated waveform*)

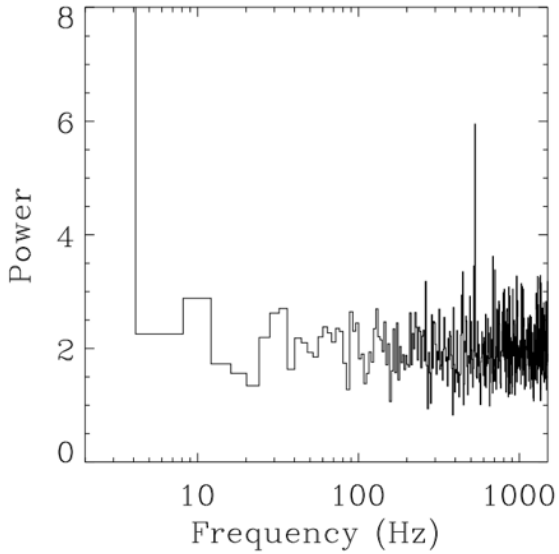

Bhattacharyya et al. (2006)

Constraints on Neutron Star Radii or M/R

- Fits of continuum spectra of X-ray bursts

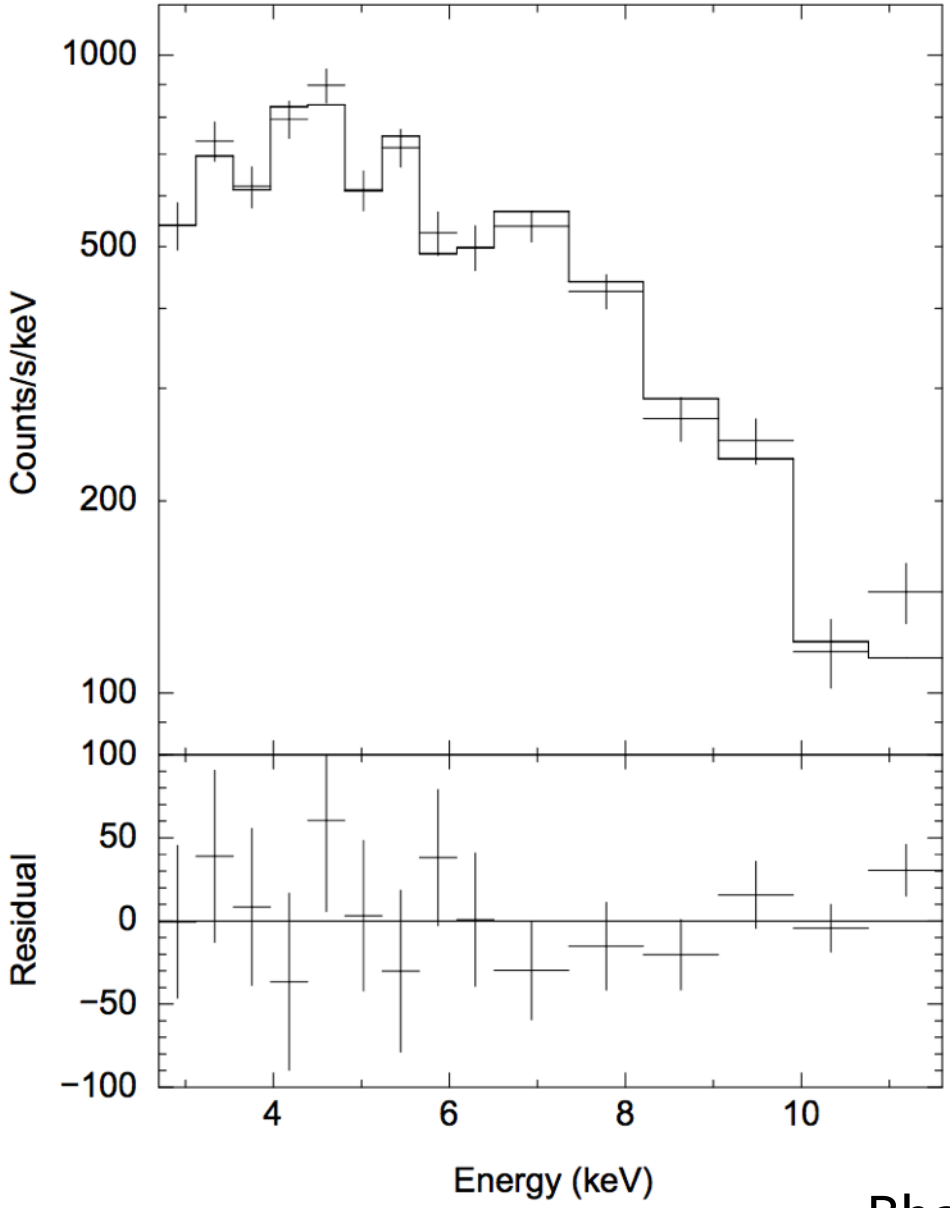

Bhattacharyya et al. (2010)

Constraints on Neutron Star Radii or M/R

- Relativistic spectral line shifts

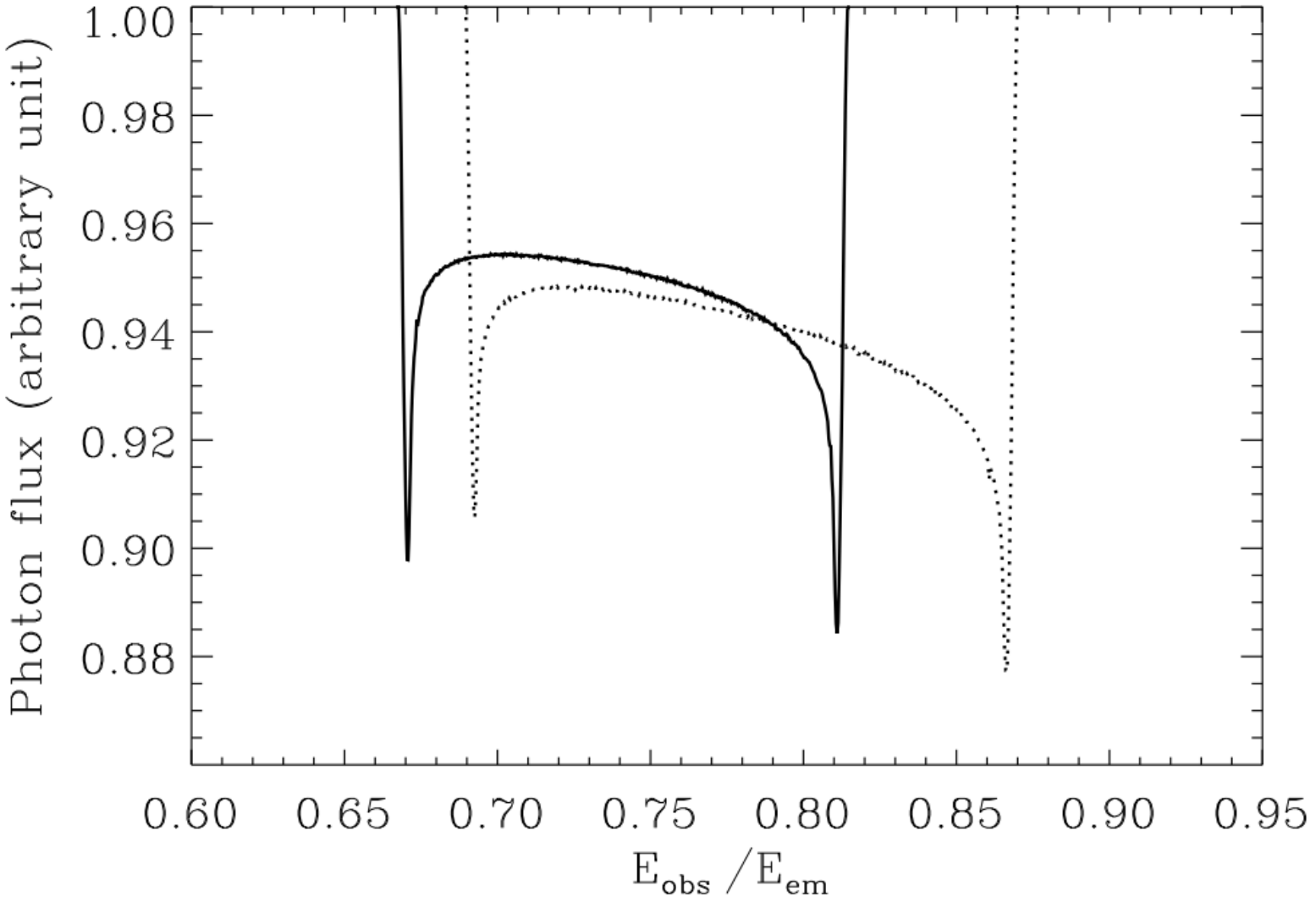

Bhattacharyya et al. (2006)

Constraints on Neutron Star Radii or M/R

- khZ QPOs in accretion disks around neutron stars

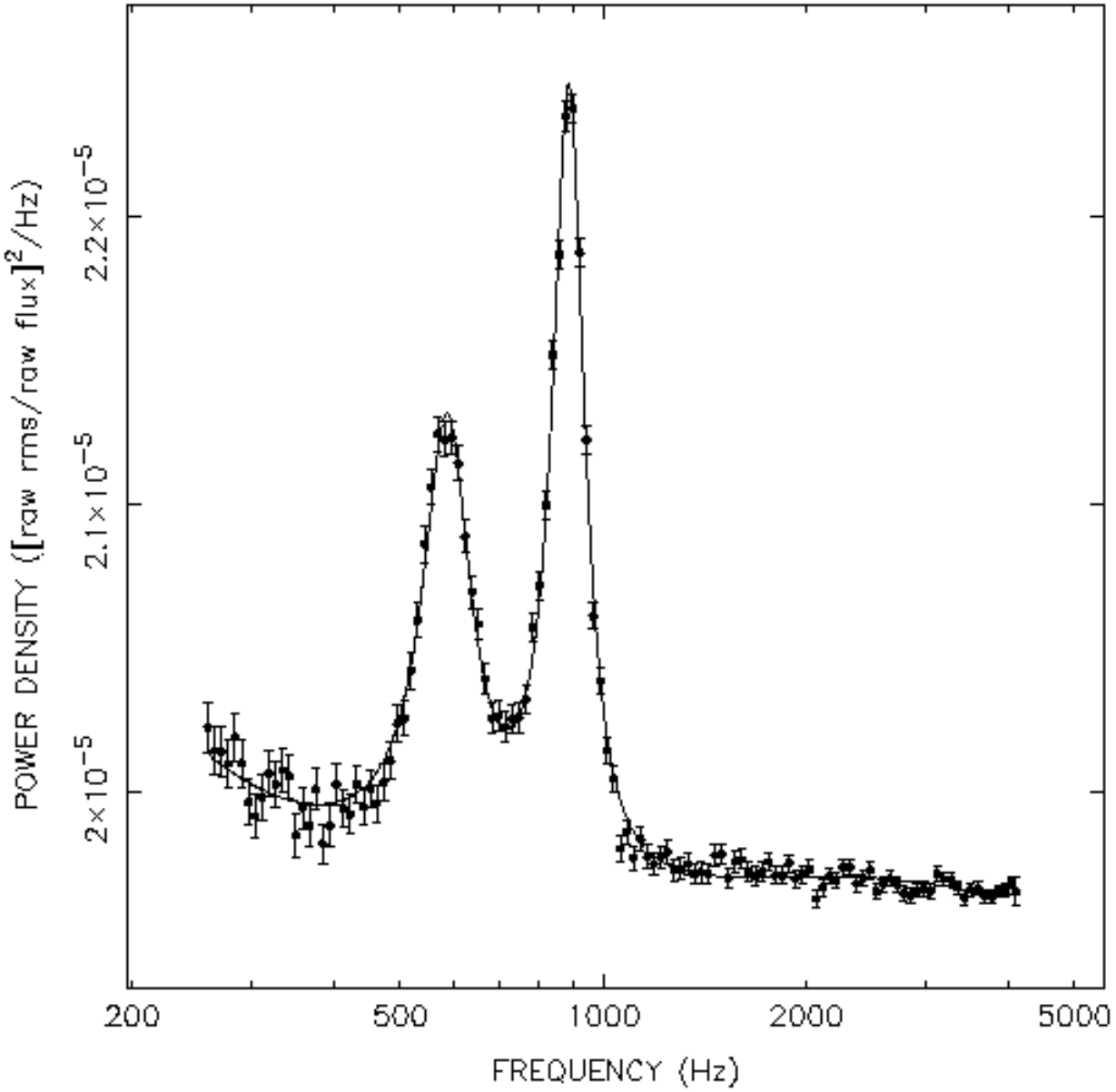

van der Klis et al. (1997)

Constraints on Neutron Star Radii or M/R

- Pericenter precession in relativistic binaries (*measuring moment of inertia in double pulsar J0737*)

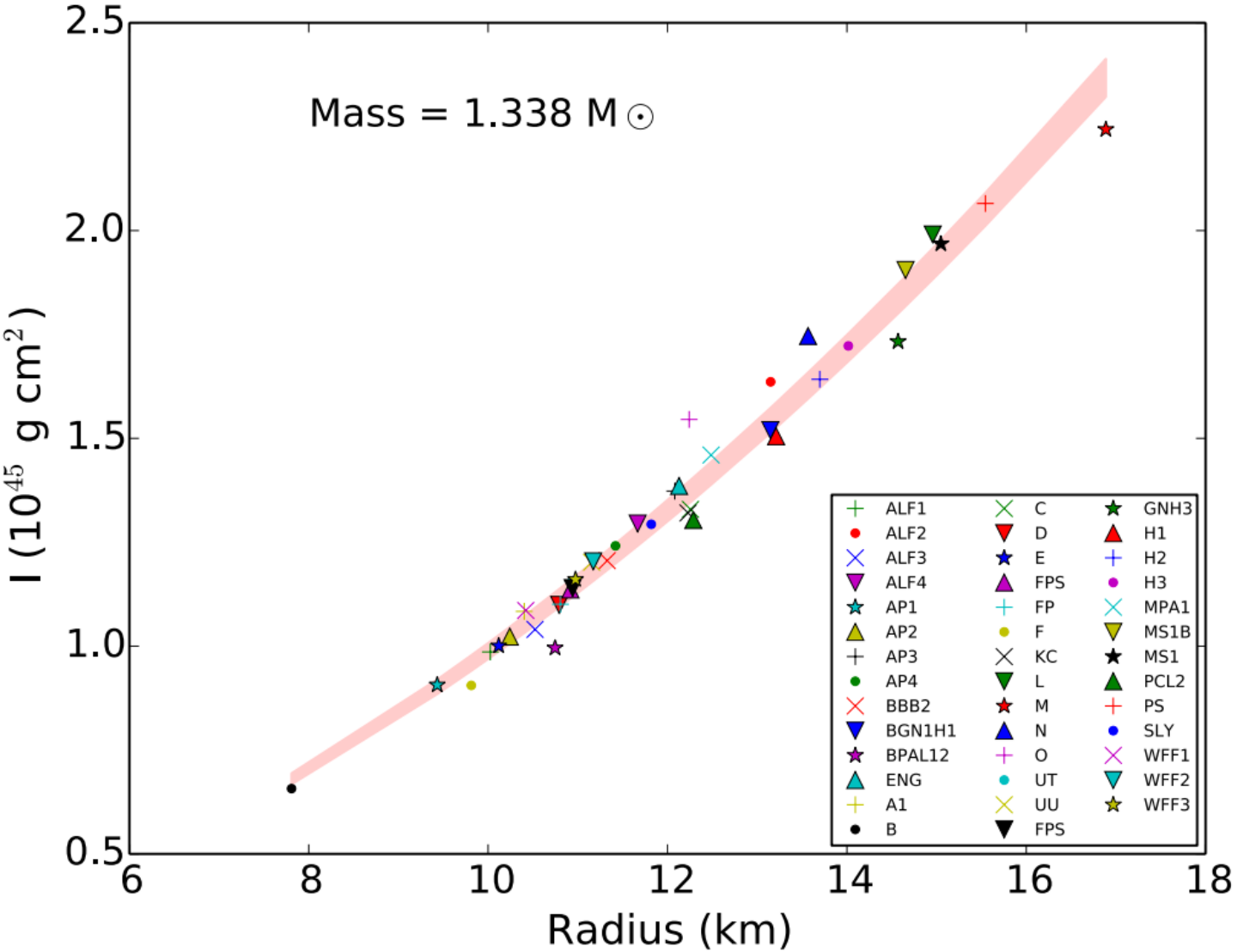

(Raithel, Ozel, Psaltis 2016)

Constraints on Neutron Star Radii

Main methods in GW spectrum:

- Tidal effects on waveform during inspiral phase of NS-NS mergers
- Tidal disruption in BH-NS mergers
- Oscillations in post-merger phase of NS-NS mergers

Description of the fluid

For a perfect fluid, we define the following *intensive properties*, all measured by an observer *comoving* with the fluid:

- n *baryon number density*
- ρ *baryon mass density*
- ε *energy density*
- p *isotropic pressure*
- h *specific enthalpy*
- s *specific entropy*

where

$$h = \frac{\epsilon + p}{\rho}$$

Description of the fluid

For a perfect fluid, we define the following *intensive properties*, all measured by an observer *comoving* with the fluid:

- n *baryon number density*
- ρ *baryon mass density*
- ε *energy density*
- p *isotropic pressure*
- h *specific enthalpy*
- s *specific entropy*

where

$$h = \frac{\epsilon + p}{\rho}$$

The *equation of state* (EOS) can be assumed to be of the form

$p=p(\rho)$, $\varepsilon=\varepsilon(\rho)$ *barotropic (cold stars)*

$p=p(\rho, s)$, $\varepsilon=\varepsilon(\rho, s)$ *non-barotropic (hot stars)*

Governing Equations

- Field equations of general relativity (GR)

$$G_{\alpha\beta} = 8\pi T_{\alpha\beta}$$

- Perfect fluid

$$T_{\alpha\beta} = (\epsilon + p)u_\alpha u_\beta + p g_{\alpha\beta}$$

- Conservation of stress-energy tensor

$$\nabla_\alpha T^{\alpha\beta} = 0$$

Governing Equations

- Field equations of general relativity (GR)

$$G_{\alpha\beta} = 8\pi T_{\alpha\beta}$$

- Perfect fluid

$$T_{\alpha\beta} = (\epsilon + p)u_\alpha u_\beta + p g_{\alpha\beta}$$

- Conservation of stress-energy tensor

$$\nabla_\alpha T^{\alpha\beta} = 0$$

- Conservation of baryons

$$\nabla_\alpha (\rho u^a) = 0$$

- 1st law of thermodynamics

$$d\epsilon = \rho T ds + h d\rho$$

Structure of Nonrotating Neutron Stars

Metric tensor:

$$ds^2 = -e^{2\Phi}c^2dt^2 + e^{2\Lambda}dr^2 + r^2d\theta^2 + r^2\sin^2\theta d\phi^2$$

Structure of Nonrotating Neutron Stars

Metric tensor:

$$ds^2 = -e^{2\Phi}c^2dt^2 + e^{2\Lambda}dr^2 + r^2d\theta^2 + r^2\sin^2\theta d\phi^2$$

- Static equilibrium (Tolman-Openheimer-Volkoff, TOV)

$$\frac{dm}{dr} = 4\pi r^2\epsilon/c^2$$

$$\frac{dp}{dr} = -\frac{G}{c^2}\frac{m\epsilon}{r^2}\left(1+\frac{p}{\epsilon}\right)\left(1+\frac{4\pi r^3 p}{mc^2}\right)\left(1-\frac{2Gm}{c^2 r}\right)^{-1}$$

Structure of Nonrotating Neutron Stars

Metric tensor:

$$ds^2 = -e^{2\Phi}c^2dt^2 + e^{2\Lambda}dr^2 + r^2d\theta^2 + r^2\sin^2\theta d\phi^2$$

- Static equilibrium (Tolman-Openheimer-Volkoff, TOV)

$$\frac{dm}{dr} = 4\pi r^2\epsilon/c^2$$

$$\frac{dp}{dr} = -\frac{G}{c^2}\frac{m\epsilon}{r^2}\left(1+\frac{p}{\epsilon}\right)\left(1+\frac{4\pi r^3 p}{mc^2}\right)\left(1-\frac{2Gm}{c^2 r}\right)^{-1}$$

- Radius and gravitational mass

$$R = r(p=0)$$

$$M = \int_0^R 4\pi r^2 \frac{\epsilon}{c^2}dr = m(r=R)$$

EOS and M-R Correspondence

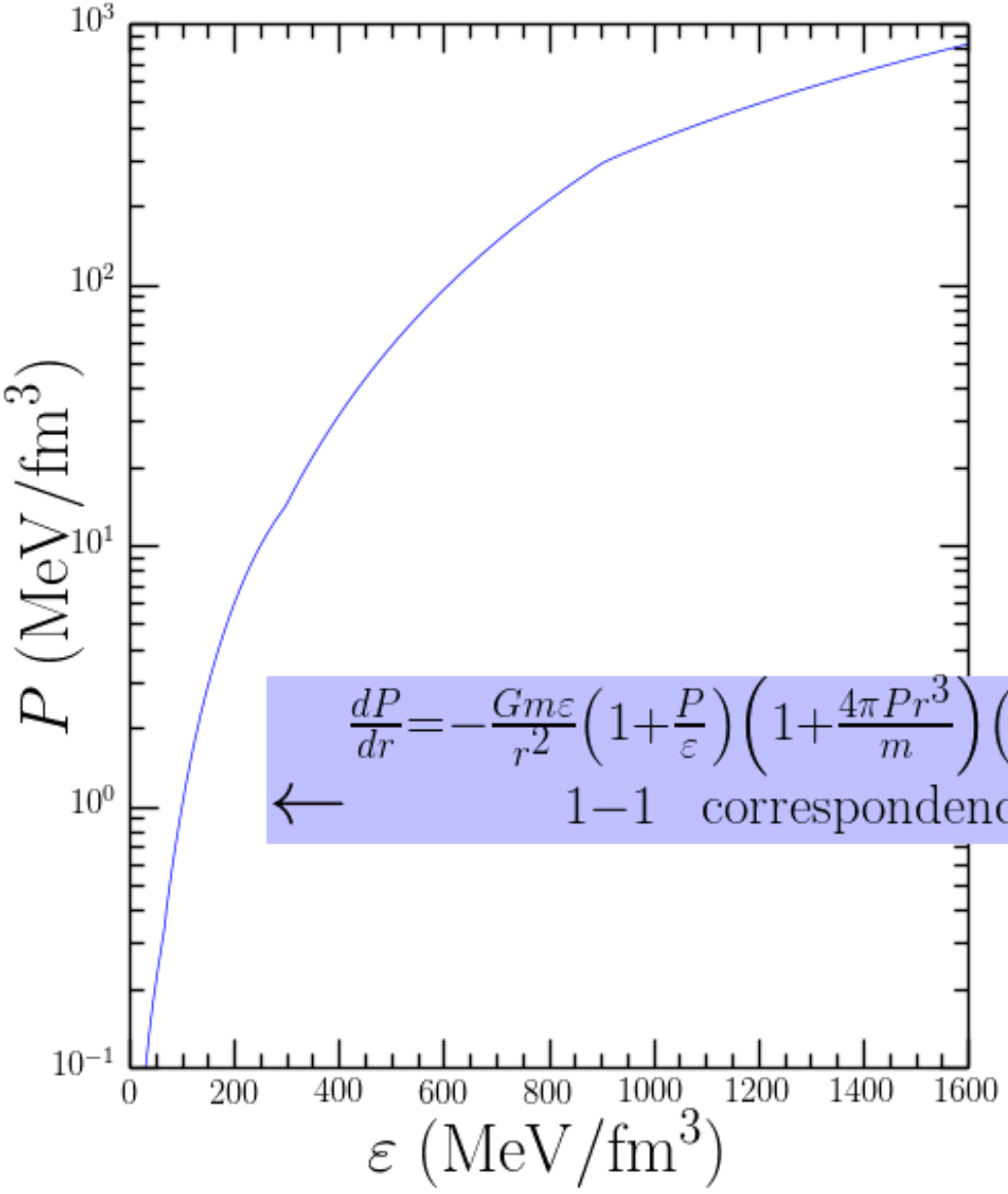

$$\frac{dP}{dr} = -\frac{Gm\varepsilon}{r^2}\left(1+\frac{P}{\varepsilon}\right)\left(1+\frac{4\pi Pr^3}{m}\right)\left(1-\frac{2Gm}{r}\right)^{-1}$$

$\leftarrow$ 1−1 correspondence $\rightarrow$

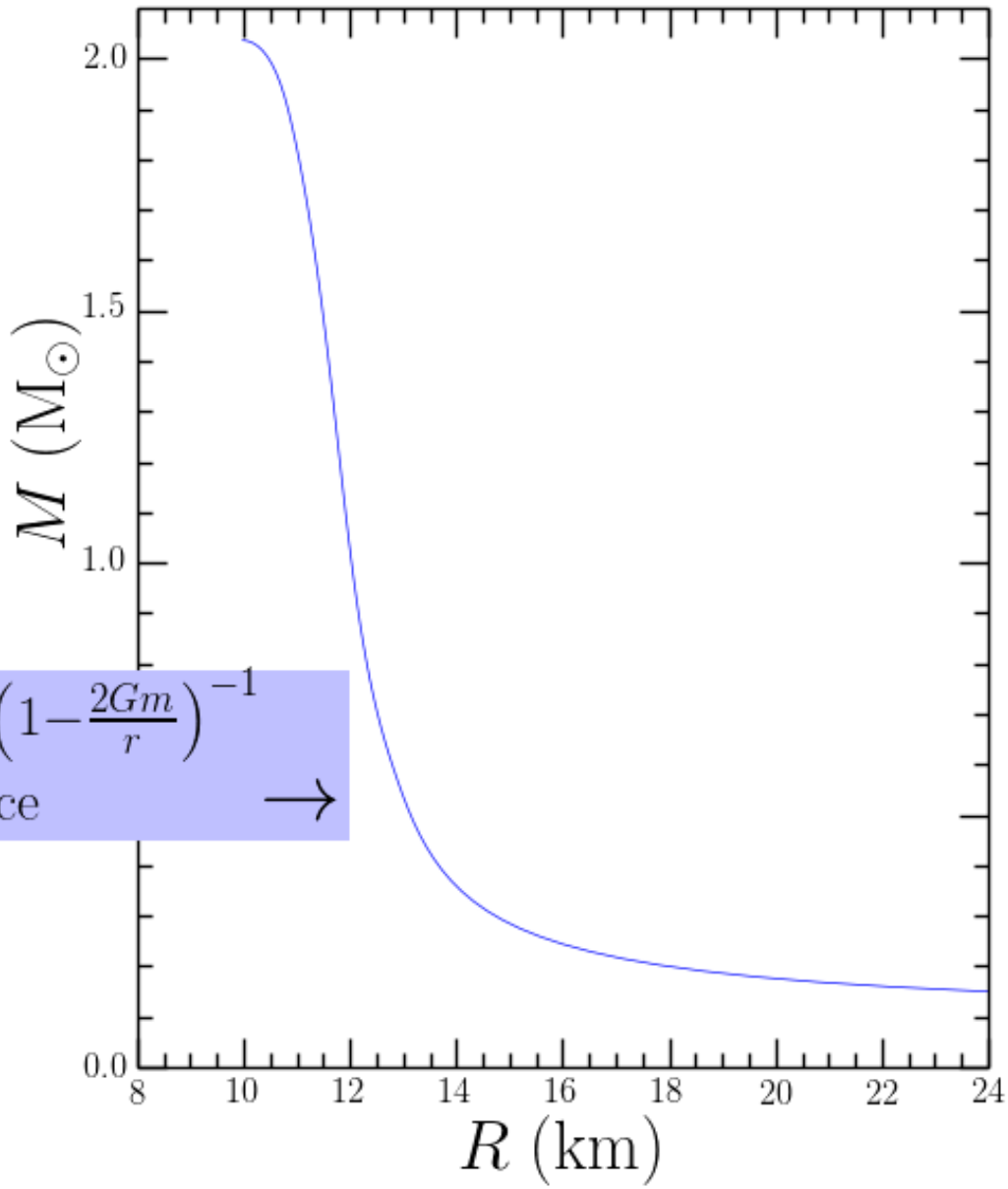

(A. Steiner)

Hybrid Stars

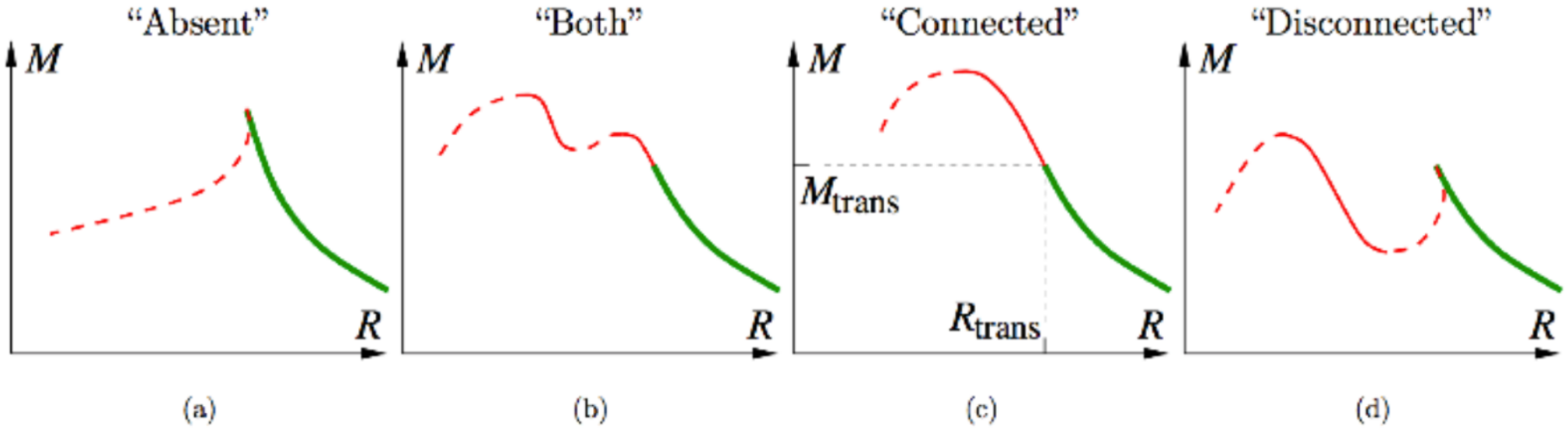

FIG. 2: Four possible topologies of the mass-radius relation for hybrid stars. The thick (green) line is the hadronic branch. Thin solid (red) lines are stable hybrid stars; thin dashed (red) lines are unstable hybrid stars. In (a) the hybrid branch is absent. In (c) there is a connected branch. In (d) there is a disconnected branch. In (b) there are both types of branch. In realistic neutron star $M(R)$ curves, the cusp that occurs in cases (a) and (d) is much smaller and harder to see [13, 14]

Alford, Han, and Prakash (2013)

Interior Structure

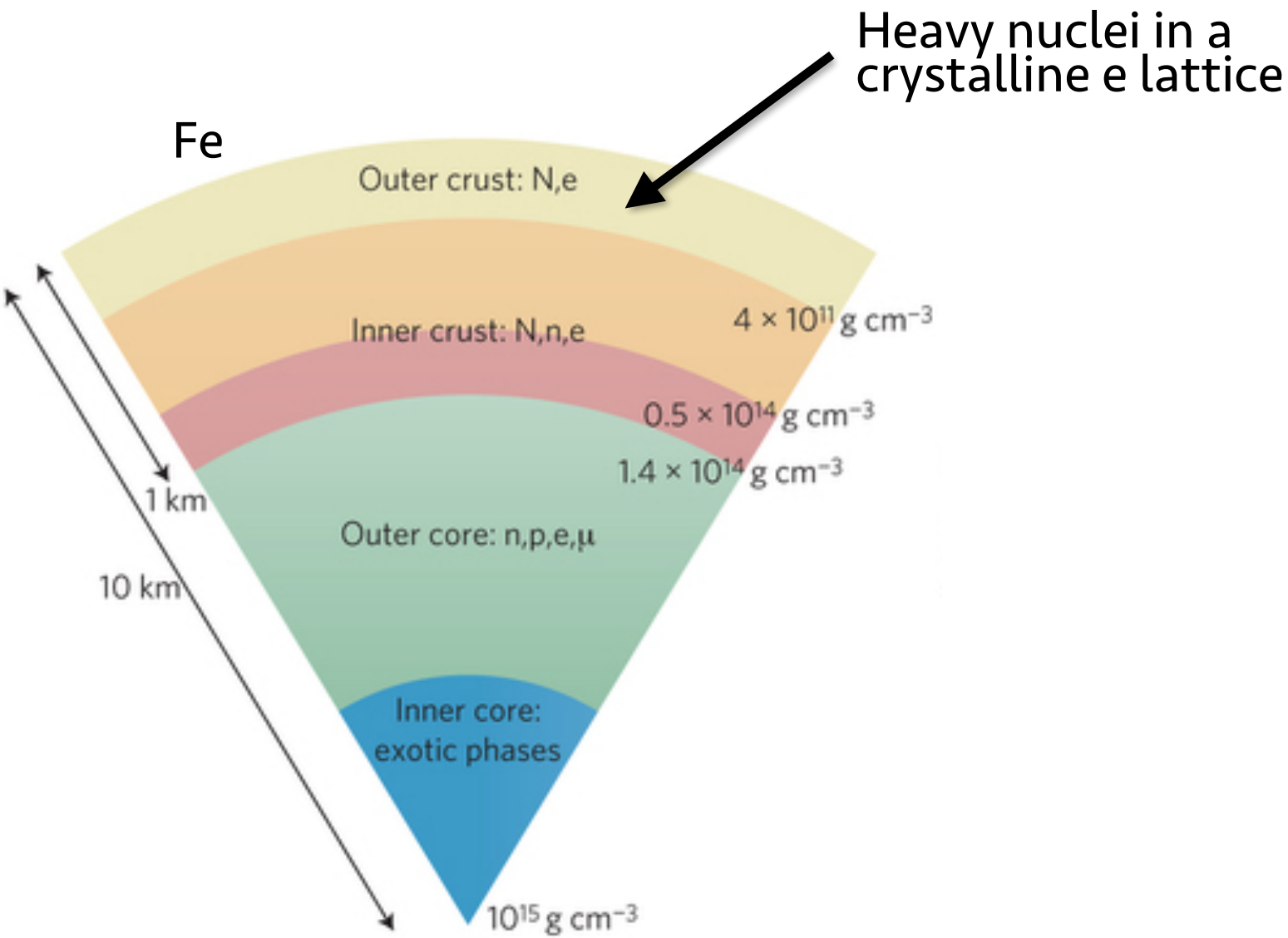

Interior Structure

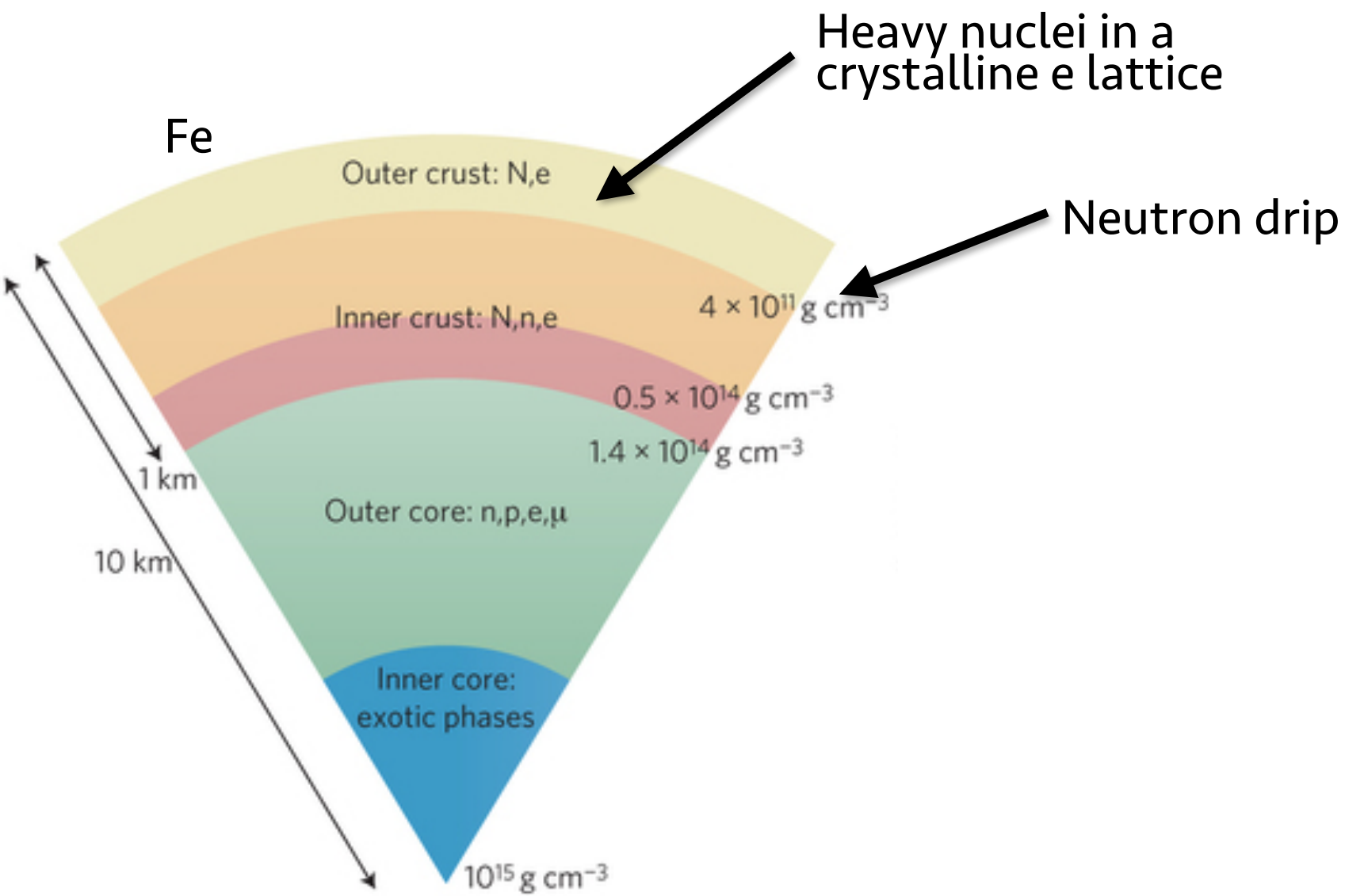

Interior Structure

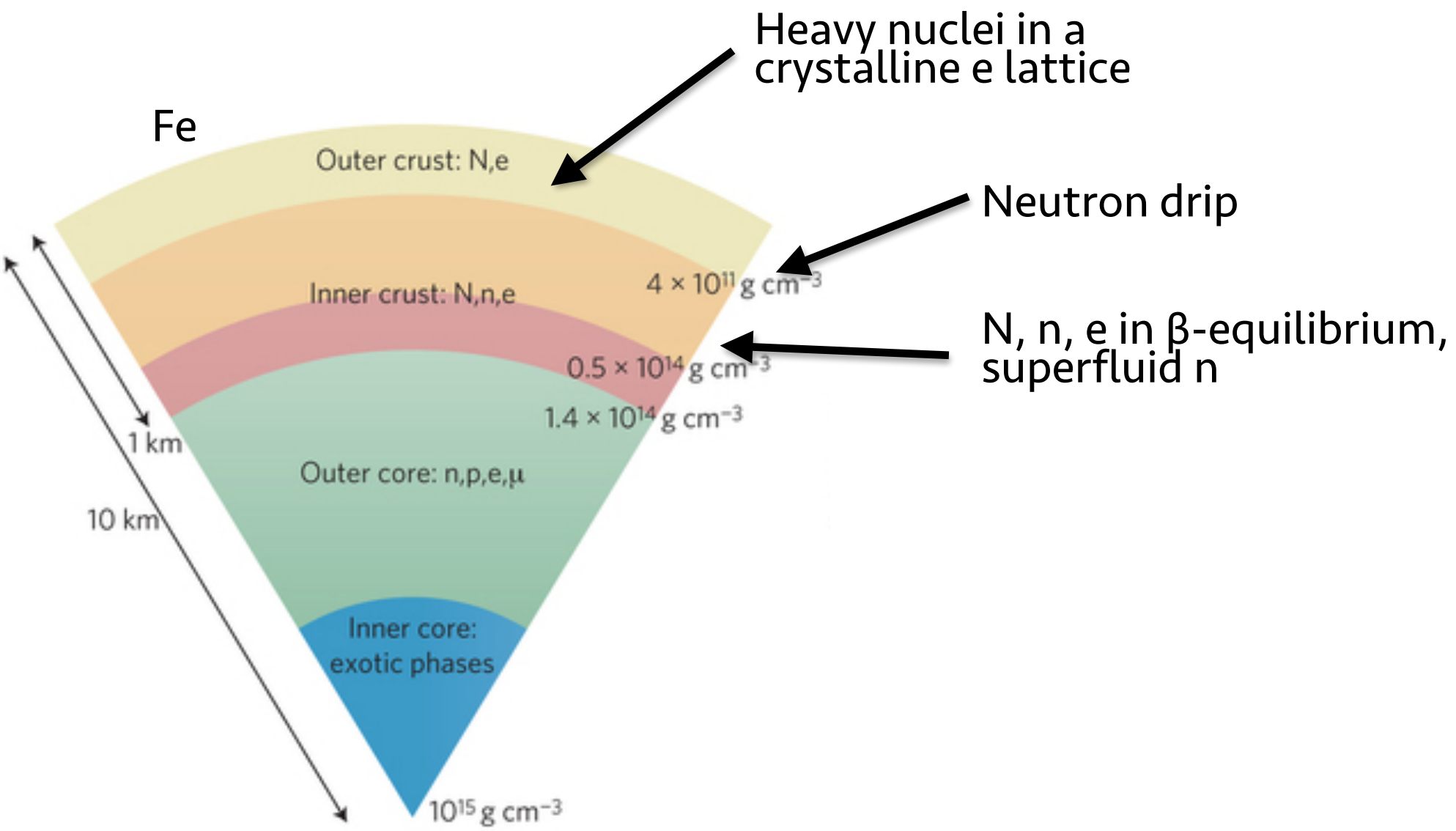

Interior Structure

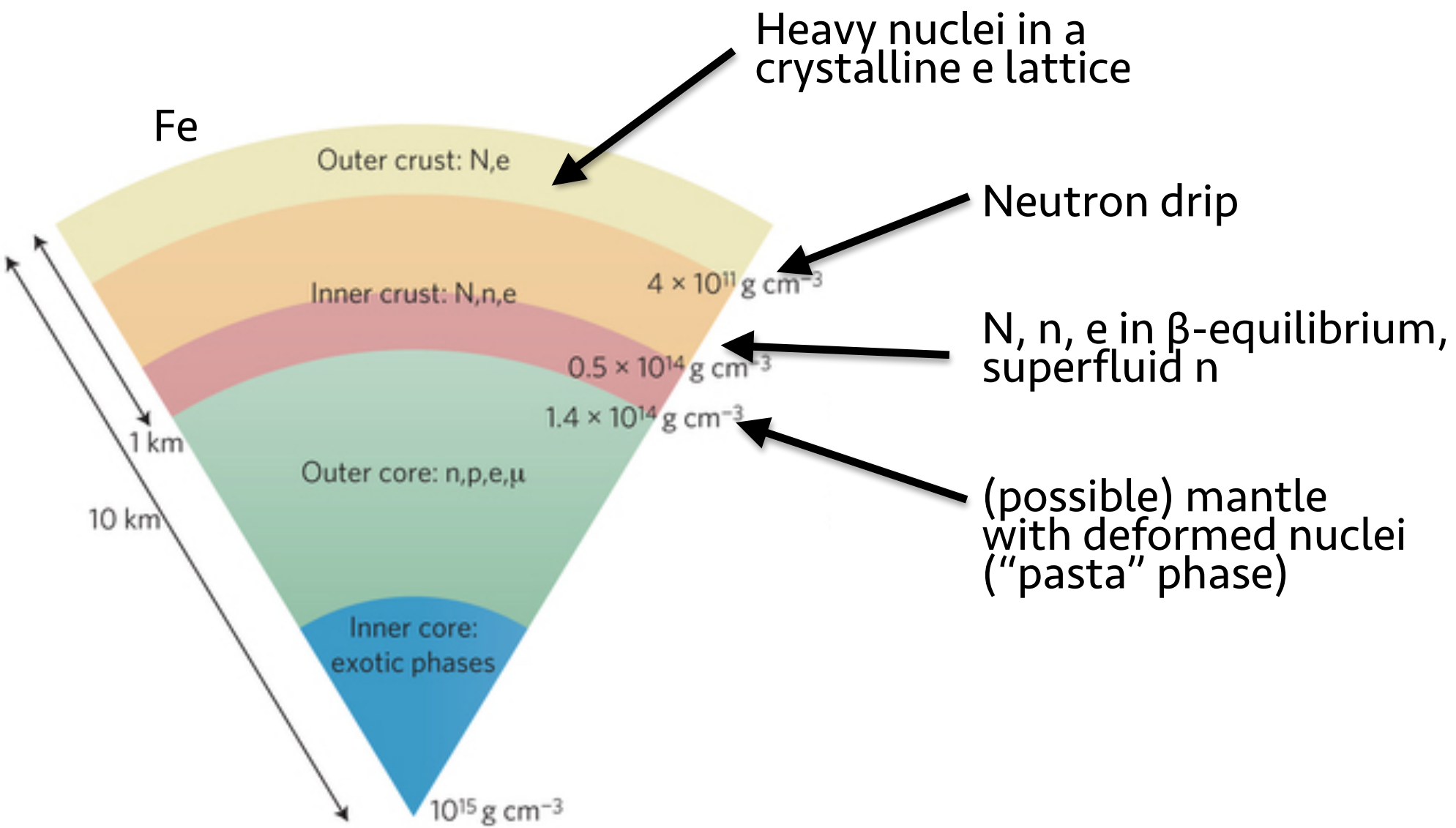

Interior Structure

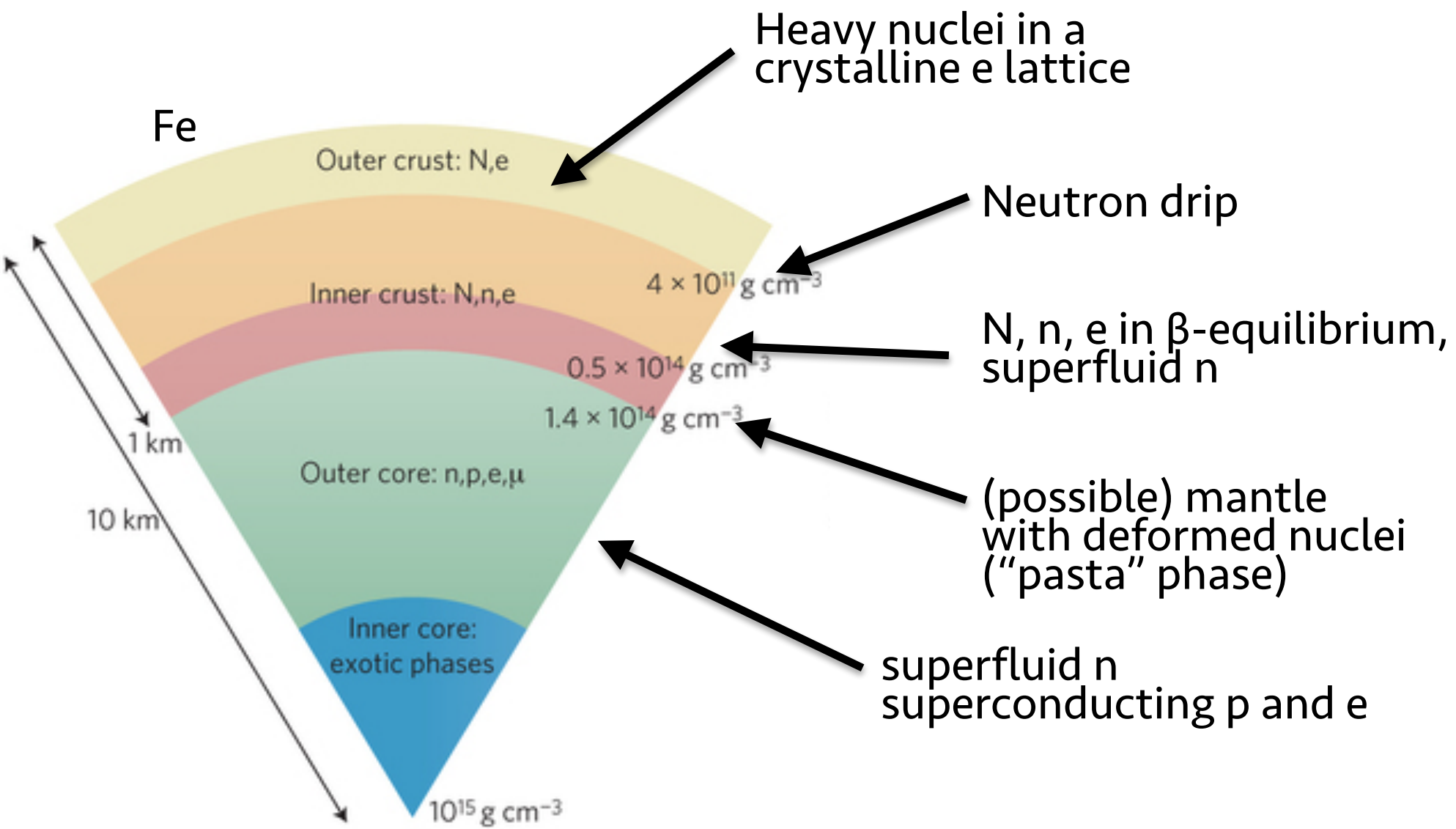

Interior Structure

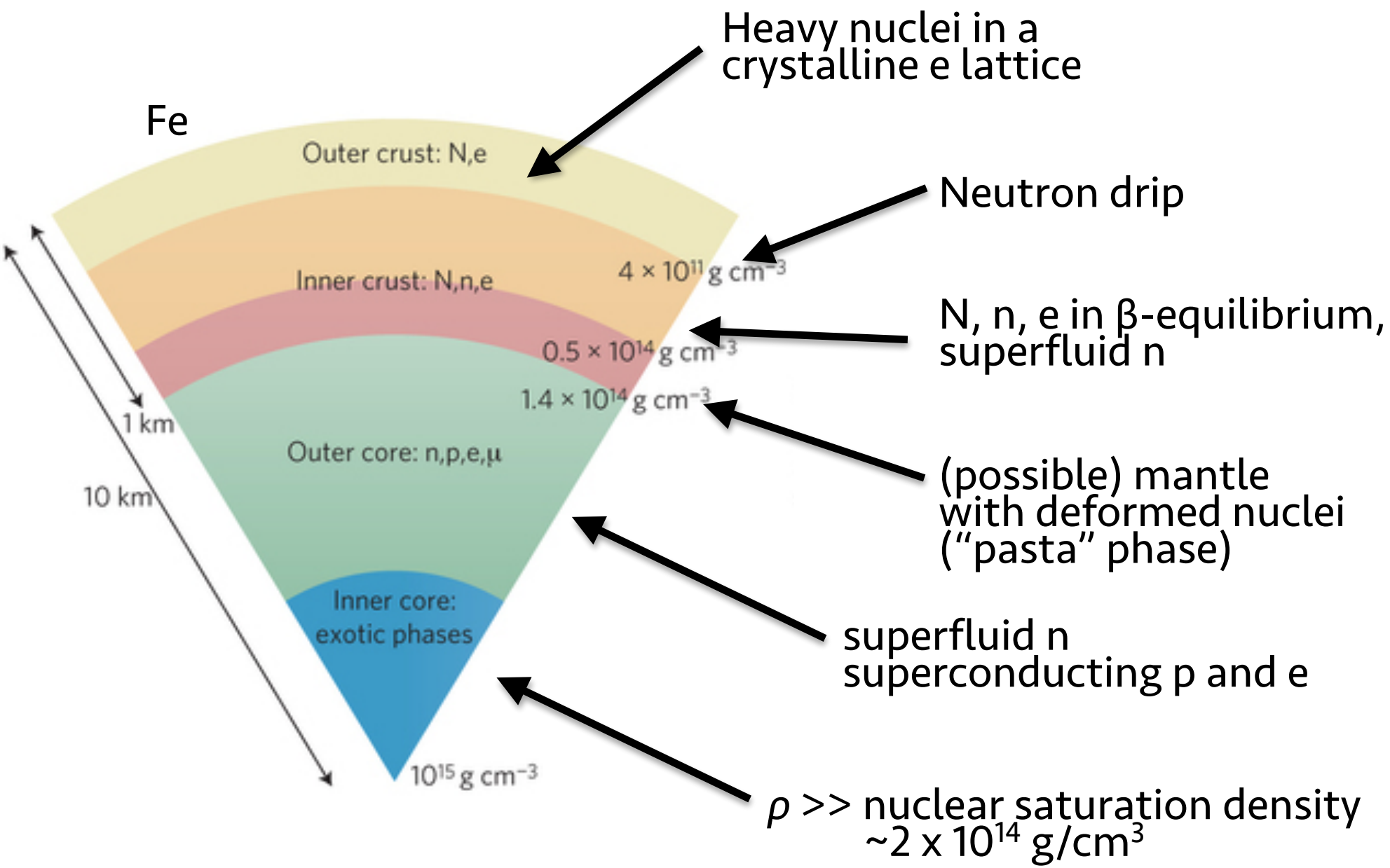

Equation of State (EOS)

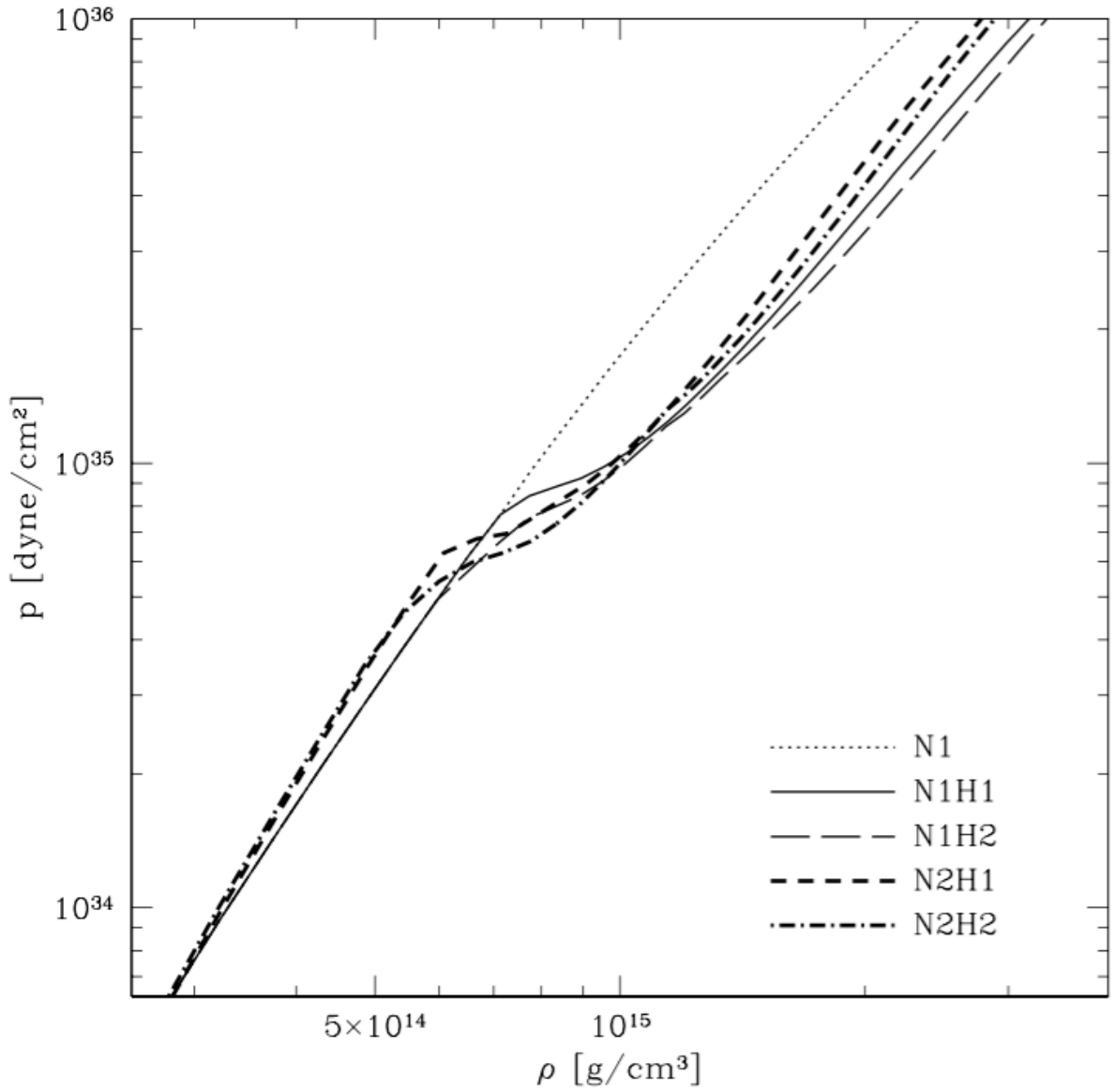

Hyperon = baryon (i.e. hadron + fermion) made of 3 quarks, with at least one strange quark:

- $\Lambda_0 = uds$
- $\Sigma^- = dds$
- $\Xi^0 = uss$
- etc...

Should appear at high density ($\rho > 2\rho_{nuc}$)
$\Rightarrow$ EOS softening

N1 = np, N1H1,N2H1 = np$\Lambda\Sigma$,
N1H2,N2H2 = np$\Lambda\Sigma\Xi$
Balberg & Gal (1997)

(E. Gourgoulhon)

Different Possible Structures

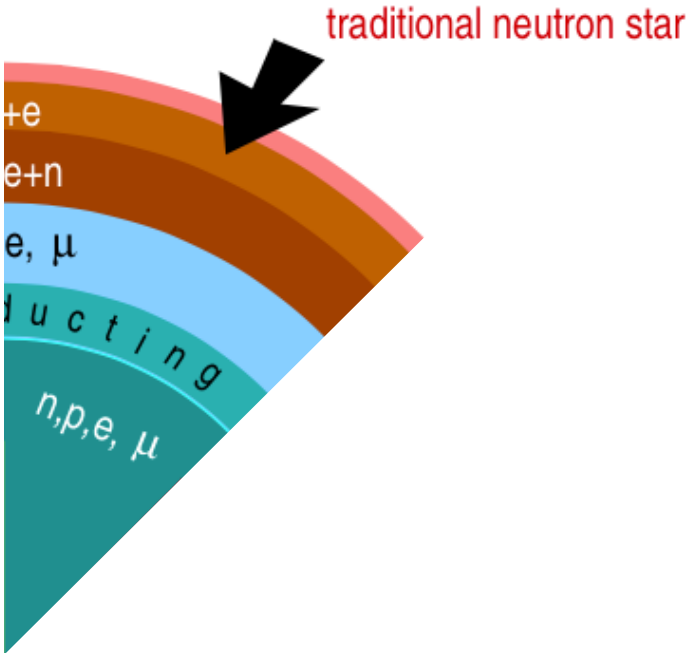

[Weber, J. Phys. G **27**, 465 (2001)]

Different Possible Structures

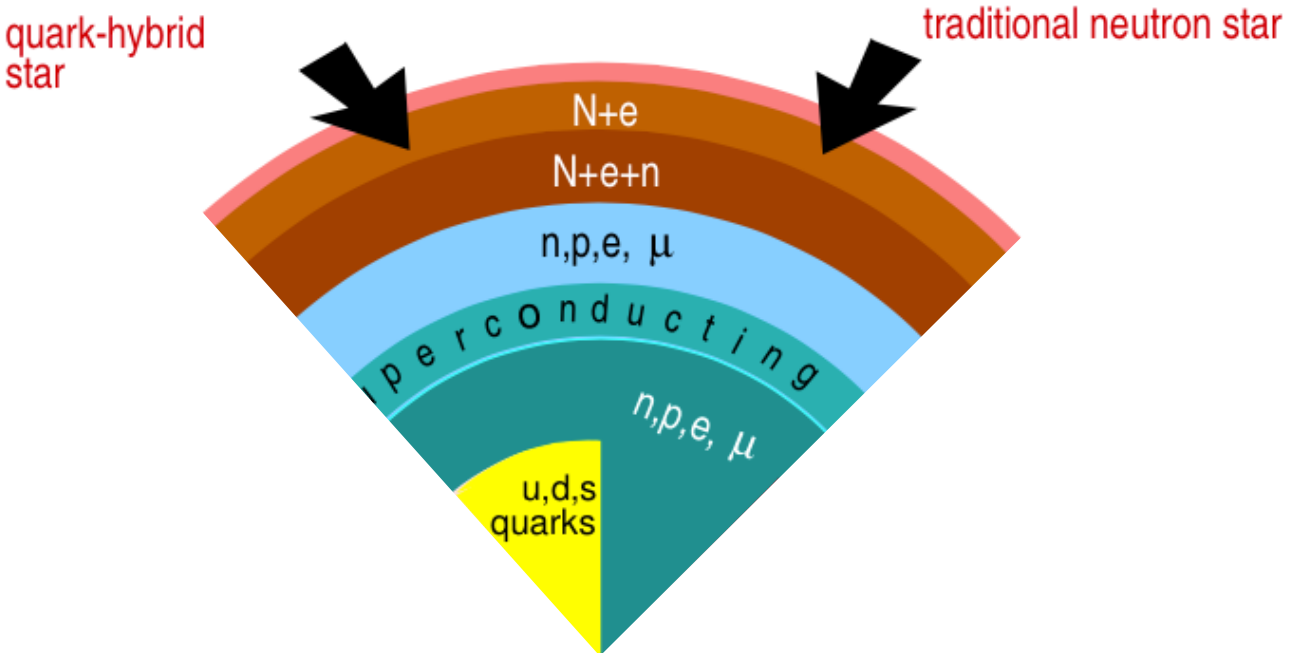

[Weber, J. Phys. G **27**, 465 (2001)]

Different Possible Structures

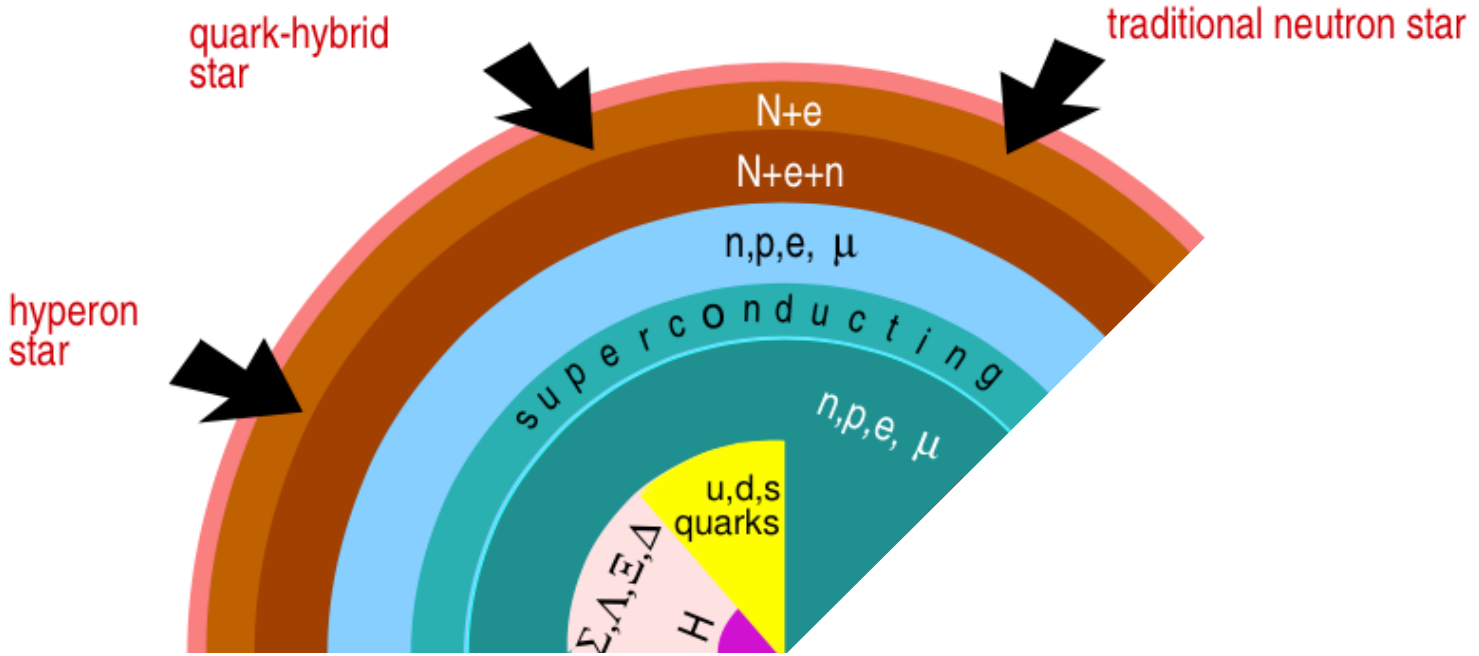

[Weber, J. Phys. G **27**, 465 (2001)]

Different Possible Structures

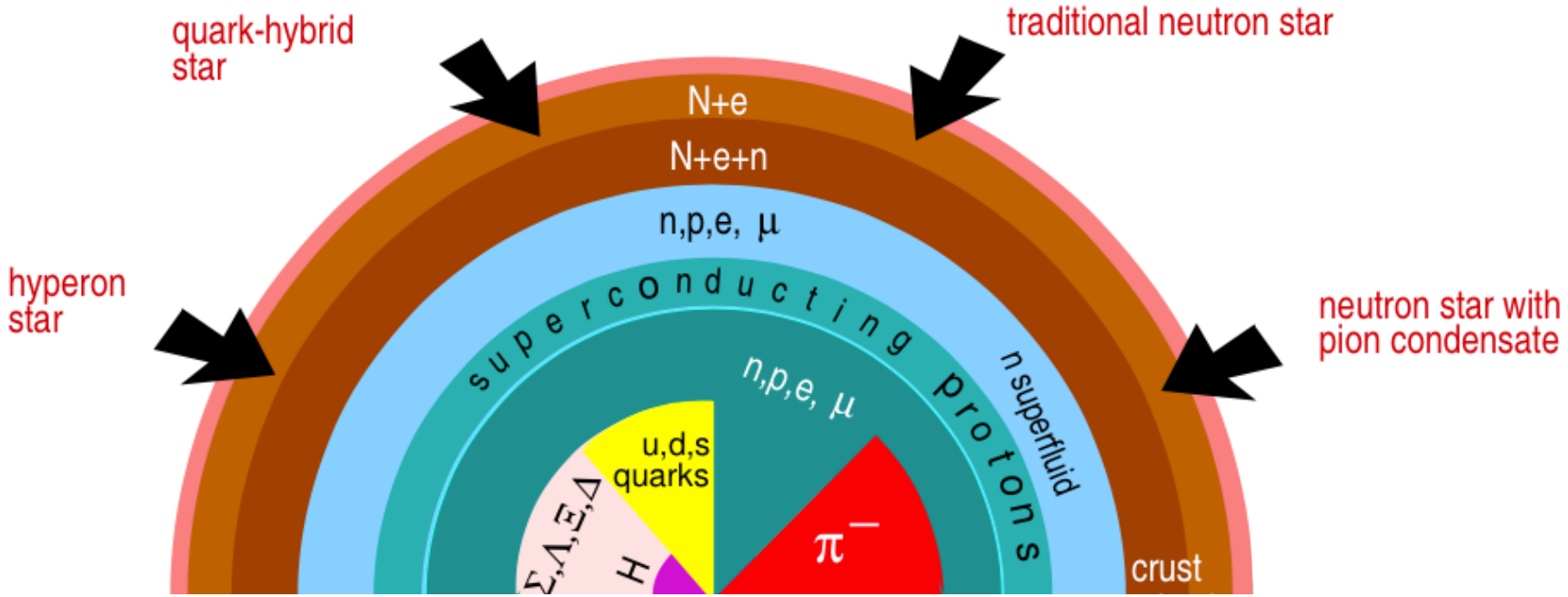

[Weber, J. Phys. G **27**, 465 (2001)]

Different Possible Structures

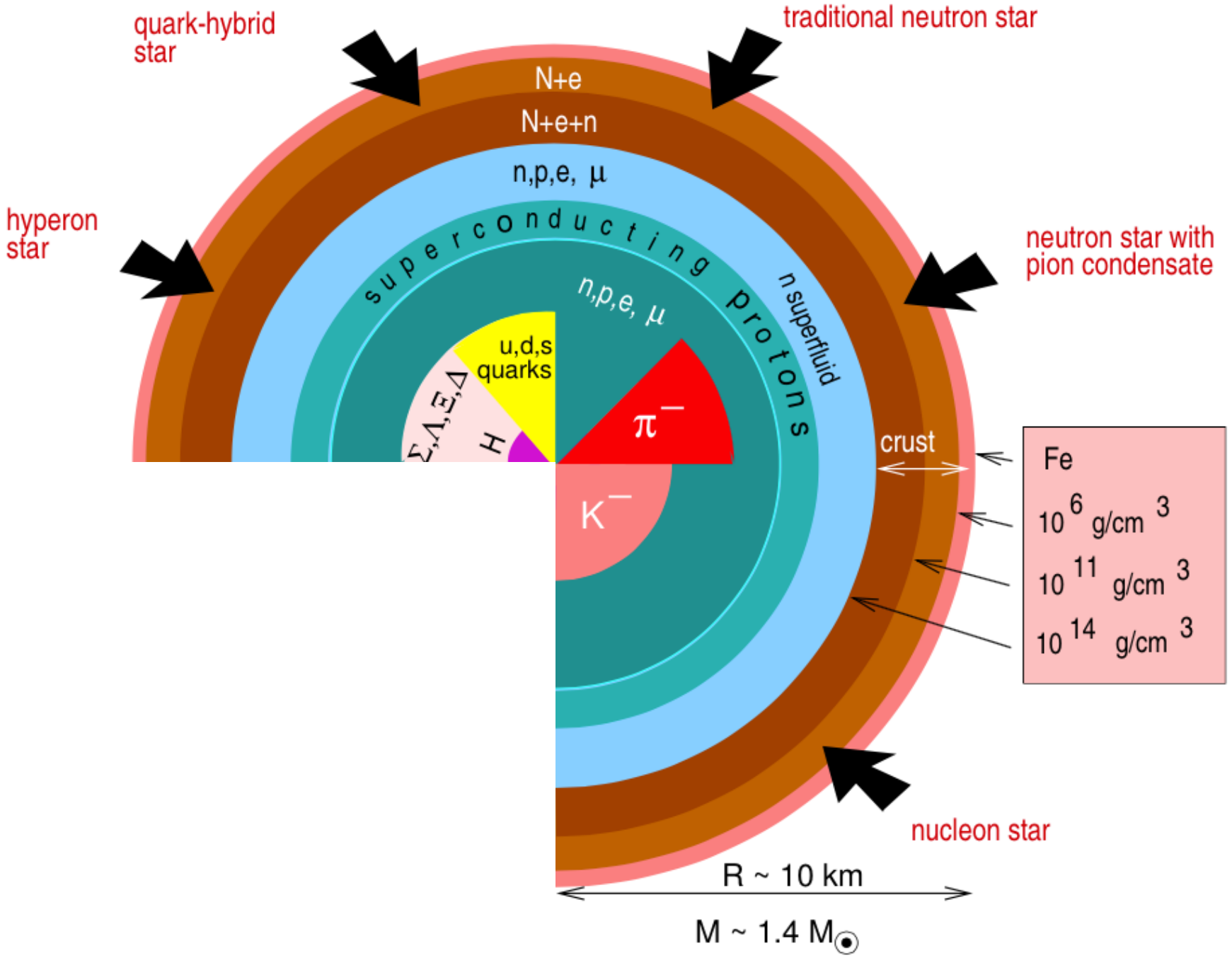

[Weber, J. Phys. G **27**, 465 (2001)]

Different Possible Structures

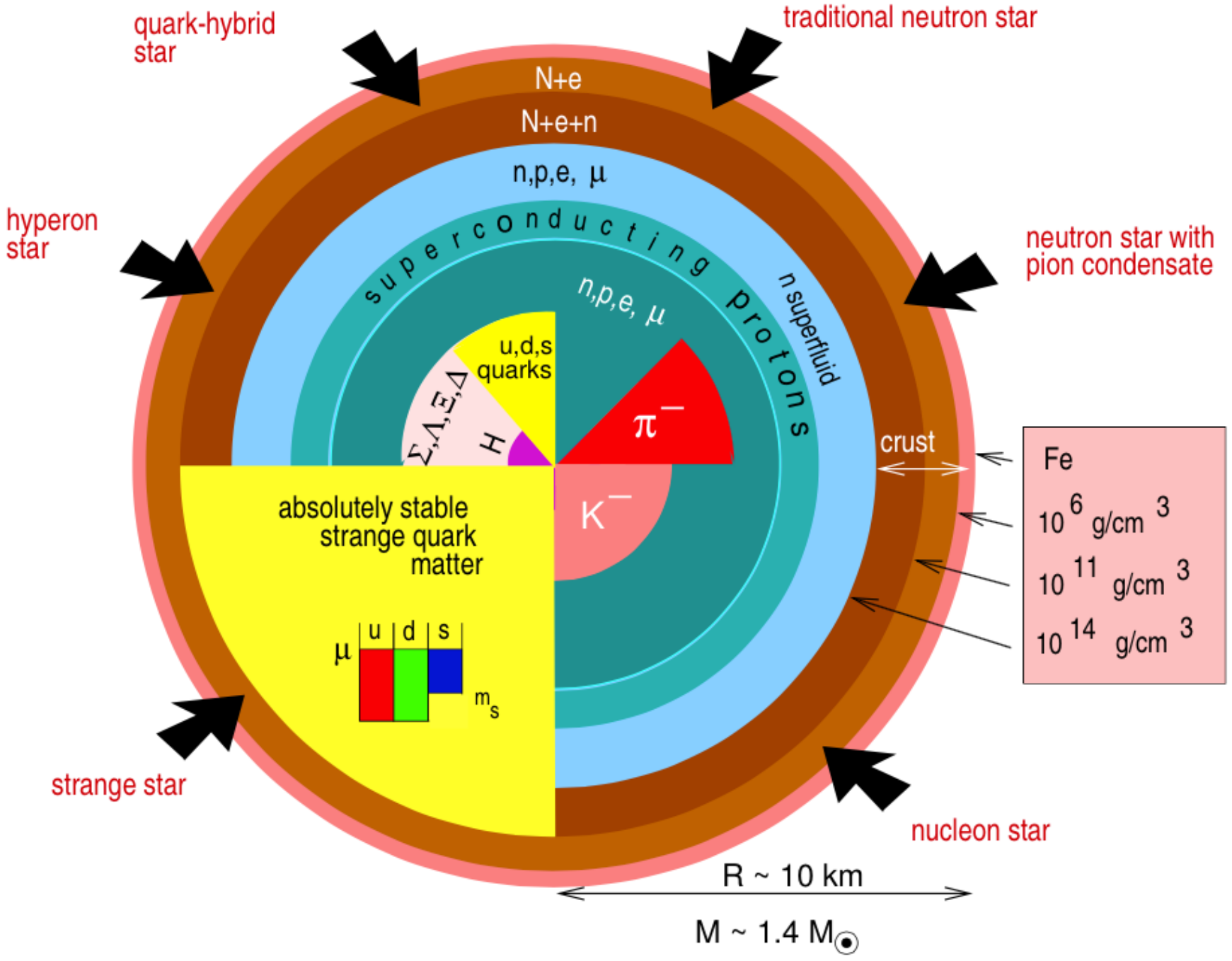

[Weber, J. Phys. G **27**, 465 (2001)]

Sample of Neutron Star Equations of State

Bauswein, Janka, Hebeler & Schwenk (2012)

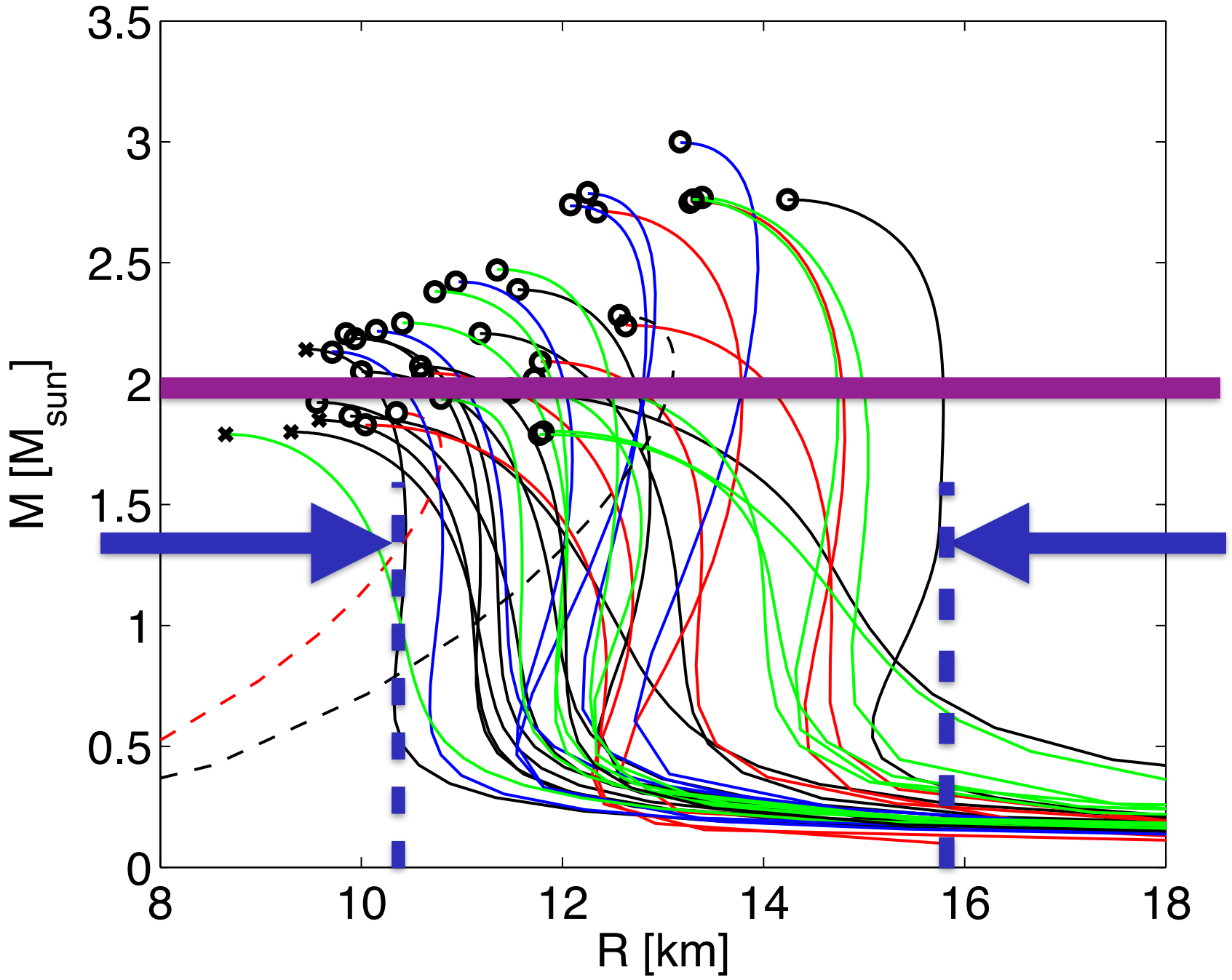

Maximally-Compact EOS

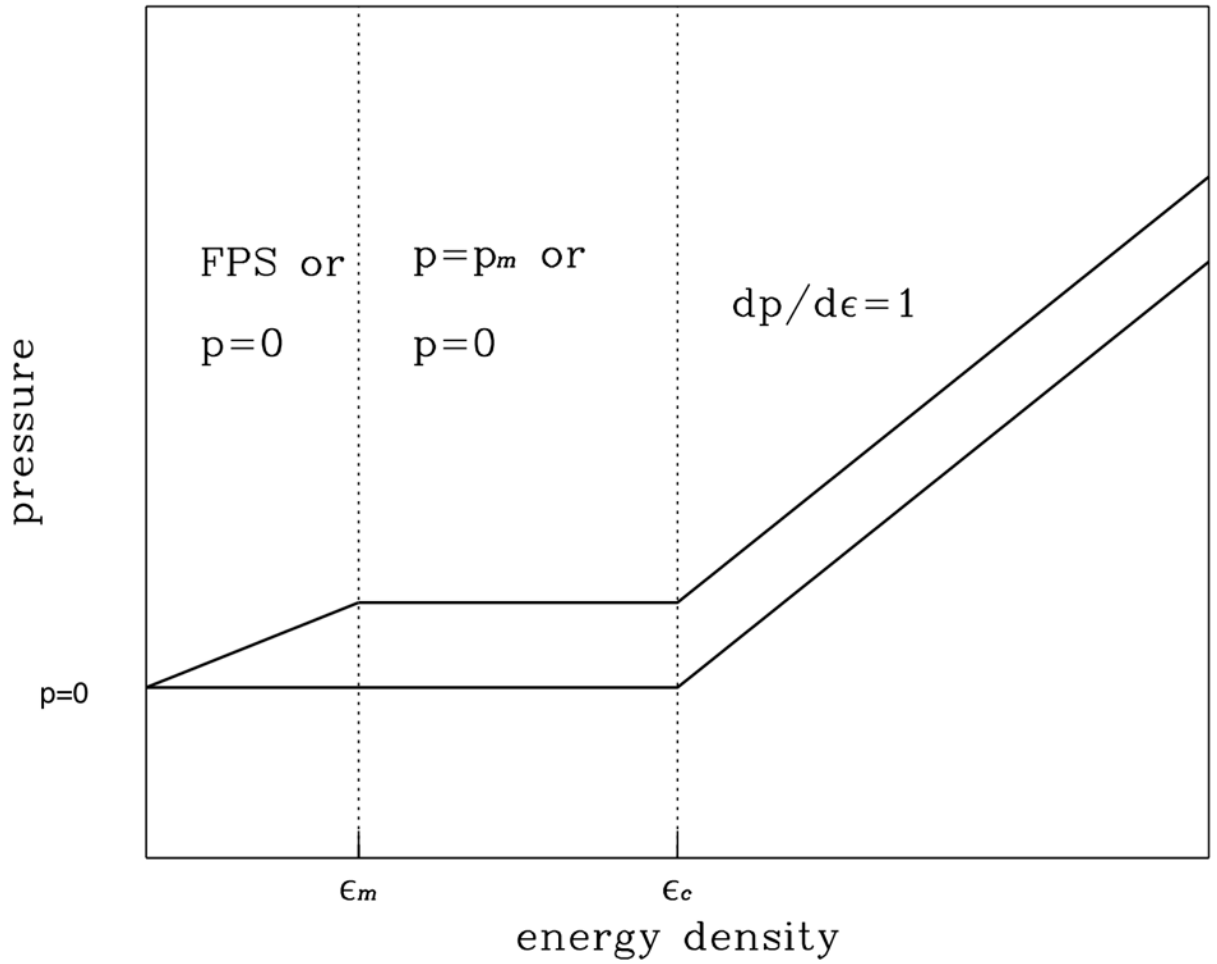

$$p(\epsilon) = \begin{cases} 0 & \epsilon \leq \epsilon_C \\ \epsilon - \epsilon_C & \epsilon \geq \epsilon_C \end{cases}$$

- Koranda, NS & Friedman (1997)

Maximally-Compact EOS Constraints

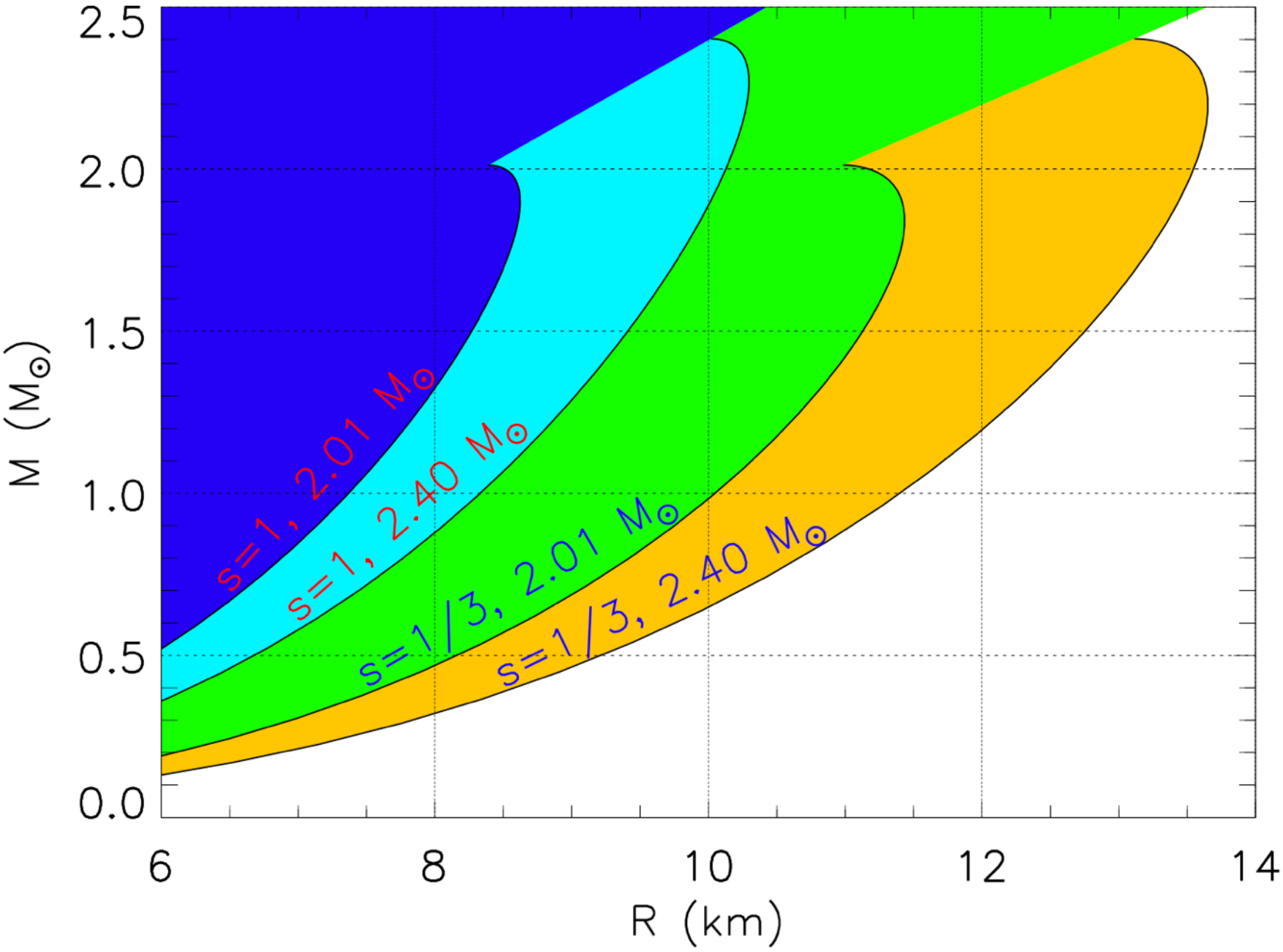

- Lattimer & Prakash (2016)

Outcome of Binary NS Mergers

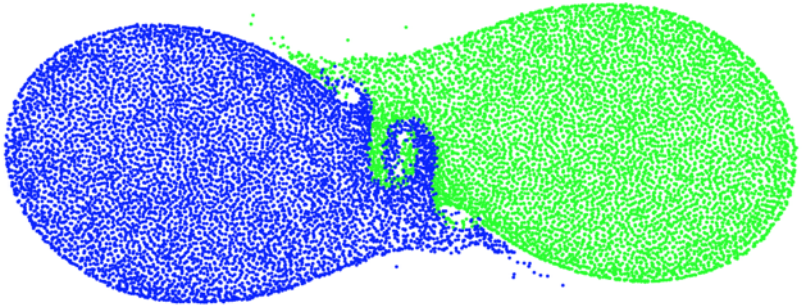

Most likely range of total mass for binary system:

$$2.4M_\odot < M_{\rm tot} < 3M_\odot$$

Because nonrotating $M_{\rm max} > 2M_\odot$ (as required by observations), a long-lived (τ >10ms) remnant is likely to be formed.

The remnant is a hypermassive neutron star (HMNS), supported by differential rotation, with a mass larger than the maximum mass allowed for uniform rotation.

Examples of Equilibrium Models

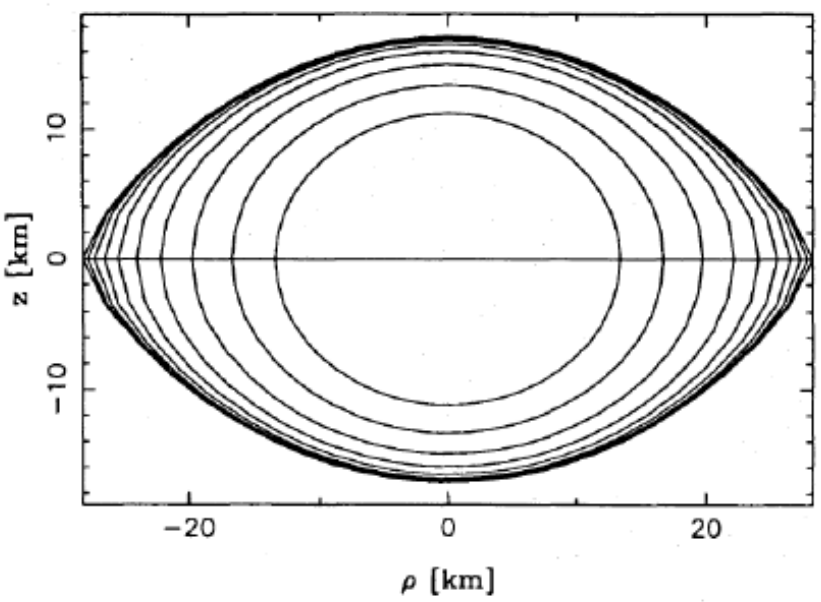

Bonazzola et al. 1993

Examples of Equilibrium Models

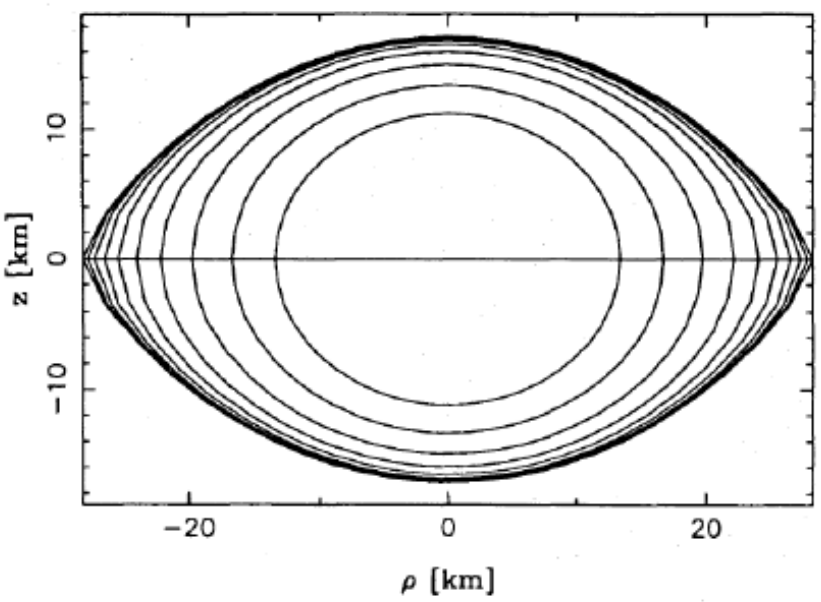

Bonazzola et al. 1993

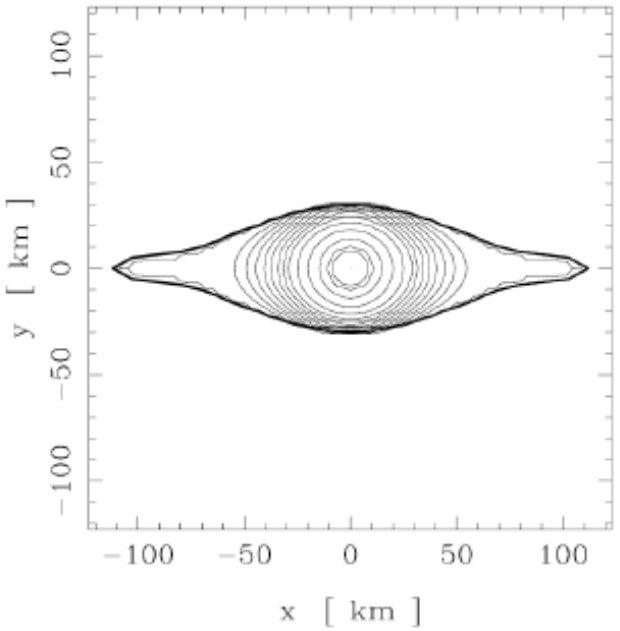

Goussard et al. 1998

Examples of Equilibrium Models

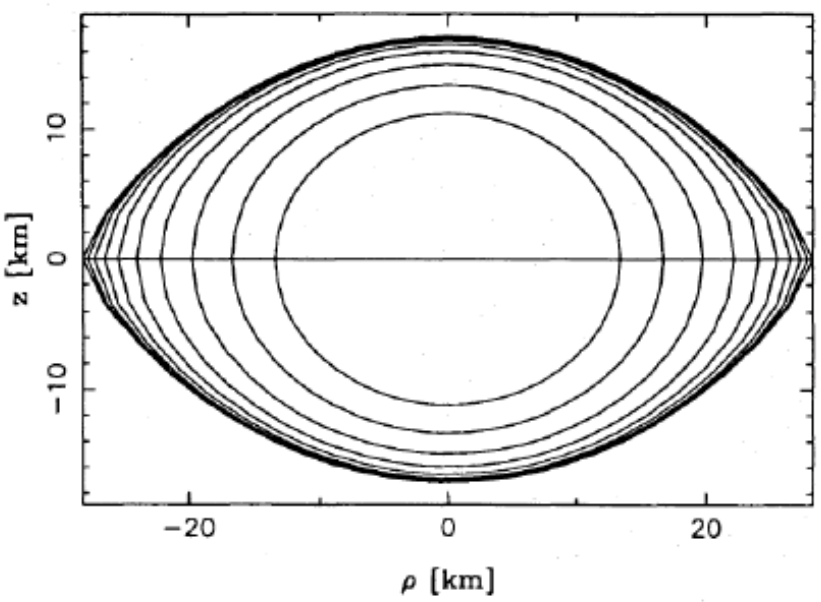

Bonazzola et al. 1993

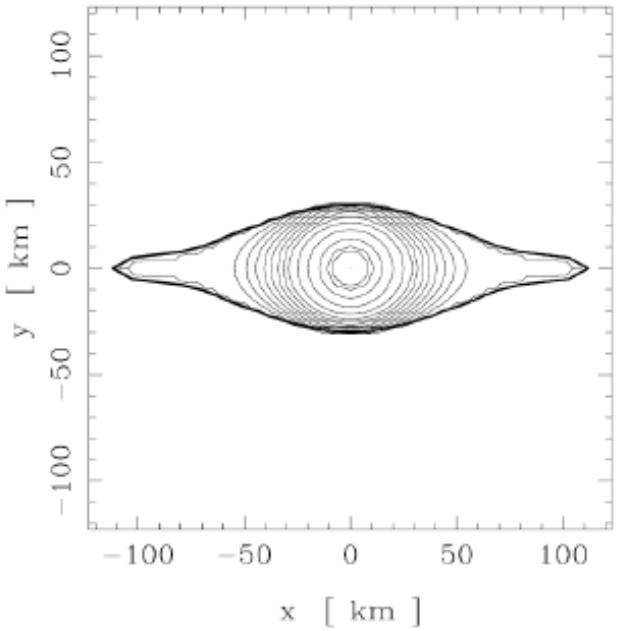

Goussard et al. 1998

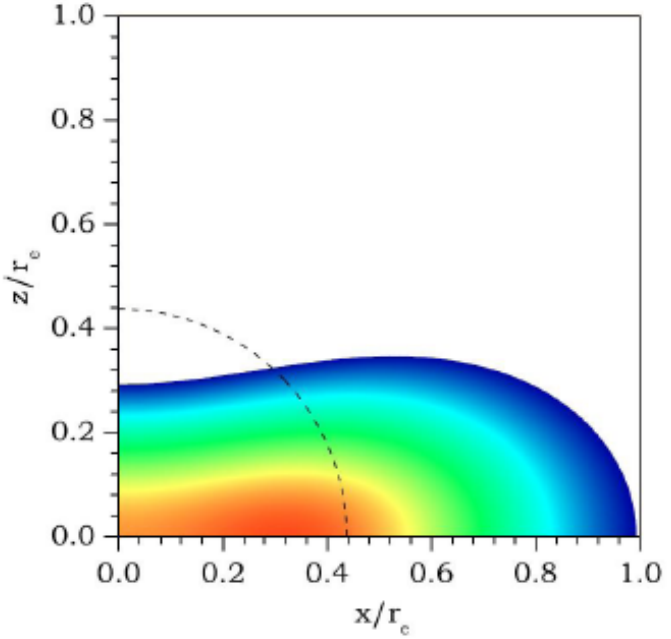

N. S., Apostolatos & Font, 2004

Examples of Equilibrium Models

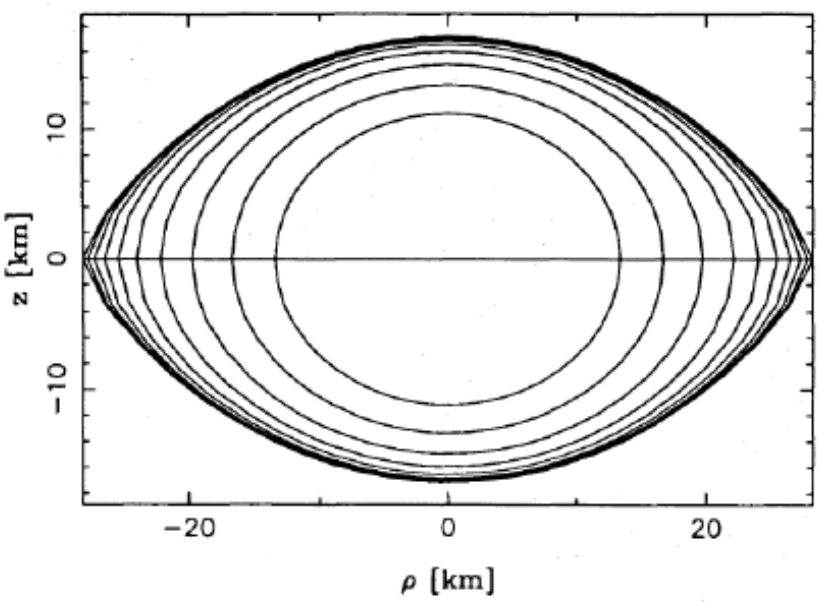

Bonazzola et al. 1993

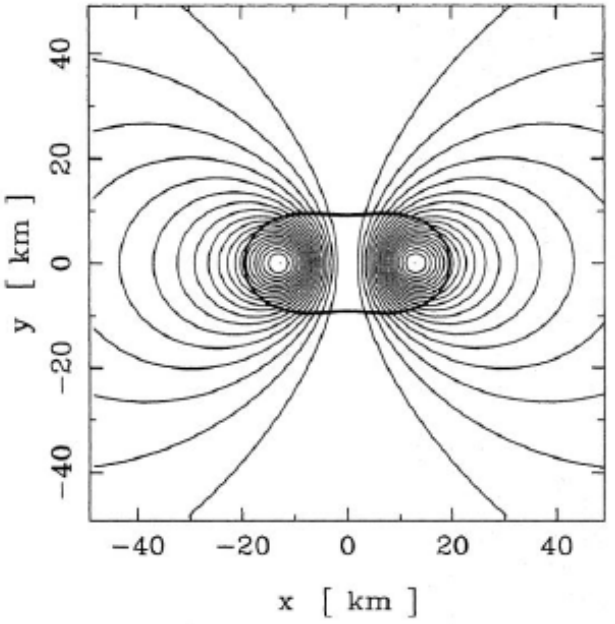

Bocquet et al. 1995

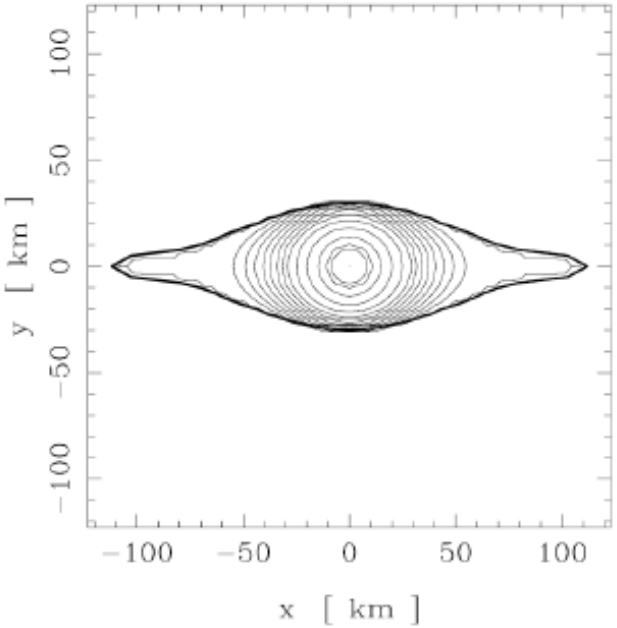

Goussard et al. 1998

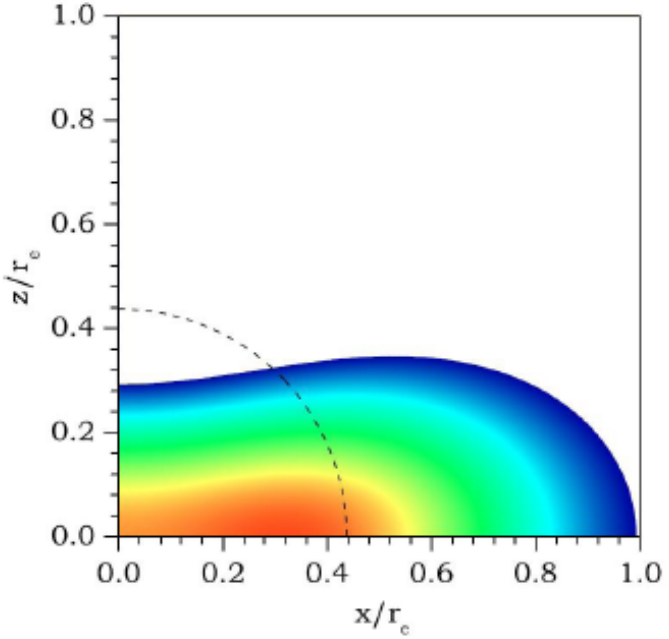

N. S., Apostolatos & Font, 2004

Rotating Equilibria in General Relativity

Assumptions on spacetime:

1. Stationary: Killing vector t^α which is timelike at spatial infinity.

2. Axisymmetric: Killing vector ϕ^α which is *spacelike* everywhere, vanishes on a *symmetry axis* and whose orbits are *closed curves*.

3. Asymptotically flat: $t^\alpha t_\alpha = -1 \quad \phi^\alpha \phi_\alpha = 1 \quad t^\alpha \phi_\alpha = 0$ at spatial infinity.

Rotating Equilibria in General Relativity

Assumptions on spacetime:

1. Stationary: Killing vector t^α which is timelike at spatial infinity.

2. Axisymmetric: Killing vector ϕ^α which is *spacelike* everywhere, vanishes on a *symmetry axis* and whose orbits are *closed curves*.

3. Asymptotically flat: $t^\alpha t_\alpha = -1 \quad \phi^\alpha \phi_\alpha = -1 \quad t^\alpha \phi_\alpha = 0$ at spatial infinity.

$\rightarrow$ We can *choose* coordinates t and ϕ such that t^α and ϕ^α are *coordinate vectors*:

$$t^\alpha = \frac{\partial}{\partial t} \qquad \phi^\alpha = \frac{\partial}{\partial \phi}$$

Rotating Equilibria in General Relativity

Assumptions on spacetime:

1. Stationary: Killing vector t^α which is timelike at spatial infinity.

2. Axisymmetric: Killing vector ϕ^α which is *spacelike* everywhere, vanishes on a *symmetry axis* and whose orbits are *closed curves*.

3. Asymptotically flat: $t^\alpha t_\alpha = -1 \quad \phi^\alpha \phi_\alpha = -1 \quad t^\alpha \phi_\alpha = 0$ at spatial infinity.

$\rightarrow$ We can *choose* coordinates t and ϕ such that t^α and ϕ^α are *coordinate vectors*:

$$t^\alpha = \frac{\partial}{\partial t} \qquad \phi^\alpha = \frac{\partial}{\partial \phi}$$

4. Circularity (no meridional currents): t^α and ϕ^α are everywhere *orthogonal* to the 2-surfaces formed by the integral curves of the remaining two coordinates x^1 and x^2.

Quasi-Isotropic Coordinates

The nonzero components of the metric involving t and φ are written as *invariant combinations* of the Killing vectors:

$$\begin{aligned} g_{tt} &= t^\alpha t_\alpha = -e^{2\nu} + \omega^2 e^{2\psi} \\ g_{t\phi} &= t^\alpha \phi_\alpha = -\omega e^{2\psi} \\ g_{\phi\phi} &= \phi^\alpha \phi_\alpha = e^{2\psi} \end{aligned}$$

Then

$$g_{\alpha\beta} = \begin{bmatrix} -e^{2\nu} + \omega^2 e^{2\psi} & 0 & 0 & -\omega e^{2\psi} \\ & g_{11} & g_{12} & 0 \\ \text{sym.} & & g_{22} & 0 \\ & & & e^{2\psi} \end{bmatrix}$$

Quasi-Isotropic Coordinates

If one chooses *orthogonal coordinates* x^1 and x^2, then $g_{12}=0$.

For the remaining components, one can choose an *isotropic gauge*, in which the (x^1, x^2) sub-space is *conformally flat*:

e.g. *cylindrical-like* coordinates:

$$e^{2\mu}(d\varpi^2 + dz^2)$$

so that, finally:

$$ds^2 = -e^{2\nu}dt^2 + e^{2\psi}(d\phi - \omega dt)^2 + e^{2\mu}(d\varpi^2 + dz^2)$$

Rotation of the Fluid

The ratio of the two components of the 4-velocity

$$\Omega \equiv \frac{u^\phi}{u^t} = \frac{d\phi/d\tau}{dt/d\tau} = \frac{d\phi}{dt}$$

is the angular velocity as seen by a nonrotating observer at infinity.

Since φ^α is a Killing vector, there is a conserved specific angular momentum:

$$u_\phi = (\Omega - \omega)e^{2\psi}u^t$$

Thus, *zero-angular momentum observers* (ZAMO's) with $u_\varphi=0$, are rotating with an angular velocity $\Omega=\omega$ w.r.t. infinity (*dragging of inertial frames*)!

Frame Dragging

Freely falling observers with conserved zero angular momentum $u_\varphi = 0$ follow inwards-falling spiral paths.

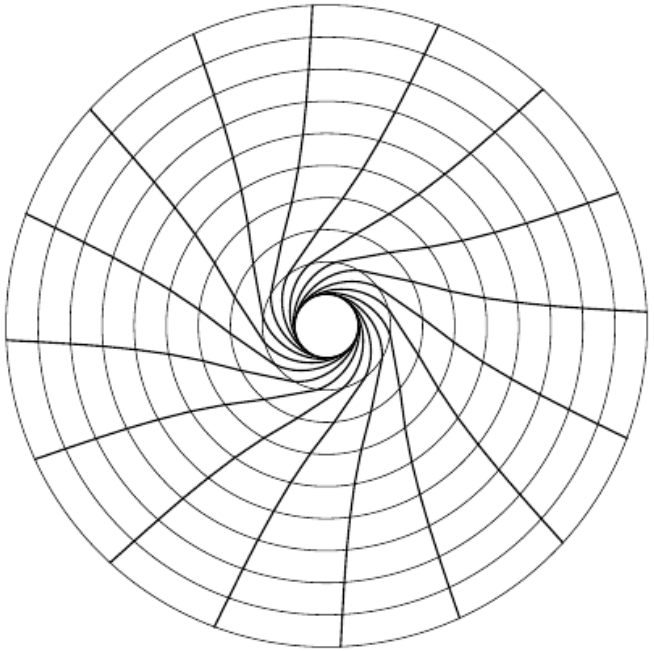

ZAMOs are *defined* as local observers with $u_\varphi = 0$ that follow circular orbits with

4-velocity $$u^\alpha_{\rm ZAMO} = u^t(t^\alpha + \omega\phi^\alpha) = e^{-\nu}(t^\alpha + \omega\phi^\alpha)$$

3-velocity $$v = 0$$

angular velocity $$\Omega = \omega$$

Radius of a Rotating Star

Consider the metric in quasi-isotropic coordinates

$$ds^2 = -e^{2\nu}dt^2 + e^{2\psi}(d\phi - \omega dt)^2 + e^{2\mu}(d\varpi^2 + dz^2)$$

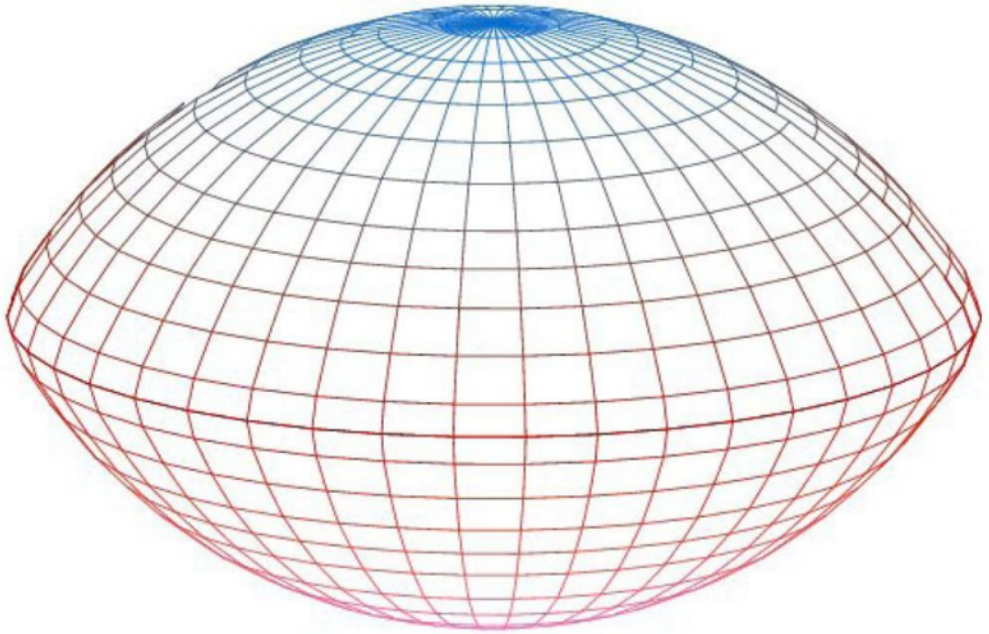

Q: What is the **radius** of the star?

Radius of a Rotating Star

Consider the metric in quasi-isotropic coordinates

$$ds^2 = -e^{2\nu}dt^2 + e^{2\psi}(d\phi - \omega dt)^2 + e^{2\mu}(d\varpi^2 + dz^2)$$

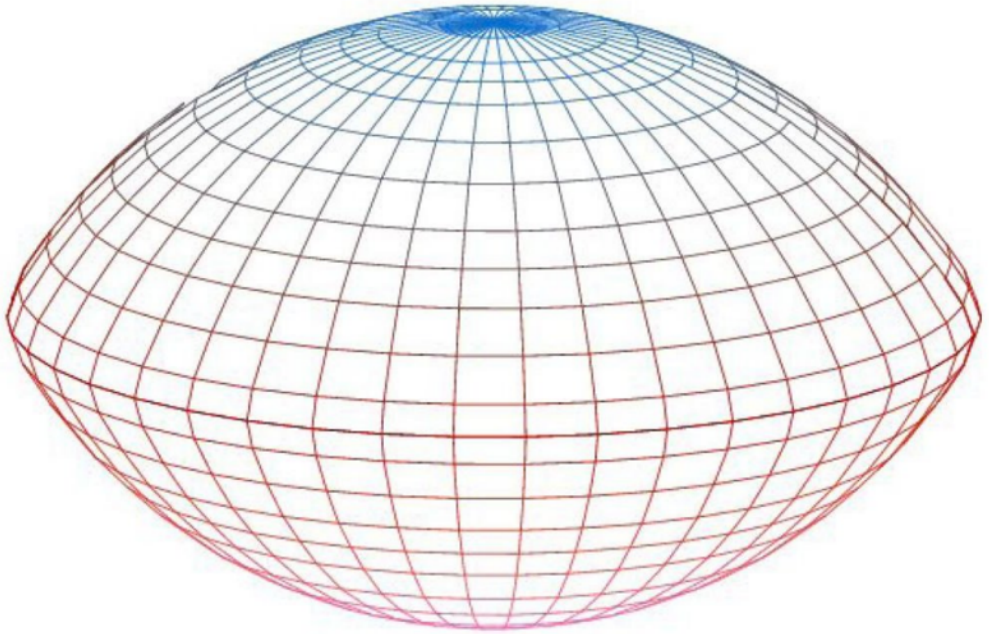

Q: What is the **radius** of the star?

A: At fixed t, ϖ, z integrate the proper length along the equator and divide by 2π.

Circumferential Radius

The proper circumference of a spatial circle at fixed t, ϖ, z is

$$\mathcal{C} = \oint ds = \int_0^{2\pi} \sqrt{g_{\phi\phi}} d\phi = 2\pi e^{\psi}$$

Thus, the *circumferential radius* is defined as

$$R := \mathcal{C}/(2\pi) = e^{\psi}$$

Summary, so far

The metric of a stationary, axisymmetric star with purely circular flow is:

$$ds^2 = -e^{2\nu}dt^2 + e^{2\psi}(d\phi - \omega dt)^2 + e^{2\mu}(d\varpi^2 + dz^2)$$

where three metric functions have an invariant meaning:

$e^{-\nu}$ *(time dilation factor)*

e^{ψ} *(circumferential radius)*

ω *(dragging of inertial frames)*

while $e^{2\mu}$ is a conformal factor for the geometry of the (ϖ,z) 2-planes.

The angular velocity Ω is measured by an observer at infinity

$$\Omega \equiv \frac{u^\phi}{u^t} = \frac{d\phi}{dt}$$

while the 3-velocity v is measured by the local zero-angular-momentum observer (ZAMO).

Field Equations

The field equations are most easily derived in a ZAMO orthonormal tetrad, where

$$T^{\hat{0}\hat{0}} = \frac{\epsilon + pv^2}{1 - v^2}, \qquad T^{\hat{0}\hat{1}} = \epsilon + p\frac{v}{1 - v^2},$$

$$T^{\hat{1}\hat{1}} = \frac{\epsilon v^2 + p}{1 - v^2}, \qquad T^{\hat{2}\hat{2}} = T^{\hat{3}\hat{3}} = p.$$

Field Equations

The field equations are most easily derived in a ZAMO orthonormal tetrad, where

$$T^{\hat{0}\hat{0}} = \frac{\epsilon + pv^2}{1 - v^2}, \qquad T^{\hat{0}\hat{1}} = \epsilon + p\frac{v}{1 - v^2},$$

$$T^{\hat{1}\hat{1}} = \frac{\epsilon v^2 + p}{1 - v^2}, \qquad T^{\hat{2}\hat{2}} = T^{\hat{3}\hat{3}} = p.$$

Then the $R_{\hat{0}\hat{0}}, R_{\hat{0}\hat{3}}$, and $R_{\hat{0}\hat{0}} - R_{\hat{3}\hat{3}}$ components of the field equations become

$$\begin{aligned}
\boldsymbol{\nabla}\cdot(B\boldsymbol{\nabla}\nu) &= \frac{1}{2}r^2\sin^2\theta B^3 e^{-4\nu}\boldsymbol{\nabla}\omega\cdot\boldsymbol{\nabla}\omega \\
&\quad + 4\pi B e^{2\zeta-2\nu}\left[\frac{(\epsilon+p)(1+v^2)}{1-v^2} + 2p\right], \\
\boldsymbol{\nabla}\cdot(r^2\sin^2\theta B^3 e^{-4\nu}\boldsymbol{\nabla}\omega) &= -16\pi r\sin\theta B^2 e^{2\zeta-4\nu}\frac{(\epsilon+p)v}{1-v^2}, \\
\boldsymbol{\nabla}\cdot(r\sin\theta\boldsymbol{\nabla}B) &= 16\pi r\sin\theta B e^{2\zeta-2\nu}p,
\end{aligned}$$

with $\zeta = \mu + \nu$ and ∇ is the *flat-space Laplacian.*

Relativistic Euler Equation

Projecting the conservation of the stress energy tensor normal to the flow:

$$\frac{\nabla_\alpha p}{(\epsilon + p)} = -u^\beta \nabla_\beta u_\alpha$$

which becomes:

$$\frac{\nabla p}{(\epsilon + p)} = \nabla \ln u^t - u^t u_\phi \nabla \Omega$$

First Integral

Define the log-enthalpy

$$H(p) := \int_0^p \frac{dp'}{\epsilon(p') + p'};$$

Then

$$\nabla(H - \ln u^t) = -F\nabla\Omega$$

where $F := u^t u_\phi$

A *first integral* exists when **either** Ω = const. or $F = F(\Omega)$

$$H - \ln u^t + \int_{\Omega_0}^{\Omega} F(\Omega')d\Omega' = \text{constant}$$

Numerical Method

Metric:

$$ds^2 = -e^{\gamma+\rho}dt^2 + e^{\gamma-\rho}r^2\sin^2\theta(d\phi-\omega dt)^2 + e^{2\alpha}(dr^2+r^2d\theta^2)$$

Field Equations:
integral form

$$\Delta[\rho e^{\gamma/2}] = S_\rho(r,\mu),$$

$$\left(\Delta + \frac{1}{r}\frac{\partial}{\partial r} - \frac{1}{r^2}\mu\frac{\partial}{\partial\mu}\right)\gamma e^{\gamma/2} = S_\gamma(r,\mu),$$

$$\left(\Delta + \frac{2}{r}\frac{\partial}{\partial r} - \frac{2}{r^2}\mu\frac{\partial}{\partial\mu}\right)\omega e^{(\gamma-2\rho)/2} = S_\omega(r,\mu),$$

$$\rho = -\frac{1}{4\pi}e^{-\gamma/2}\int_0^\infty dr'\int_{-1}^1 d\mu'\int_0^{2\pi} d\phi' r'^2 S_\rho(r',\mu')\frac{1}{|\mathbf{r}-\mathbf{r}'|},$$

$$r\sin\theta\gamma = \frac{1}{2\pi}e^{-\gamma/2}\int_0^\infty dr'\int_0^{2\pi} d\theta' r'^2\sin\theta' S_\gamma(r',\theta')\log|\mathbf{r}-\mathbf{r}'|,$$

$$r\sin\theta\cos\phi\,\omega = -\frac{1}{4\pi}e^{(2\rho-\gamma)/2}\int_0^\infty dr'\int_0^\pi d\theta'\int_0^{2\pi} d\phi' r'^3\sin^2\theta'\cos\phi' S_\omega(r',\theta')\frac{1}{|\mathbf{r}-\mathbf{r}'|}.$$

RNS code, NS & Friedman

Komatsu, Eriguchi & Hachisu (1989) method

Cook, Shapiro & Teukolsky (1994)
compactified radial coordinate

$$\begin{aligned}\alpha_{,\mu} = &-\nu_{,\mu} - \{(1-\mu^2)(1+rB^{-1}B_{,r})^2 + [\mu-(1-\mu^2)B^{-1}B_{,\mu}]^2\}^{-1}\\
&\left[\tfrac{1}{2}B^{-1}\{r^2B_{,rr} - [(1-\mu^2)B_{,\mu}]_{,\mu} - 2\mu B_{,\mu}\}[-\mu+(1-\mu^2)B^{-1}B_{,\mu}]\right.\\
&+rB^{-1}B_{,r}[\tfrac{1}{2}\mu+\mu rB^{-1}B_{,r}+\tfrac{1}{2}(1-\mu^2)B^{-1}B_{,\mu}]\\
&+\tfrac{3}{2}B^{-1}B_{,\mu}[-\mu^2+\mu(1-\mu^2)B^{-1}B_{,\mu}] - (1-\mu^2)rB^{-1}B_{,\mu r}(1+rB^{-1}B_{,r})\\
&-\mu r^2\nu_{,r}^2 - 2(1-\mu^2)r\nu_{,\mu}\nu_{,r} + \mu(1-\mu^2)\nu_{,\mu}^2 - 2(1-\mu^2)r^2B^{-1}B_{,r}\\
&\times\nu_{,\mu}\nu_{,r} + (1-\mu^2)B^{-1}B_{,\mu}[r^2\nu_{,r}^2 - (1-\mu^2)\nu_{,\mu}^2] + (1-\mu^2)B^2e^{-4\nu}\\
&\times[\tfrac{1}{4}\mu r^4\omega_{,r}^2 + \tfrac{1}{2}(1-\mu^2)r^3\omega_{,\mu}\omega_{,r} - \tfrac{1}{4}\mu(1-\mu^2)r^2\omega_{,\mu}^2 + \tfrac{1}{2}(1-\mu^2)\\
&\left.\times r^4B^{-1}B_{,r}\omega_{,\mu}\omega_{,r} - \tfrac{1}{4}(1-\mu^2)r^2B^{-1}B_{,\mu}[r^2\omega_{,r}^2 - (1-\mu^2)\omega_{,\mu}^2]\}\right],\end{aligned}$$

Differential Rotation

For polytropic EOS the specific angular momentum measured by proper time of matter is

$$j \equiv u^t u_\phi = j(\Omega)$$

Rotation Law:

$$\Omega = \Omega_C - \frac{(\Omega-\omega) r^2 \sin^2\theta\, e^{-2\rho}}{A^2\left[1-(\Omega-\omega)^2 r^2 \sin^2\theta\, e^{-2\rho}\right]}$$

Dimensionless constant:

$$\hat{A} = A/r_e$$

Limits:

$$\hat{A}^{-1} \rightarrow \begin{cases} 0 & \text{uniform rotation} \\ \infty & j-\text{constant rotation law} \end{cases}$$

Specific angular momentum conserved during homologous collapse:

$$\tilde{j} \equiv u_\phi \left(\frac{\varepsilon + p}{\rho_0}\right)$$

Satisfies Rayleigh criterion for local dynamical stability to axisymmetric perturbations:

$$\frac{d\tilde{j}}{d\Omega} < 0$$

Equilibrium Quantities

Using the unit normal $\hat{n}^\alpha$ to the *t*=const. spacelike surfaces and the proper volume

$$dV = \sqrt{|^3 g|} d^3x$$

one can define various *extensive* equilibrium quantities

$$\begin{aligned}
M &= \int \left(T_{\alpha\beta} - \frac{1}{2} g_{\alpha\beta} T \right) t^\alpha \hat{n}^\beta dV && \textit{gravitational mass} \\
M_0 &= \int \rho u_\alpha \hat{n}^\alpha dV && \textit{baryon mass} \\
U &= \int \rho \epsilon u_\alpha \hat{n}^\alpha dV && \textit{internal energy} \\
J &= \int T_{\alpha\beta} \phi^\alpha n^\beta dV && \textit{angular momentum} \\
T &= \frac{1}{2} \int \Omega dJ && \textit{rotational energy} \\
W &= M - (M_0 + U + T) && \textit{gravitational binding energy} \\
I &= J/\Omega && \textit{moment of inertia}
\end{aligned}$$

The Virial Theorems

The well-known Newtonian Virial theorem for equilibrium configurations

$$2T + (3\gamma - 1)U + W = 0$$

has been generalized in GR by Bonazzola & Gourgoulhon

$$\begin{aligned}
\lambda_3 \equiv\ & 4\pi \int_0^{+\infty} \int_0^{\pi} \left[3p + (\varepsilon + p) \frac{v^2}{1 - v^2} \right] \mathrm{e}^{2\mu + \psi}\, r\, \mathrm{d}r\, \mathrm{d}\theta \\
& \times \left\{ \int_0^{+\infty} \int_0^{\pi} \left[\partial\nu \partial\nu - \frac{1}{2} \partial\mu \partial\psi \right.\right. \\
& + \frac{\mathrm{e}^{2\mu - 2\psi}}{2} r \sin^2\theta \left(\frac{\partial\mu}{\partial r} + \frac{1}{r \tan\theta} \frac{\partial\mu}{\partial\theta} \right) \\
& + \frac{1}{4r} \left(1 - \mathrm{e}^{2\mu - 2\psi} r^2 \sin^2\theta \right) \left(\frac{\partial\psi}{\partial r} + \frac{1}{r \tan\theta} \frac{\partial\psi}{\partial\theta} \right. \\
& \left.\left.\left. - \frac{1}{r \sin^2\theta} \right) - \frac{3}{8} \mathrm{e}^{2\psi - 2\nu} \partial\omega \partial\omega \right] \mathrm{e}^{\psi}\, r\, \mathrm{d}r\, \mathrm{d}\theta \right\}^{-1},
\end{aligned}$$

Comparison of Different Codes

N.S., Living Reviews in Relativity (2003)

	AKM	Lorene/ rotstar	SF (260×400)	SF (70×200)	BGSM	KEH
$\bar{p}_{\rm c}$	1.0					
$r_{\rm p}/r_{\rm e}$	0.7				1×10^{-3}	
$\bar{\Omega}$	1.41170848318	9×10^{-6}	3×10^{-4}	3×10^{-3}	1×10^{-2}	1×10^{-2}
$\bar{M}$	0.135798178809	2×10^{-4}	2×10^{-5}	2×10^{-3}	9×10^{-3}	2×10^{-2}
$\bar{M}_0$	0.186338658186	2×10^{-4}	2×10^{-4}	3×10^{-3}	1×10^{-2}	2×10^{-3}
$\bar{R}_{\rm circ}$	0.345476187602	5×10^{-5}	3×10^{-5}	5×10^{-4}	3×10^{-3}	1×10^{-3}
$\bar{J}$	0.0140585992949	2×10^{-5}	4×10^{-4}	5×10^{-4}	2×10^{-2}	2×10^{-2}
$Z_{\rm p}$	1.70735395213	1×10^{-5}	4×10^{-5}	1×10^{-4}	2×10^{-2}	6×10^{-2}
$Z^{\rm f}_{\rm eq}$	-0.162534082217	2×10^{-4}	2×10^{-3}	2×10^{-2}	4×10^{-2}	2×10^{-2}
$Z^{\rm b}_{\rm eq}$	11.3539142587	7×10^{-6}	7×10^{-5}	1×10^{-3}	8×10^{-2}	2×10^{-1}
|GRV3|	4×10^{-13}	3×10^{-6}	3×10^{-5}	1×10^{-3}	4×10^{-3}	1×10^{-1}

AKM: Ansorg et al.

Lorene/rotstar + BGSM: Meudon group

SF: RNS code

KEH: original KEH code (not compactified)

Equilibria of Rotating Stars

Uniformly rotating equilibrium models for a realistic neutron star equation of state.

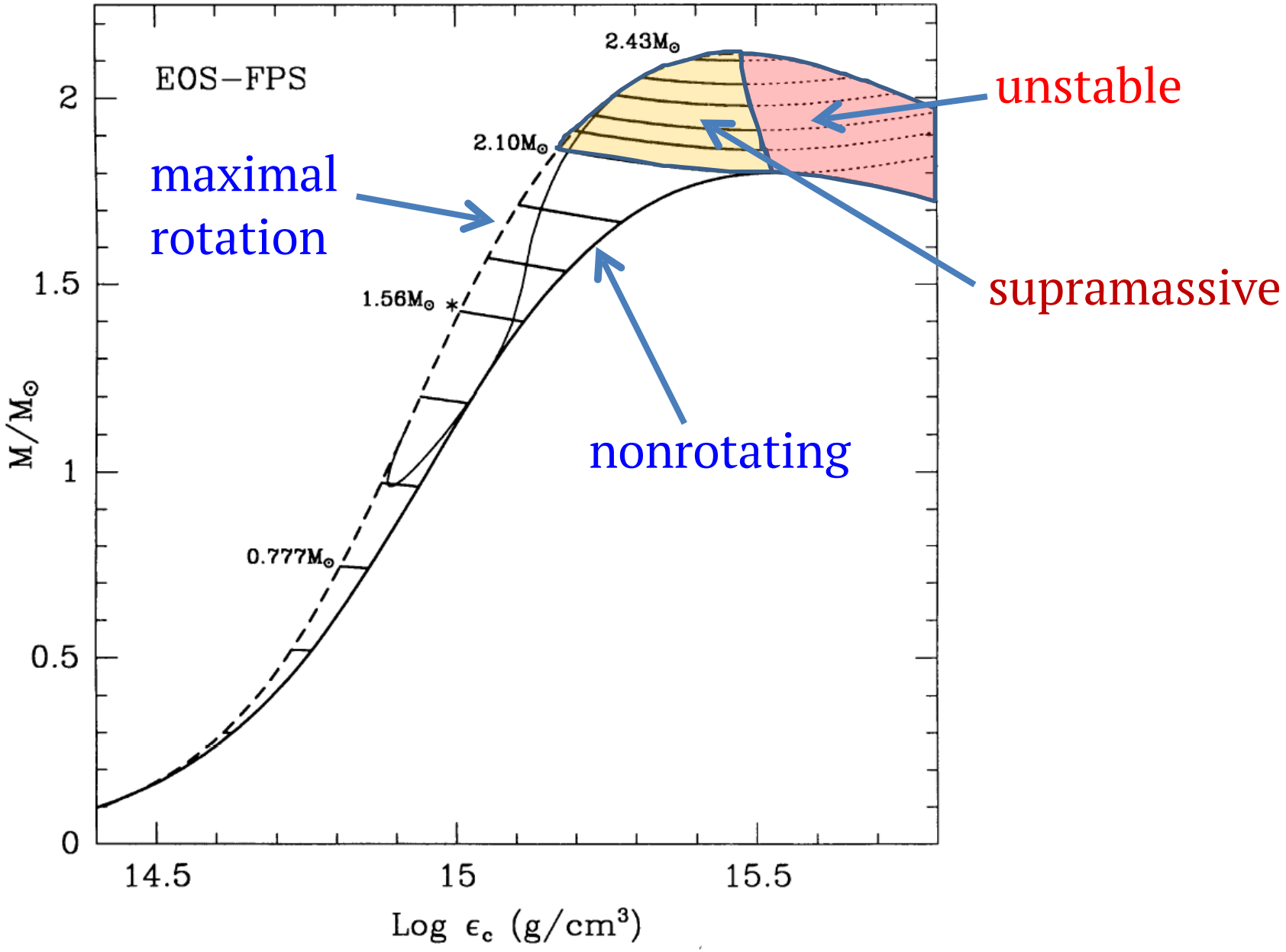

Axisymmetric Instability to Collapse

Rotating stars are subject to a ***secular*** axisymmetric instability, if:

$$\left(\frac{\partial M}{\partial \epsilon_c}\right)_J < 0$$

(Friedman, Ipser & Sorkin, 1988).

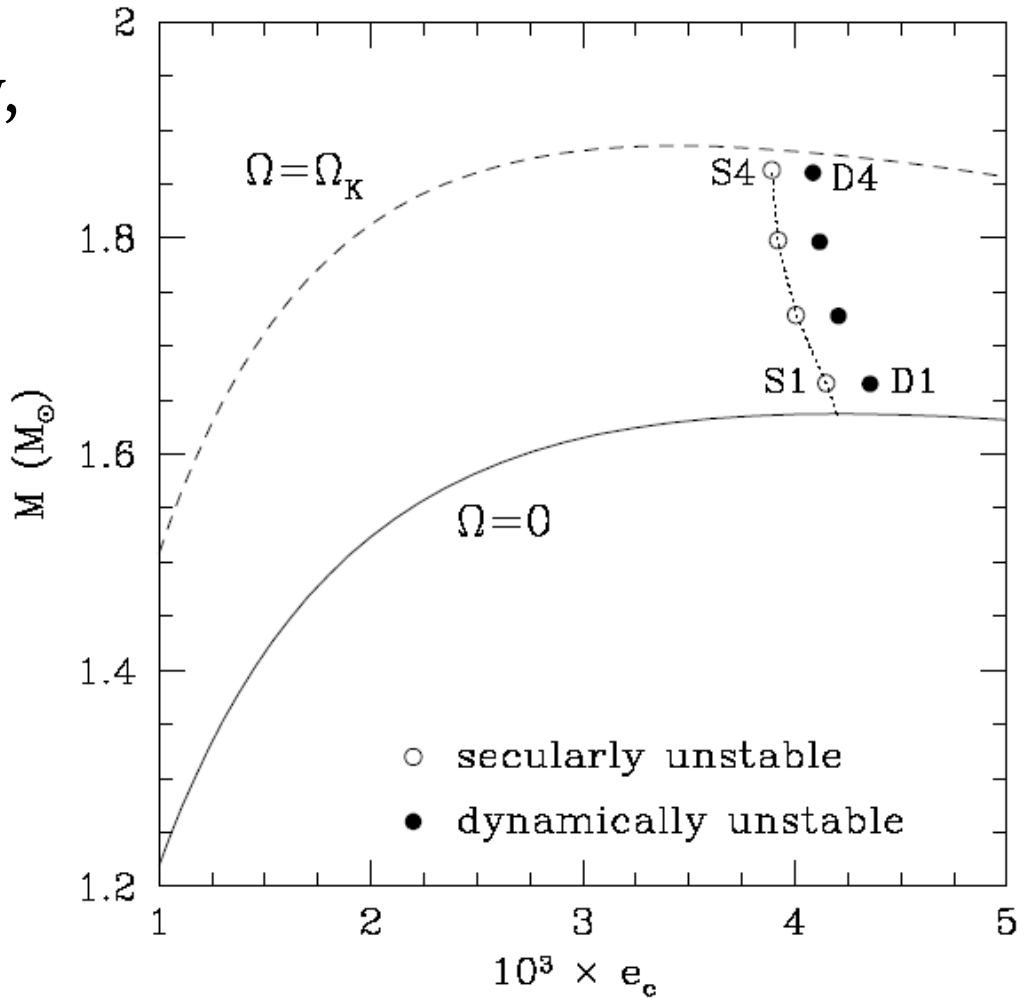

Axisymmetric Instability to Collapse

Rotating stars are subject to a ***secular*** axisymmetric instability, if:

$$\left(\frac{\partial M}{\partial \epsilon_c}\right)_J < 0$$

(Friedman, Ipser & Sorkin, 1988).

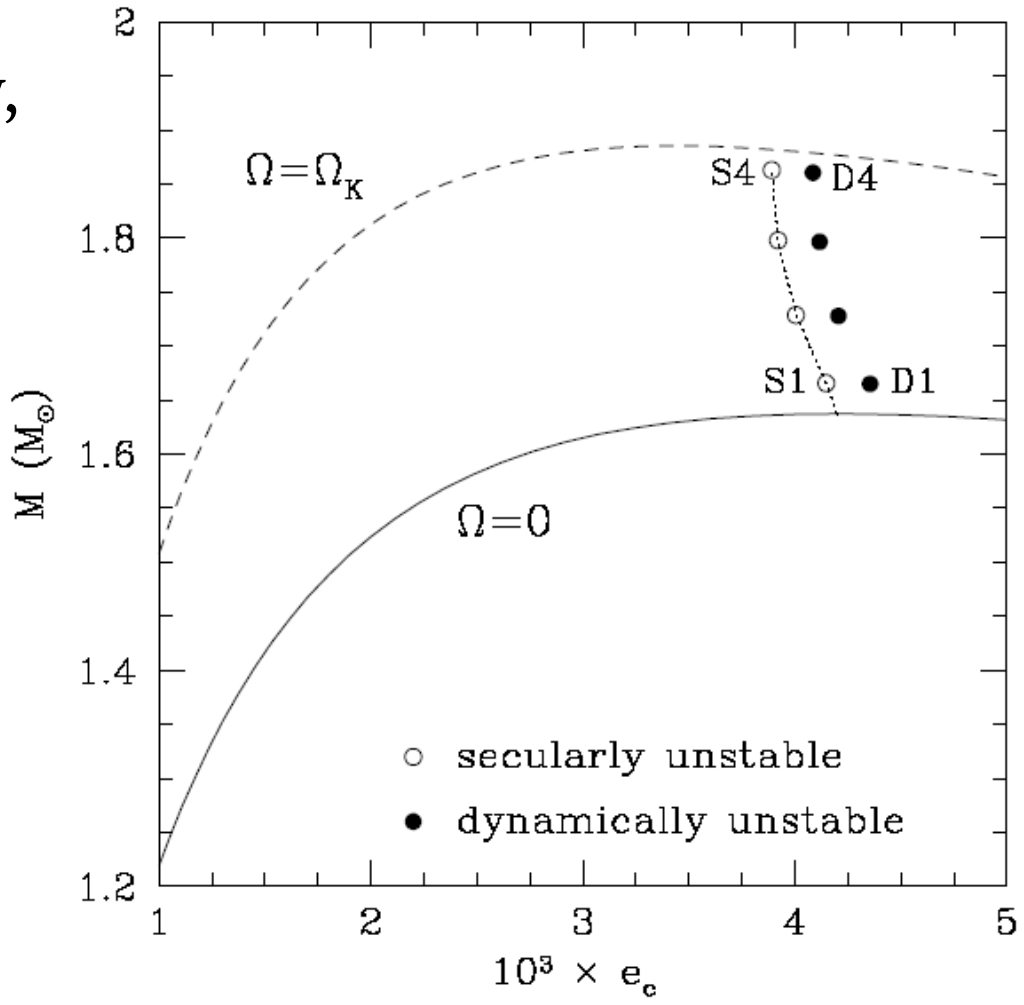

Dynamical instability soon after onset of secular instability.

Axisymmetric Instability to Collapse

Rotating stars are subject to a ***secular*** axisymmetric instability, if:

$$\left(\frac{\partial M}{\partial \epsilon_c}\right)_J < 0$$

(Friedman, Ipser & Sorkin, 1988).

A neutron star can collapse to a Kerr BH during:

a) *Core collapse* of massive star

b) *Accretion-induced collapse*

c) *Binary neutron star merger*

d) *Spin-down* of a supramassive pulsar

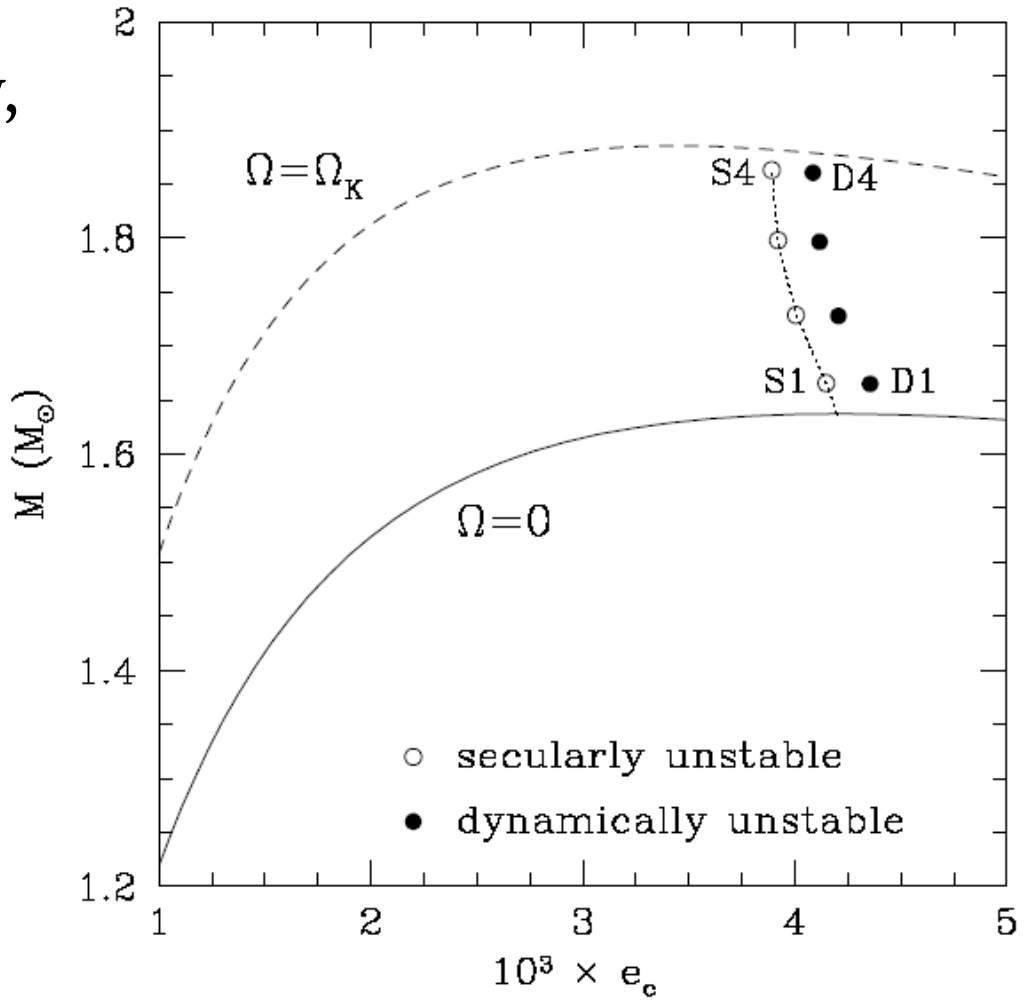

Dynamical instability soon after onset of secular instability.

Equilibrium Sequences (II)

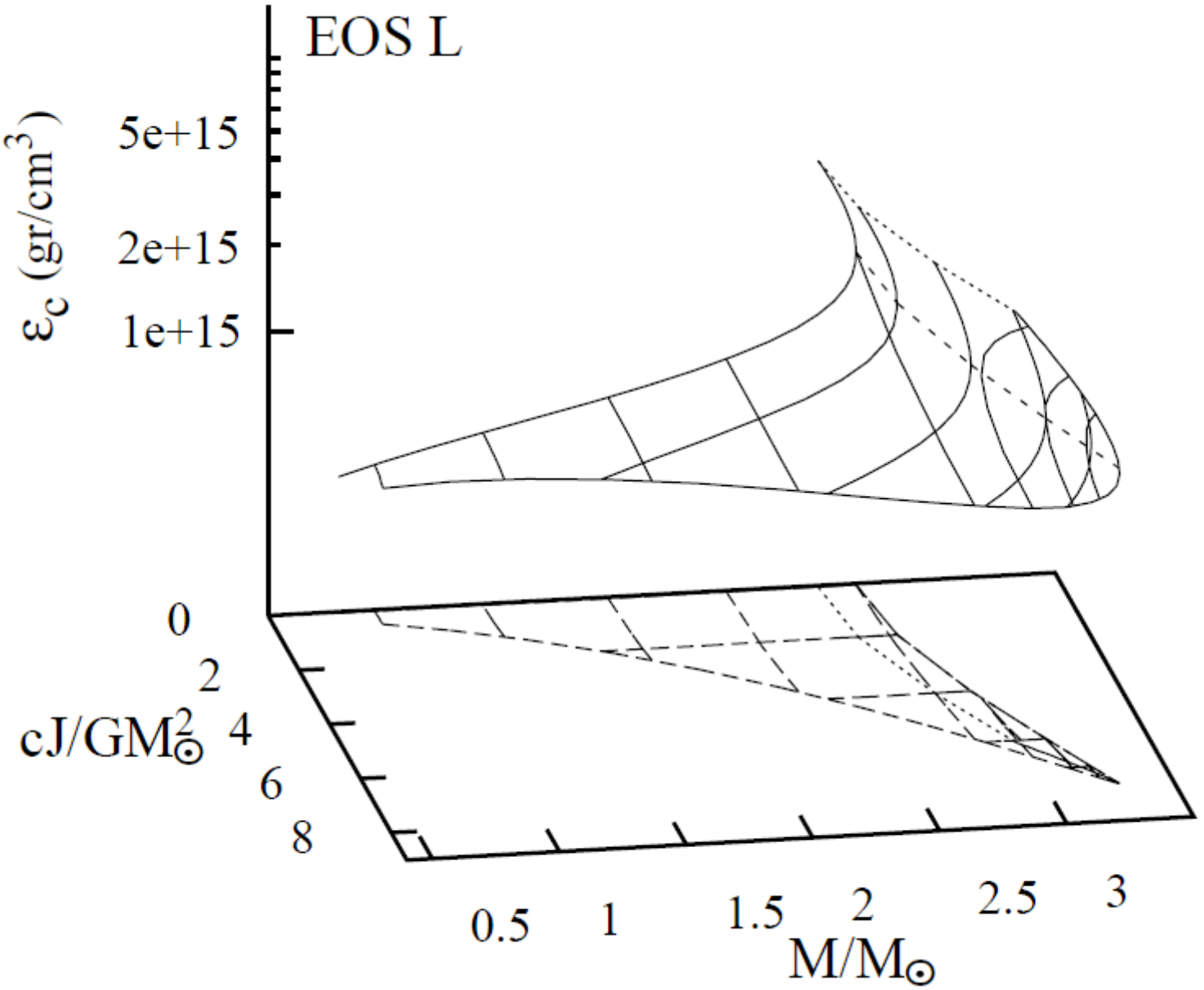

(NS & Friedman 1995)

Differentially Rotating Models

hypermassive stars

Threshold mass

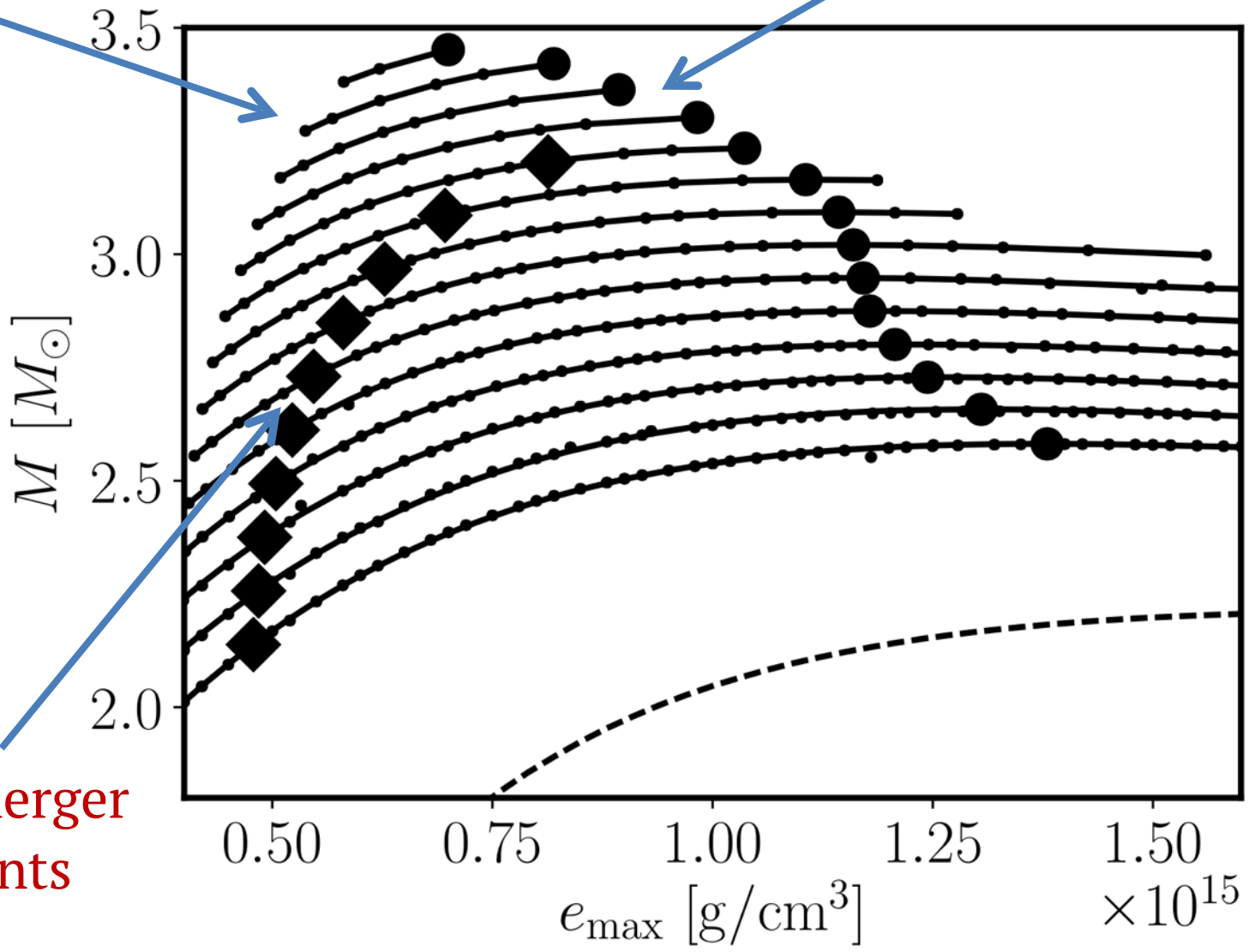

BNS merger remnants

(Bauswein & NS 2017)

Equilibrium neutron star solutions: Scalar-Tensor Theory

Observational constraints

$\alpha_0 < 0.0035$ $(Cassini)$ and $\beta > -4.5$

(Damour & Esposito-Farese (1996,1998), Will (2006), Freire et al (2012), Antoniadis et al (2013))

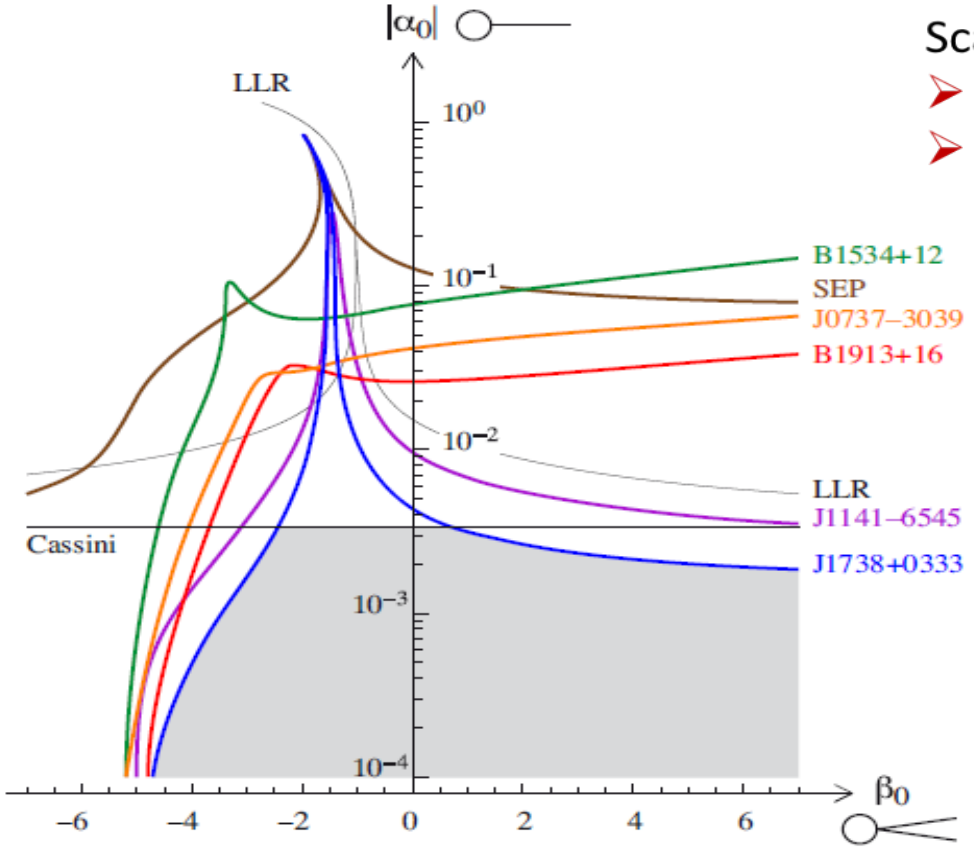

Freire et al (2012)

Scalarized solutions exist only for

- $\beta < -4.35$ in the static case and
- $\beta < -3.9$ in the rapidly rotating case.

Equilibrium neutron star solutions:
Scalar-Tensor Theory

Spontaneous Scalarizarion is possible for β<-4.35 **(Damour+Esposito-Farese 1993)** introducing macroscopically (and observationally) significant modifications to the structure of the star[52].

The solutions become nonunique: for certain ranges of the parameter space: NS solutions in GR coexist with scalarized NSs.

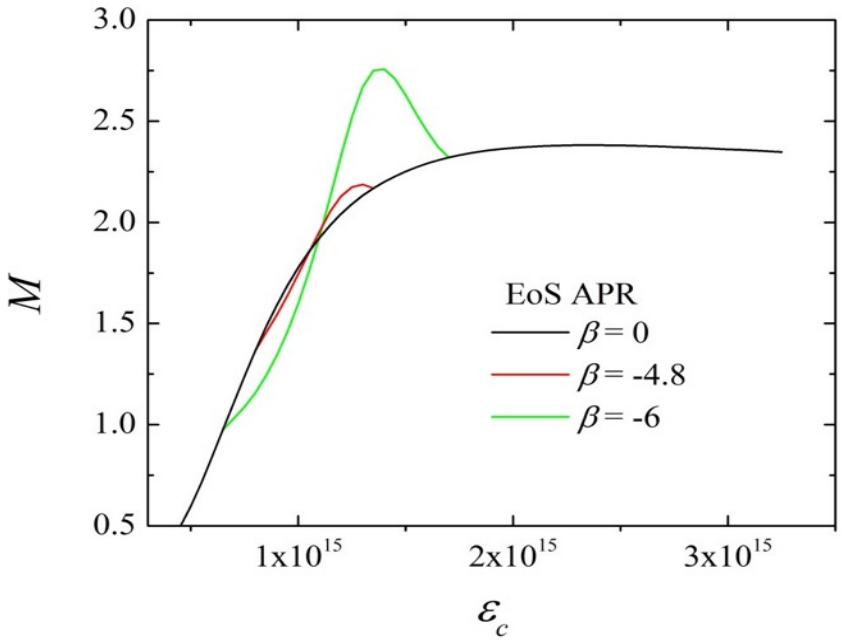

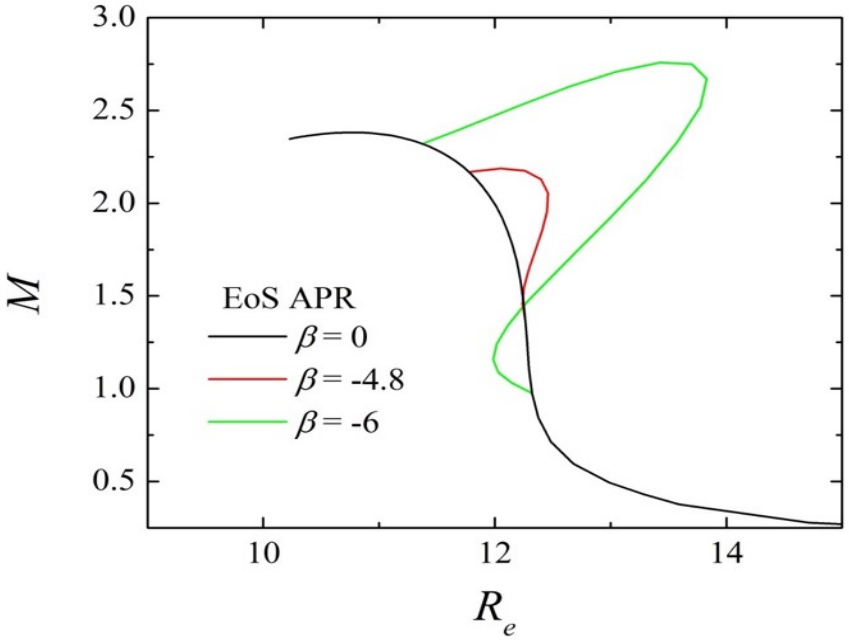

The solutions with nontrivial scalar field are energetically more favorable than their GR counterpart (Harada 1997, Harada 1998, Sotani+Kokkotas 2004).

Rotating stars in scalar-tensor gravity

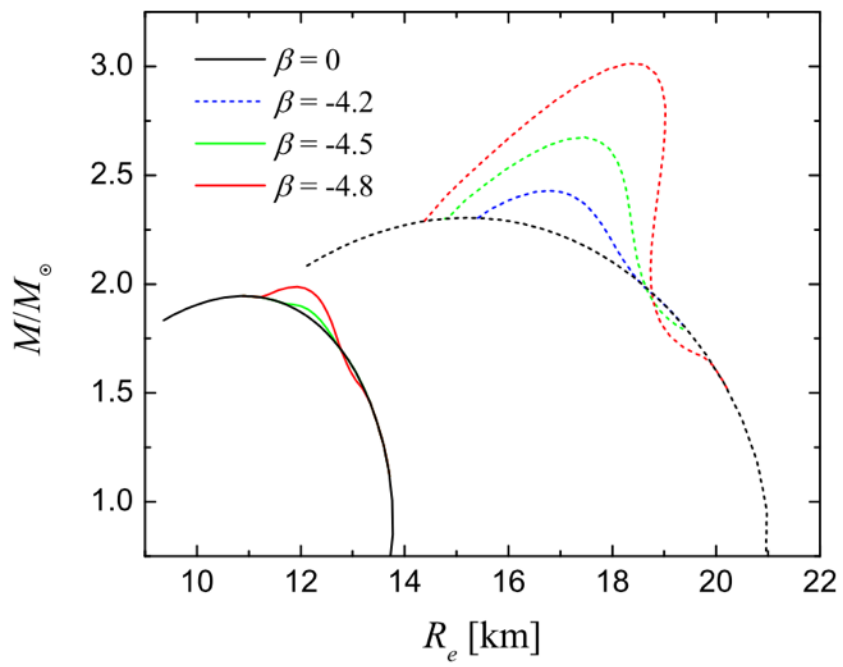

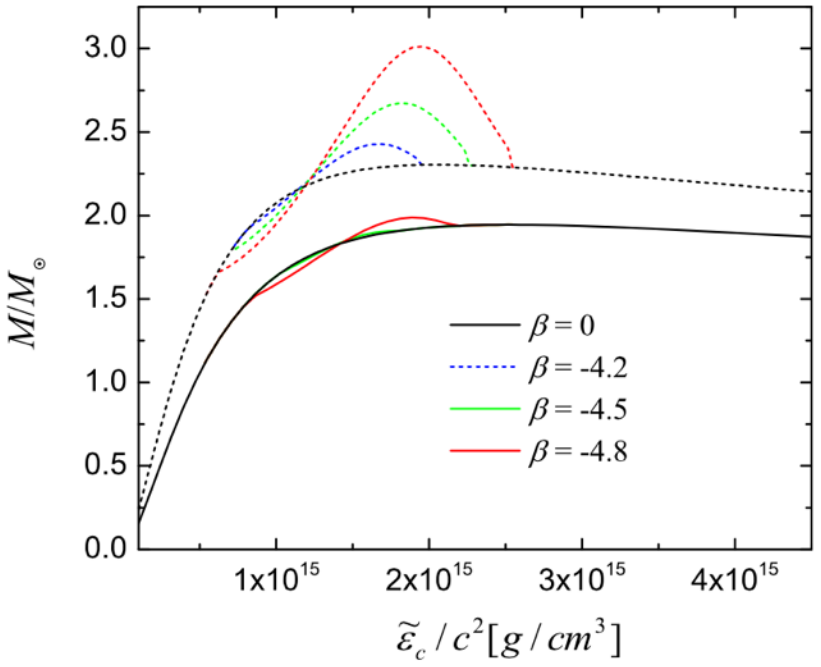

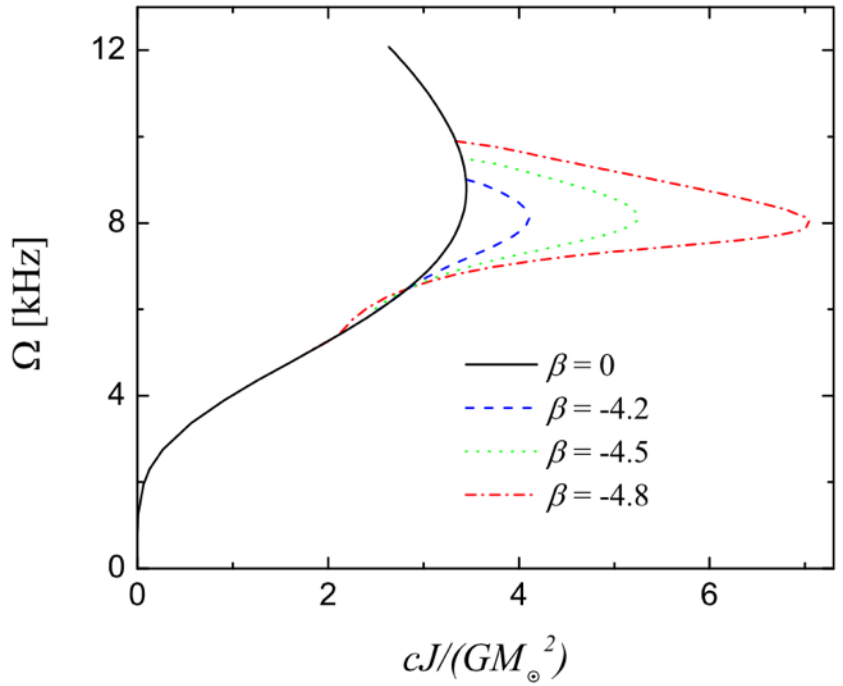

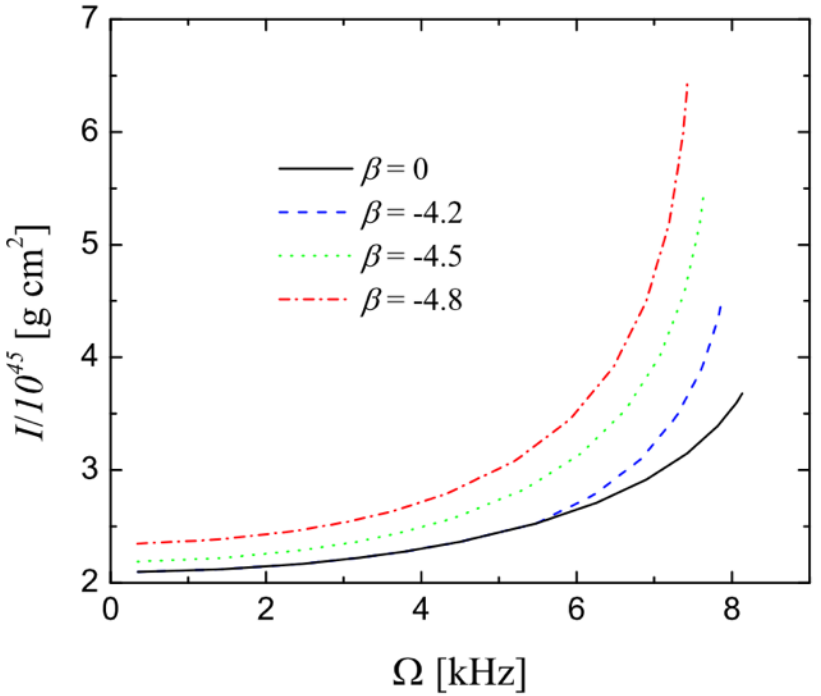

(Doneva, Yazadjiev, NS & Kokkotas, 2013)

Post-TOV approximation

The gravity theory degeneracy problem:

Exists even if we do know the correct equation of state

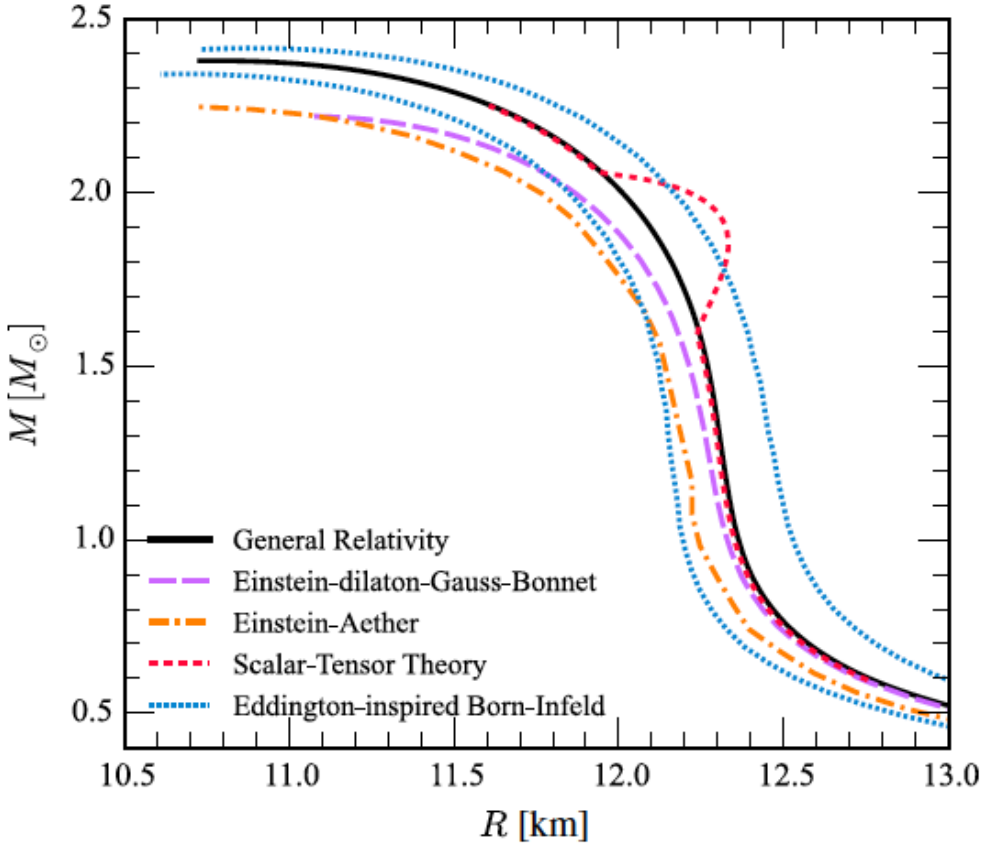

The logic underpinning the formalism is that by parametrizing the deviation of the stellar structure equations from their GR counterparts, thus producing a set of post-TOV equations.

Glampedakis, Pappas, Silva, Berti (2015, 2016)

Post-TOV approximation

Post-TOV equations: *describe smooth modifications of he TOV equations, parametrized by the post-TOV parameters*

$$\frac{dp}{dr} = \left(\frac{dp}{dr}\right)_{\rm GR} - \frac{\rho m}{r^2}\mathcal{P} \qquad \frac{dm}{dr} = \left(\frac{dm}{dr}\right)_{\rm GR} + 4\pi r^2 \rho \mathcal{M}$$

where

$$\mathcal{P} \equiv \pi_1 \frac{m^3}{r^5\rho} + \pi_2 \frac{m^2}{r^2} + \pi_3 r^2 p + \pi_4 \frac{\Pi p}{\rho}$$

$$\mathcal{M} \equiv \mu_1 \frac{m^3}{r^5\rho} + \mu_2 \frac{m^2}{r^2} + \mu_3 r^2 p + \mu_4 \frac{\Pi p}{\rho} + \mu_5 \frac{\Pi^3 r}{m}$$

Glampedakis, Pappas, Silva, Berti (2015, 2016)

Astrophysical Implications

Dynamical scalarization – NS mergers

Even if the two NS are not scalarized when separated, in close binary system they **develop strong scalar field**.

Coupling function $\alpha(\varphi) = \beta\varphi$

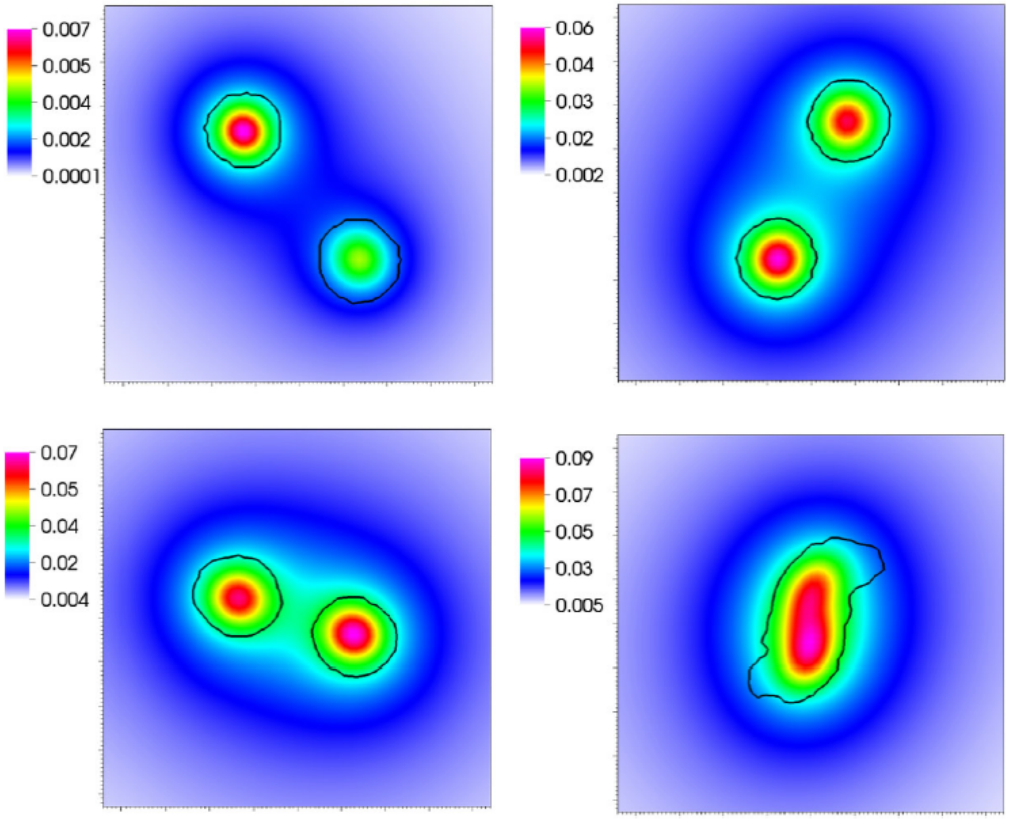

The observational signature of the scalarized merging neutron stars has been studied in Barause et al (2013), Palenzuela et al (2014), Shibata et al (2014), Sampson (2014), Taniguchi et al (2015).

Post-Merger Gravitational Waves

The GW signal can be divided into three distinct phases: *inspiral*, *merger* and *post-merger ringdown*.

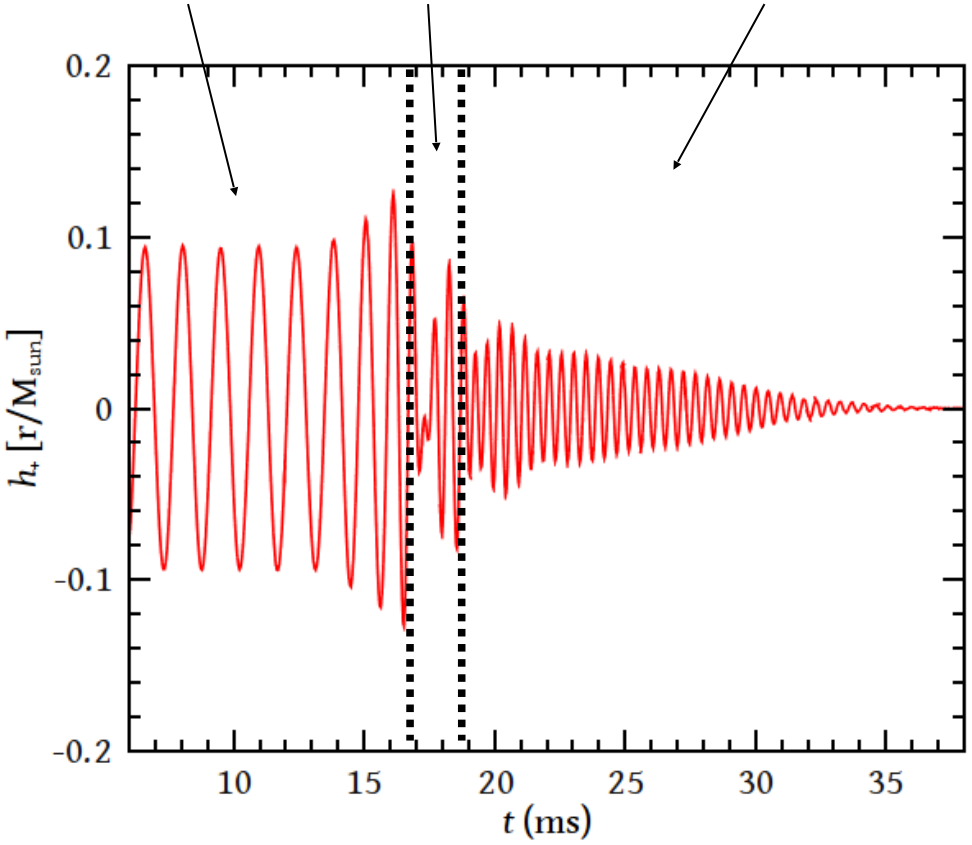

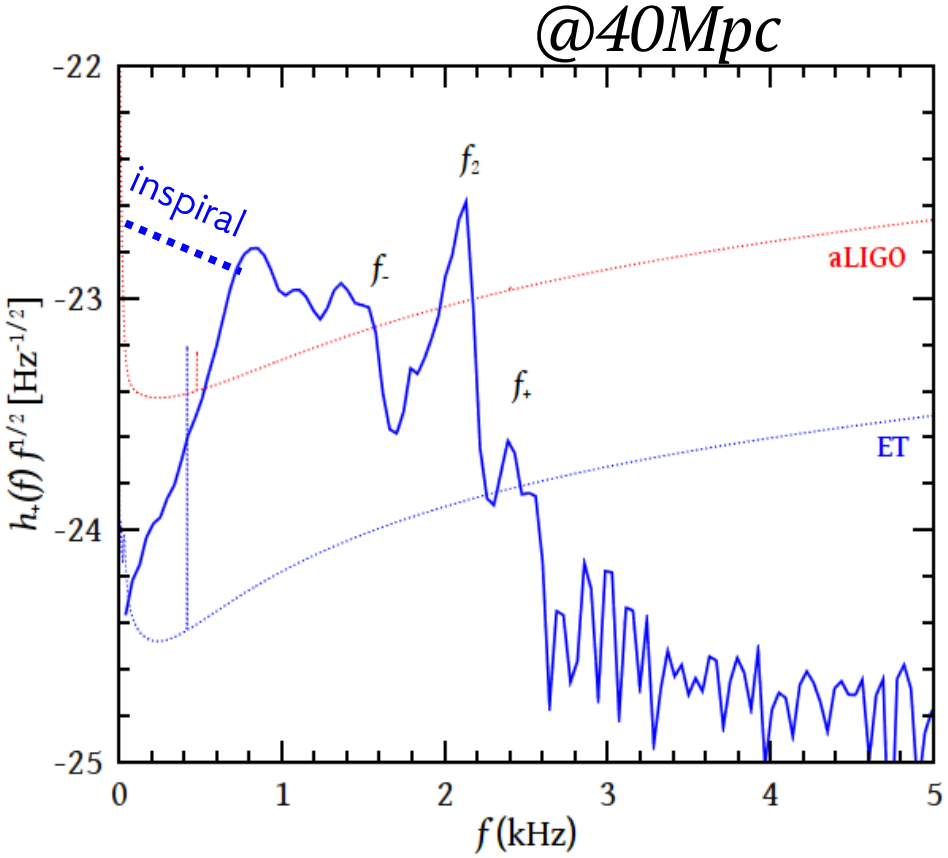

Several peaks stand above the aLIGO/VIRGO or ET sensitivity curves and are potentially detectable. Are these *oscillations* of the HMNS?

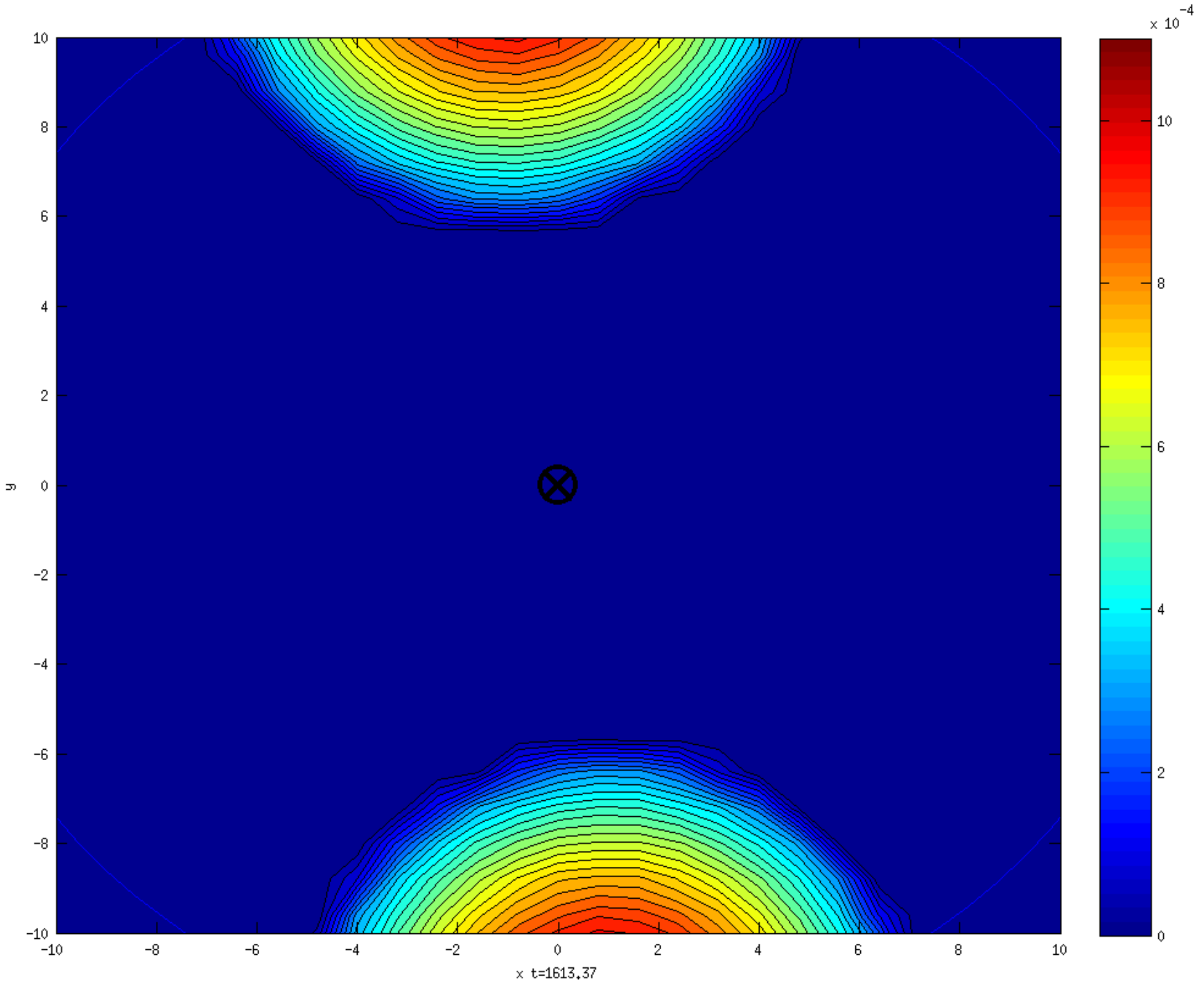
x 10^-4
10
8
6
4
2
0
-2
-4
-6
-8
-10
y
-10
-8
-6
-4
-2
0
2
4
6
8
10
x t=1613.37

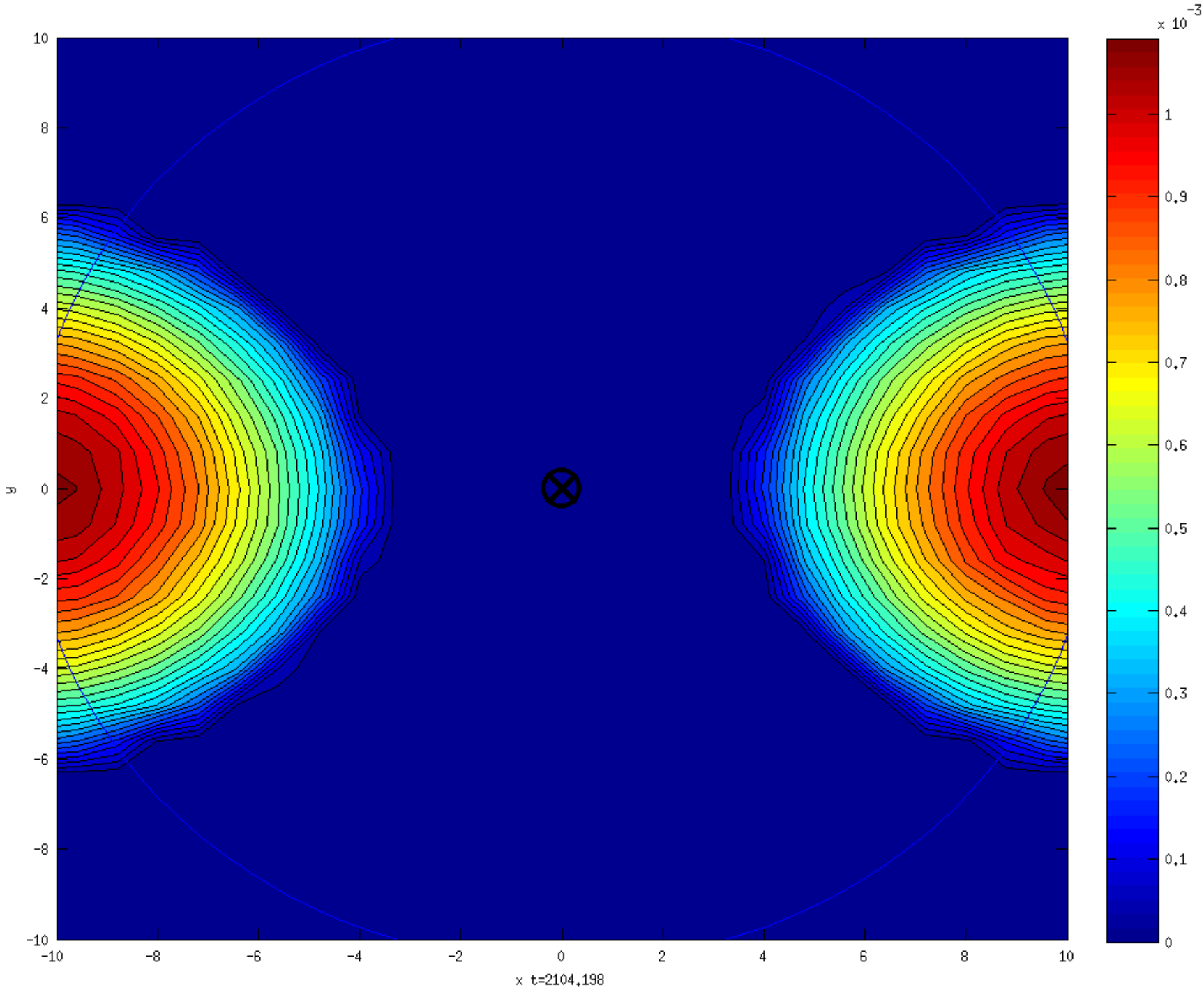
x 10^-3
1
0.9
0.8
0.7
0.6
0.5
0.4
0.3
0.2
0.1
0
10
8
6
4
2
0
-2
-4
-6
-8
-10
y
-10
-8
-6
-4
-2
0
2
4
6
8
10
x t=2104.198

Equal mass: Lattimer-Swesty 1.35+1.35

GRAVITATIONAL WAVES

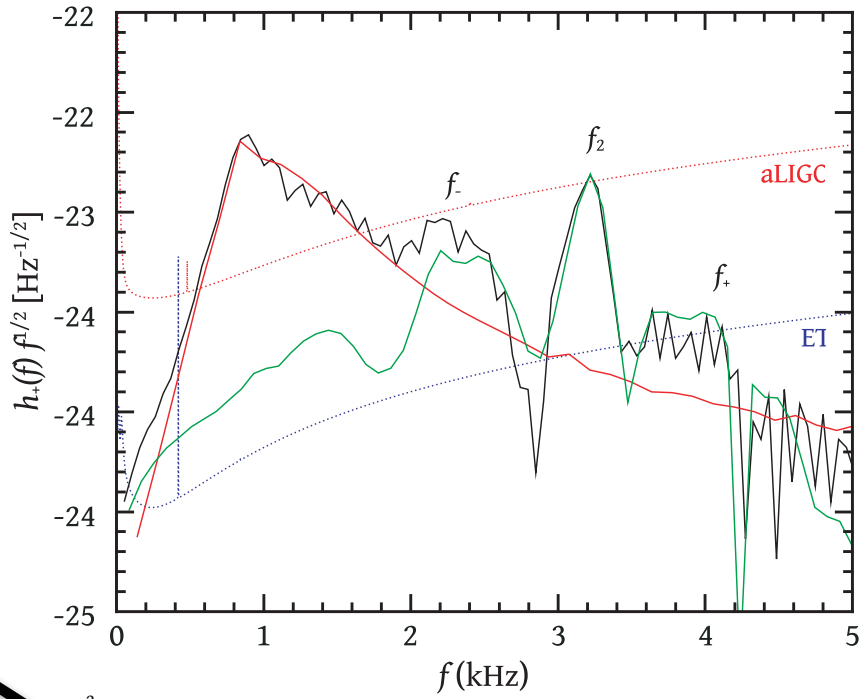

m=0 radial mode

m=2 quadrupole mode

HYDRODYNAMICS

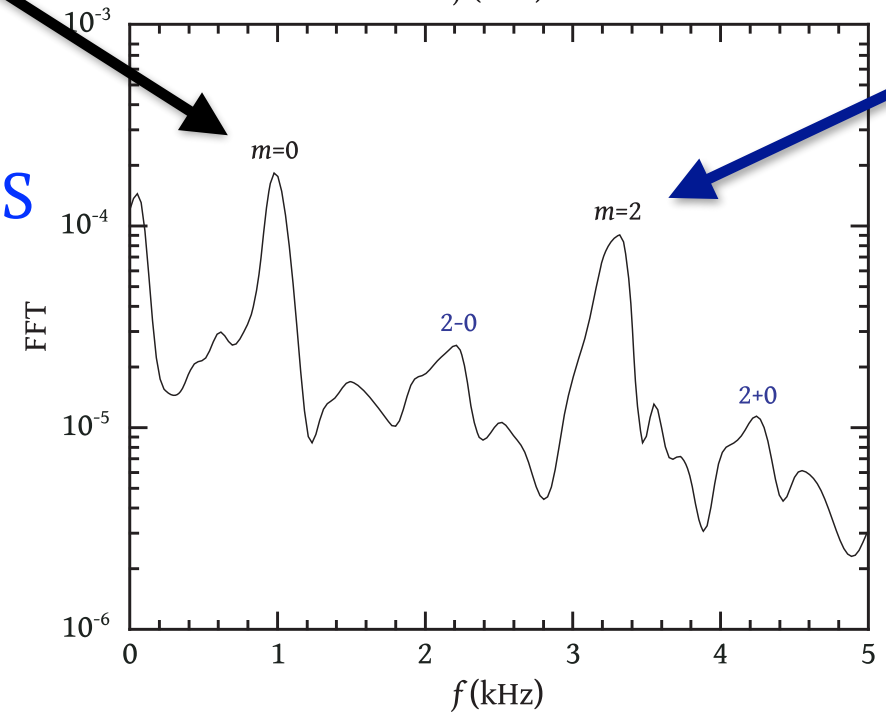

Equal mass: Lattimer-Swesty 1.35+1.35

GRAVITATIONAL WAVES

HYDRODYNAMICS

m=0 radial mode

m=2 quadrupole mode

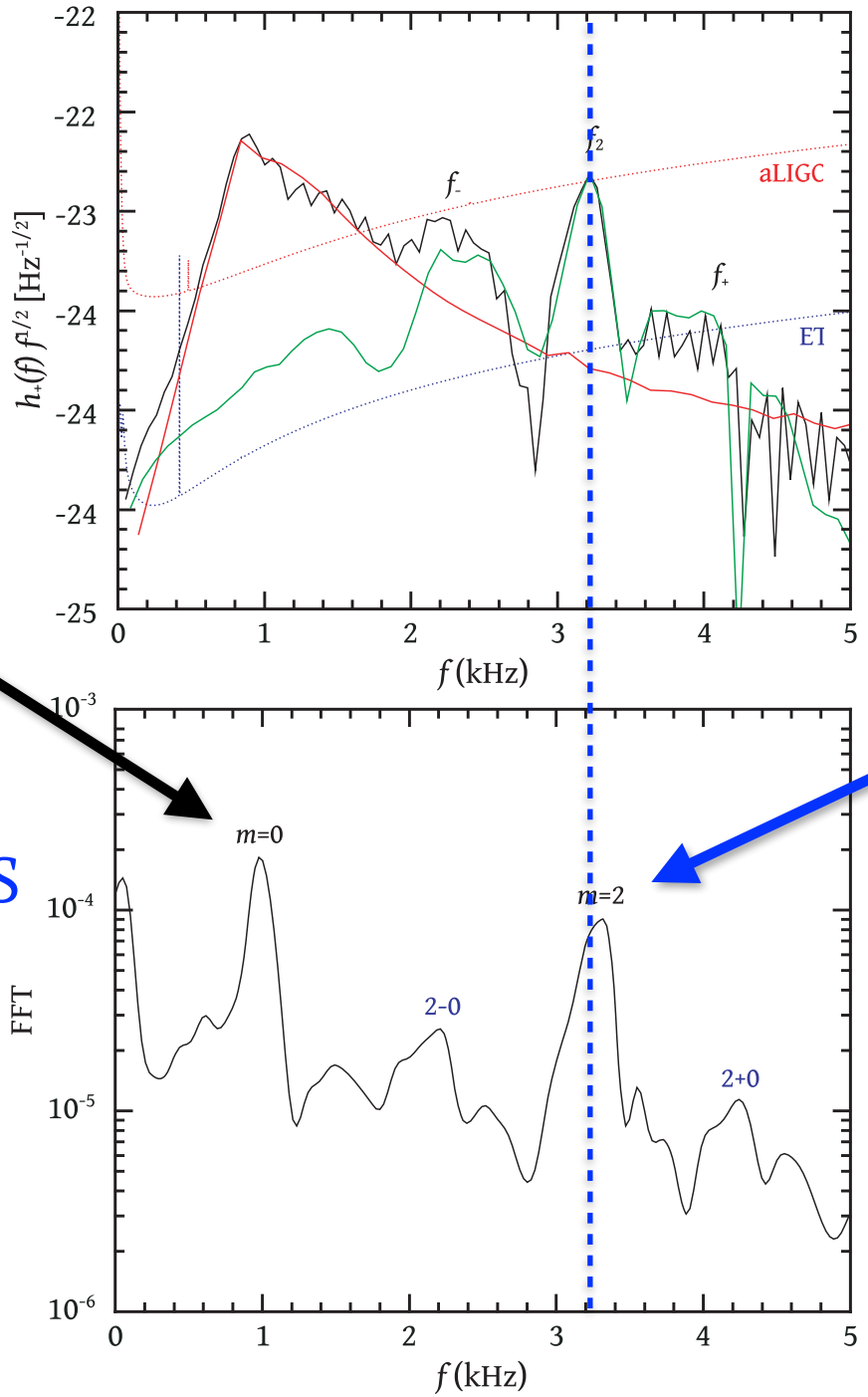

Equal mass: Lattimer-Swesty 1.35+1.35

GRAVITATIONAL WAVES

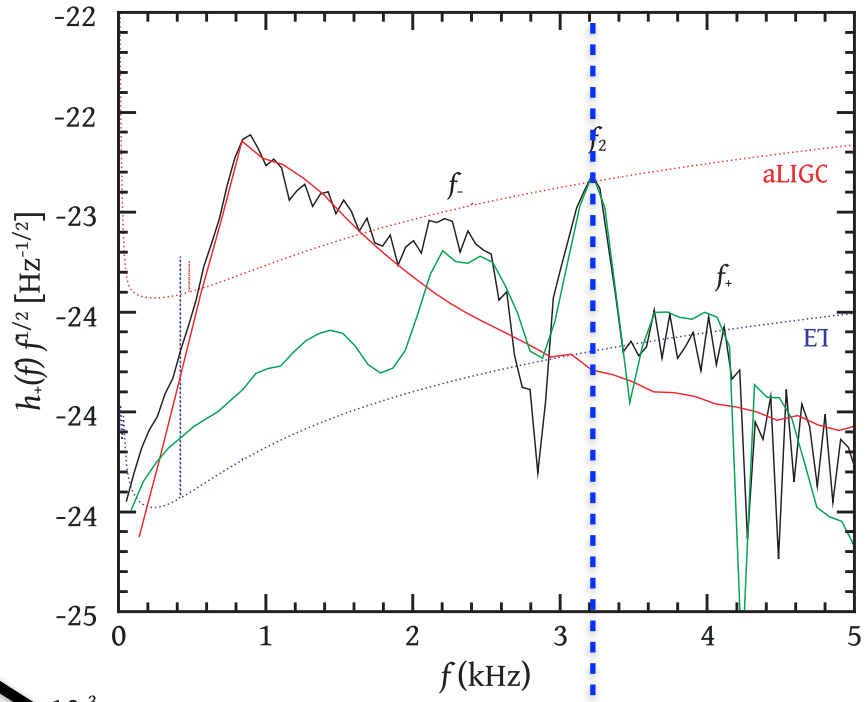

m=0 radial mode

HYDRODYNAMICS

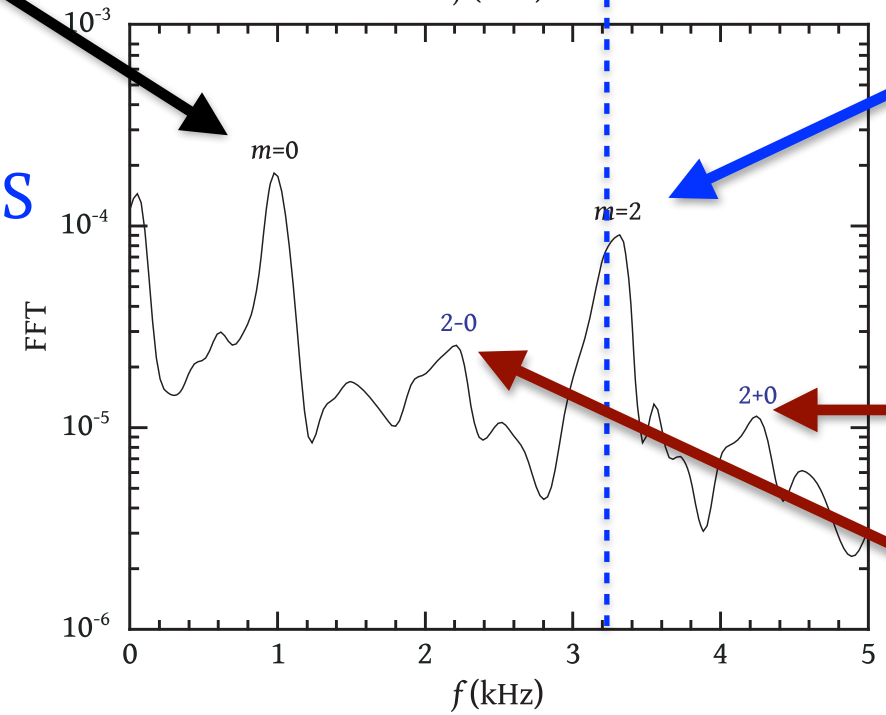

m=2 quadrupole mode

"2-0" and "2+0" quasi-linear combination frequency

Equal mass: Lattimer-Swesty 1.35+1.35

GRAVITATIONAL WAVES

HYDRODYNAMICS

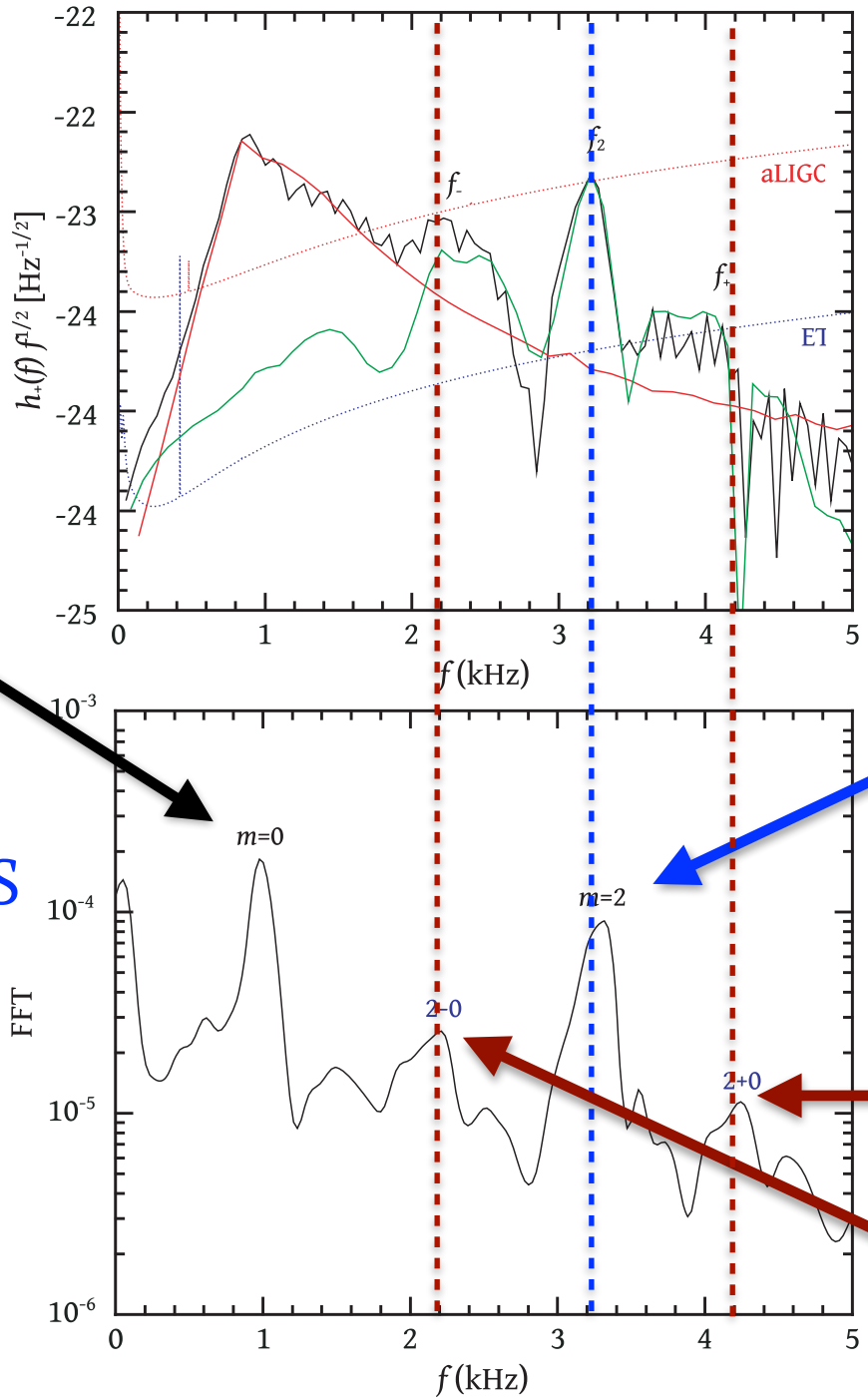

m=0 radial mode

m=2 quadrupole mode

"2-0" and "2+0" quasi-linear combination frequency

Radial Oscillations

Consider first a spherical Newtonian star, with radius *R*. The mass contained within an internal radius *r* is $\mathcal{M}_r$.

The conservation of mass (continuity) and momentum are

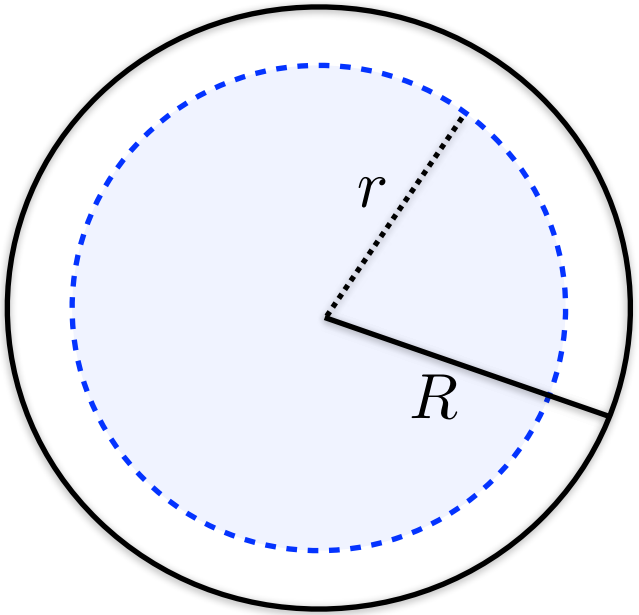

$$\frac{\partial \mathcal{M}_r}{\partial r} = 4\pi r^2 \rho$$

$$\ddot{r} = -4\pi r^2 \left(\frac{\partial P}{\partial \mathcal{M}_r}\right) - \frac{G\mathcal{M}_r}{r^2}$$

Radial Oscillations

Consider first a spherical Newtonian star, with radius *R*. The mass contained within an internal radius *r* is $\mathcal{M}_r$.

The conservation of mass (continuity) and momentum are

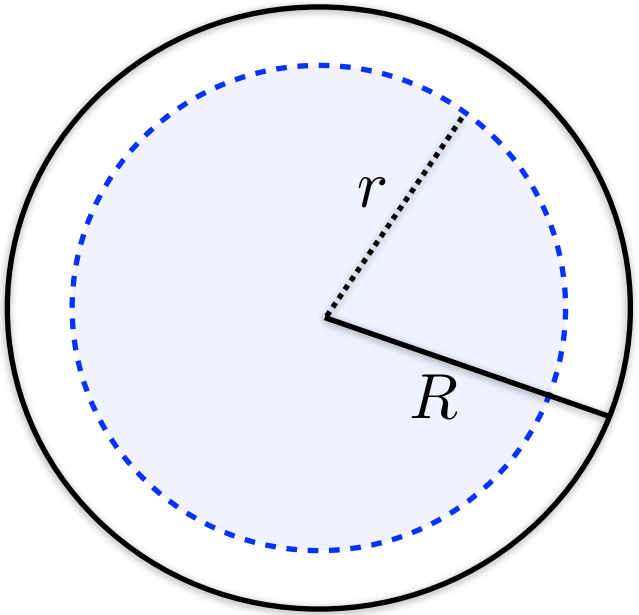

$$\frac{\partial \mathcal{M}_r}{\partial r} = 4\pi r^2 \rho$$

$$\ddot{r} = -4\pi r^2 \left(\frac{\partial P}{\partial \mathcal{M}_r}\right) - \frac{G\mathcal{M}_r}{r^2}$$

Next, consider small *Lagrangian perturbations*

$$|\delta r / r_0| \ll 1 \text{ and } |\delta\rho/\rho_0| \ll 1$$

Then

$$\frac{\delta\rho}{\rho_0} = -3\,\frac{\delta r}{r_0} - r_0\,\frac{\partial\,(\delta r/r_0)}{\partial r_0}$$

$$\rho_0 r_0\,\frac{d^2\,\delta r/r_0}{dt^2} = -\left(4\,\frac{\delta r}{r_0} + \frac{\delta P}{P_0}\right)\frac{\partial P_0}{\partial r_0} - P_0\frac{\partial\,(\delta P/P_0)}{\partial r_0}$$

Radial Oscillations

If we assume a *harmonic time dependence*

$$\frac{\delta r(t, r_0)}{r_0} = \frac{\delta r(r_0)}{r_0} e^{i\sigma t} = \zeta(r_0)\, e^{i\sigma t}$$

Then

$$\frac{d\zeta}{dr} = -\frac{1}{r}\left(3\zeta + \frac{1}{\Gamma_1}\frac{\delta P}{P}\right)$$

$$\frac{d\left(\delta P/P\right)}{dr} = -\frac{d\ln P}{dr}\left(4\zeta + \frac{\sigma^2 r^3}{G\mathcal{M}_r}\zeta + \frac{\delta P}{P}\right)$$

Radial Oscillations

If we assume a *harmonic time dependence*

$$\frac{\delta r(t, r_0)}{r_0} = \frac{\delta r(r_0)}{r_0} e^{i\sigma t} = \zeta(r_0)\, e^{i\sigma t}$$

Then

$$\frac{d\zeta}{dr} = -\frac{1}{r}\left(3\zeta + \frac{1}{\Gamma_1}\frac{\delta P}{P}\right)$$

$$\frac{d\left(\delta P/P\right)}{dr} = -\frac{d\ln P}{dr}\left(4\zeta + \frac{\sigma^2 r^3}{G\mathcal{M}_r}\zeta + \frac{\delta P}{P}\right)$$

where $\Gamma_1 = \left(\dfrac{\partial \ln P}{\partial \ln \rho}\right)_{\rm ad}$ is the *adiabatic index* in equilibrium.

We have assumed *adiabatic oscillations*, so that

$$\frac{\delta P}{P_0} = \Gamma_1 \frac{\delta \rho}{\rho_0}$$

Examples

- Assuming *uniform density*, the fundamental mode has ζ = const. and

$$\sigma_0^2 = \frac{4\pi}{3} G\rho(3\Gamma_1 - 4)$$

which reveals a fundamental scaling between frequency and density

$$\sigma \sim \sqrt{\rho} \sim \sqrt{M/R^3}$$

Examples

- Assuming *uniform density*, the fundamental mode has ζ = const. and

$$\sigma_0^2 = \frac{4\pi}{3} G\rho(3\Gamma_1 - 4)$$

which reveals a fundamental scaling between frequency and density

$$\sigma \sim \sqrt{\rho} \sim \sqrt{M/R^3}$$

- For n=2 polytropes, the first three eigenfunctions are:

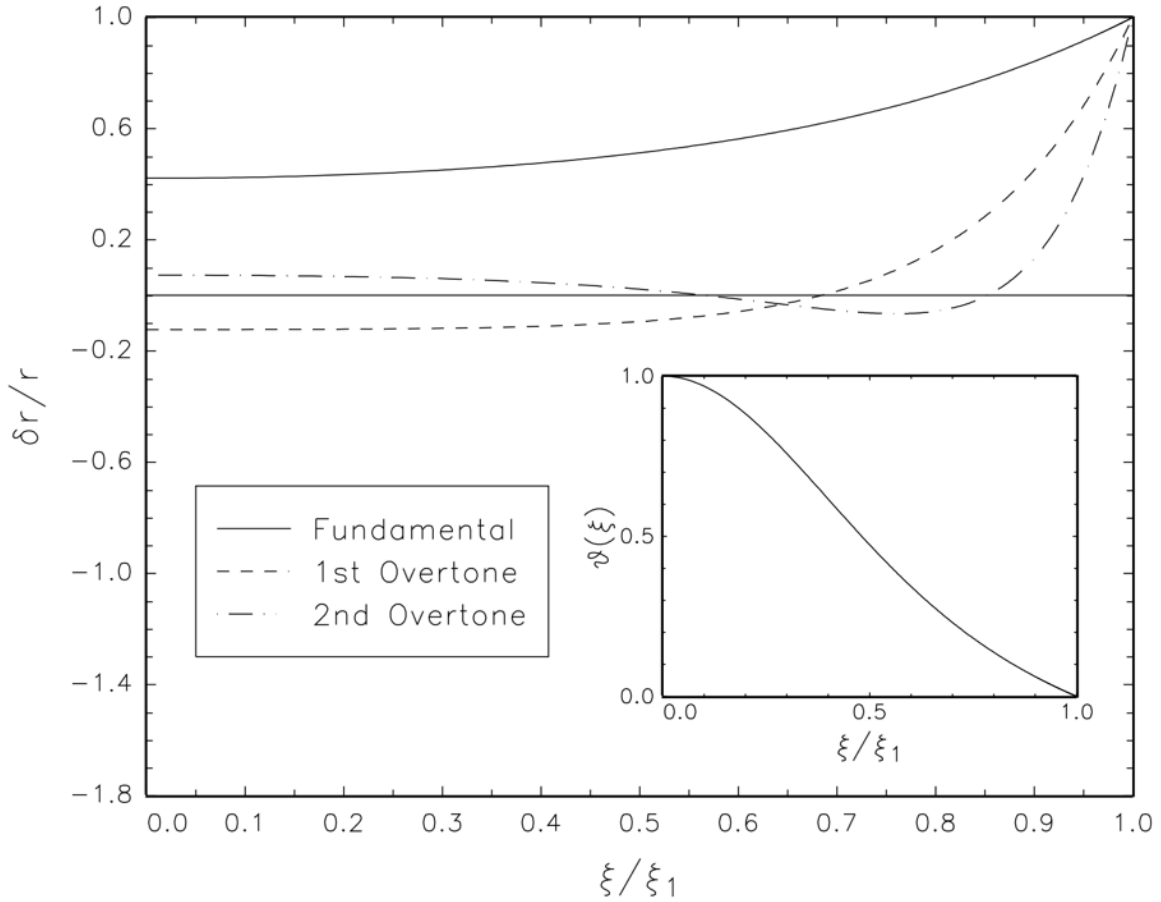

Nonradial Oscillations

For nonradial oscillations, we need to considered the general system of the Poisson equation plus energy and momentum conservation, without symmetries

$$\nabla^2 \Phi = 4\pi G\rho$$

$$\frac{\partial \rho}{\partial t} + \boldsymbol{\nabla} \bullet (\rho \mathbf{v}) = 0$$

$$\rho \left(\frac{\partial}{\partial t} + \mathbf{v} \bullet \boldsymbol{\nabla} \right) \mathbf{v} = -\boldsymbol{\nabla} P - \rho \boldsymbol{\nabla} \Phi$$

Nonradial Oscillations

For nonradial oscillations, we need to considered the general system of the Poisson equation plus energy and momentum conservation, without symmetries

$$\nabla^2 \Phi = 4\pi G\rho$$

$$\frac{\partial \rho}{\partial t} + \boldsymbol{\nabla} \bullet (\rho \mathbf{v}) = 0$$

$$\rho \left(\frac{\partial}{\partial t} + \mathbf{v} \bullet \boldsymbol{\nabla} \right) \mathbf{v} = -\boldsymbol{\nabla} P - \rho \, \boldsymbol{\nabla} \Phi$$

The displacement vector with harmonic time dependence

$$\boldsymbol{\xi}(\mathbf{r}, t) = \boldsymbol{\xi}(\mathbf{r})\, e^{i\sigma t}$$

is then decomposed in terms of spherical harmonics as

$$\begin{aligned} \boldsymbol{\xi}(r, \theta, \varphi) &= \xi_r(r, \theta, \varphi)\, \mathbf{e}_{\boldsymbol{r}} + \xi_\theta(r, \theta, \varphi)\, \mathbf{e}_{\boldsymbol{\theta}} + \xi_\varphi(r, \theta, \varphi)\, \mathbf{e}_{\boldsymbol{\varphi}} \\ &= \left[\xi_r(r)\, \mathbf{e}_{\boldsymbol{r}} + \xi_t(r)\, \mathbf{e}_{\boldsymbol{\theta}} \frac{\partial}{\partial \theta} + \xi_t(r)\, \mathbf{e}_{\boldsymbol{\varphi}} \frac{1}{\sin\theta} \frac{\partial}{\partial \varphi} \right] Y_{\ell m}(\theta, \varphi) \end{aligned}$$

Nonradial Oscillations

Notice that

$$Y_{\ell m}(\theta,\varphi) = \sqrt{\frac{2\ell+1}{4\pi}\frac{(\ell-m)!}{(\ell+m)!}}\, P_\ell^m(\cos\theta)\, e^{im\varphi}$$

The Eulerian perturbation in the density is

$$\rho'(r,\theta,\phi,t) = \rho'(r) Y_{lm}(\theta,\phi) e^{i\sigma t}$$

The perturbed system of equations is of 4th order (because of the perturbation in Φ) and admits normal mode solutions that are characterized by the spherical harmonic indices *l*, *m* and the radial order *n*.

Nonradial Oscillations

Notice that

$$Y_{\ell m}(\theta,\varphi) = \sqrt{\frac{2\ell+1}{4\pi}\frac{(\ell-m)!}{(\ell+m)!}}\, P_\ell^m(\cos\theta)\, e^{im\varphi}$$

The Eulerian perturbation in the density is

$$\rho'(r,\theta,\phi,t) = \rho'(r) Y_{lm}(\theta,\phi) e^{i\sigma t}$$

The perturbed system of equations is of 4th order (because of the perturbation in Φ) and admits normal mode solutions that are characterized by the spherical harmonic indices *l*, *m* and the radial order *n*.

A general perturbation in the density is then

$$\rho'(r,\theta,\phi,t) = \sum_l^\infty \sum_m^\infty \sum_n^\infty a_{lmn}\rho'_n(r) P_l^m(\theta,\phi) e^{i(\sigma_{lmn}t + m\phi)}$$

(but only the *m*=0 case is relevant for spherical stars).

Nonradial Oscillations

$\ell = 0$

$\ell = 1$

$\ell = 2$

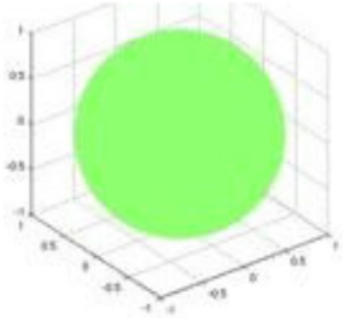

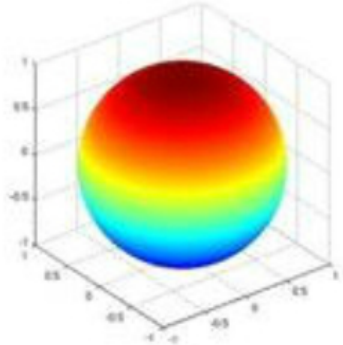

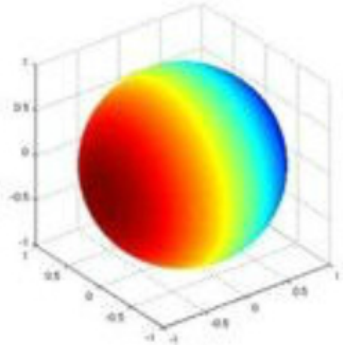

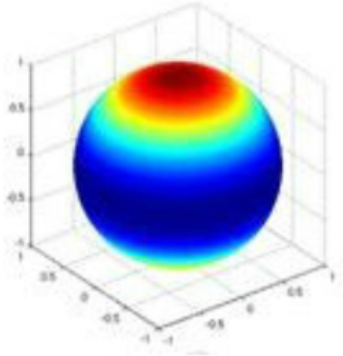

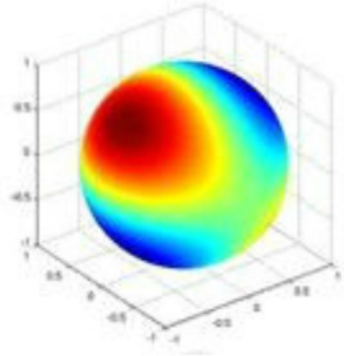

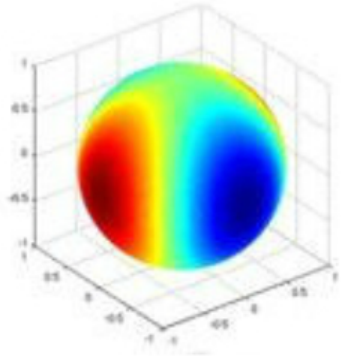

$m = 0$ (zonal)

$m = 1$

$m = 2$

$$\cos(m\phi)\ P_\ell^m(\cos\theta)$$

$l = m$ (sectoral)

$l \neq m$ (tesseral)

Nonradial Oscillations of Neutron Stars

Main oscillation modes:

1. *f*-modes / *p*-modes

   fluid modes restored by pressure

2. *g*-modes

   restored by gravity/buoyancy in non-isentropic stars

3. inertial modes (*r*-modes)

   restored by the Coriolis force in rotating stars

4. *w*-modes

   spacetime modes (similar to black hole modes)

GW-detection: *f*-, *p*-, *g*-, *r*-modes : stable oscillations

instabilities

Mode Excitation

Various ways to excite modes:

1. Core collapse
2. Binary merger (if HMNS forms)
3. Star quakes (e.g. SGR activity)
4. Secular instabilities (*f*-modes, *r*-modes)
5. Dynamical instabilities (bar-mode, $T/W > 0.27$)
6. Low T/W instabilities

Frequency and Pattern Speed

For a nonrotating, uniform density star the *f*-mode frequency is

$$\omega^2 = \frac{2l(l-1)}{2l+1}\frac{GM}{R^3}$$

For *l* = 2, this is ~2 kHz for a typical neutron star.

Frequency and Pattern Speed

For a nonrotating, uniform density star the *f*-mode frequency is

$$\omega^2 = \frac{2l(l-1)}{2l+1}\frac{GM}{R^3}$$

For *l* = 2, this is ~2 kHz for a typical neutron star.

Since oscillations are proportional to $e^{i\omega t + m\phi}$, surfaces of constant phase correspond to

$$m\phi + \omega t = \text{const.} \quad \Rightarrow \quad \frac{d\phi}{dt} = -\frac{\omega}{m} := \omega_p$$

which defines the pattern speed, with which a mode revolves around the star (notice that the *m* = 0 modes are standing waves).

Nonradial Oscillations of Relativistic Stars

In GR, nonradial oscillations with l > 1 radiate gravitational waves and modes become quasi-normal, acquiring an imaginary part.

$$\omega = \sigma + \frac{i}{\tau_{\mathrm{GW}}}$$

The spacetime metric is perturbed as

$$\begin{aligned} ds^2 = &- e^{2\nu}\left(1 + r^l H_0^{lm} Y_{lm} e^{i\omega t}\right) dt^2 - 2i\omega r^{l+1} H_1^{lm} Y_{lm} e^{i\omega t} dt dr \\ &+ e^{2\lambda}\left(1 - r^l H_0^{lm} Y_{lm} e^{i\omega t}\right) dr^2 + r^2\left(1 - r^l K^{lm} Y_{lm} e^{i\omega t}\right)\left(d\theta^2 + \sin^2\theta d\phi^2\right) \end{aligned}$$

and the displacement vector is

$$\begin{aligned} \xi_r &= e^{\lambda} r^{l-1} W^{lm} Y_{lm} e^{i\omega t}, \\ \xi_\theta &= -r^l V^{lm} \partial_\theta Y_{lm} e^{i\omega t}, \\ \xi_\phi &= -r^l V^{lm} \partial_\phi Y_{lm} e^{i\omega t}, \end{aligned}$$

Quasi-normal Modes

The perturbation in the energy density is

$$\delta\varepsilon = r^l \delta\varepsilon^{lm} Y_{lm} e^{i\omega t}$$

A useful redefinition of variables is

$$X^{lm} = \omega^2(\varepsilon + p)e^{-\nu}V^{lm} - \frac{1}{r}\frac{dp}{dr}e^{\nu-\lambda}W^{lm} + \frac{e^{\nu}}{2}(\varepsilon + p)H_0^{lm}$$

One then arrives at a 4th-order system of equations that can be solved for arbitrary complex eigenfrequencies (mathing to BH perturbations in the exterior), which includes both incoming and outgoing gravitational waves.

Quasi-normal Modes

The perturbation in the energy density is

$$\delta\varepsilon = r^l \delta\varepsilon^{lm} Y_{lm} e^{i\omega t}$$

A useful redefinition of variables is

$$X^{lm} = \omega^2(\varepsilon + p)e^{-\nu}V^{lm} - \frac{1}{r}\frac{dp}{dr}e^{\nu-\lambda}W^{lm} + \frac{e^{\nu}}{2}(\varepsilon + p)H_0^{lm}$$

One then arrives at a 4th-order system of equations that can be solved for arbitrary complex eigenfrequencies (mathing to BH perturbations in the exterior), which includes both incoming and outgoing gravitational waves.

A discrete set of *quasi-normal modes* is obtained by requiring *purely outgoing* gravitational waves.

The Perturbed System for Spherical Stars

$$H_1^{lm\prime} = -\frac{1}{r}\left[l+1+\frac{2me^{2\lambda}}{r}+4\pi r^2 e^{2\lambda}(p-\epsilon)\right]H_1^{lm} + \frac{e^{2\lambda}}{r}\left[H_0^{lm}+K^{lm}-16\pi(\epsilon+p)V^{lm}\right],$$

$$K^{lm\prime} = \frac{1}{r}H_0^{lm}+\frac{l(l+1)}{2r}H_1^{lm}-\left[\frac{l+1}{r}-\nu'\right]K^{lm}-8\pi(\epsilon+p)\frac{e^{\lambda}}{r}W^{lm},$$

$$W^{lm\prime} = -\frac{l+1}{r}W^{lm}+re^{\lambda}\left[\frac{e^{-\nu}}{\upsilon_s^2(\epsilon+p)}X^{lm}-\frac{l(l+1)}{r^2}V^{lm}+\frac{1}{2}H_0^{lm}+K^{lm}\right],$$

$$X^{lm\prime} = -\frac{l}{r}X^{lm}+\frac{(\epsilon+p)e^{\nu}}{2}\left\{\left(\frac{1}{r}-\nu'\right)H_0^{lm}+\left(r\omega^2e^{-2\nu}+\frac{l(l+1)}{2r}\right)H_1^{lm} + \left(3\nu'-\frac{1}{r}\right)K^{lm}-\frac{2l(l+1)}{r^2}\nu'V^{lm} -\frac{2}{r}\left[4\pi(\epsilon+p)e^{\lambda}+\omega^2e^{\lambda-2\nu}-\frac{r^2}{2}\left(\frac{2e^{-\lambda}}{r^2}\nu'\right)'\right]W^{lm}\right\},$$

Eigenfunction of Quadrupole Oscillation

Typical example of the eigenfunction $\delta\rho(r, \theta)$ for the $l = 2$ mode:

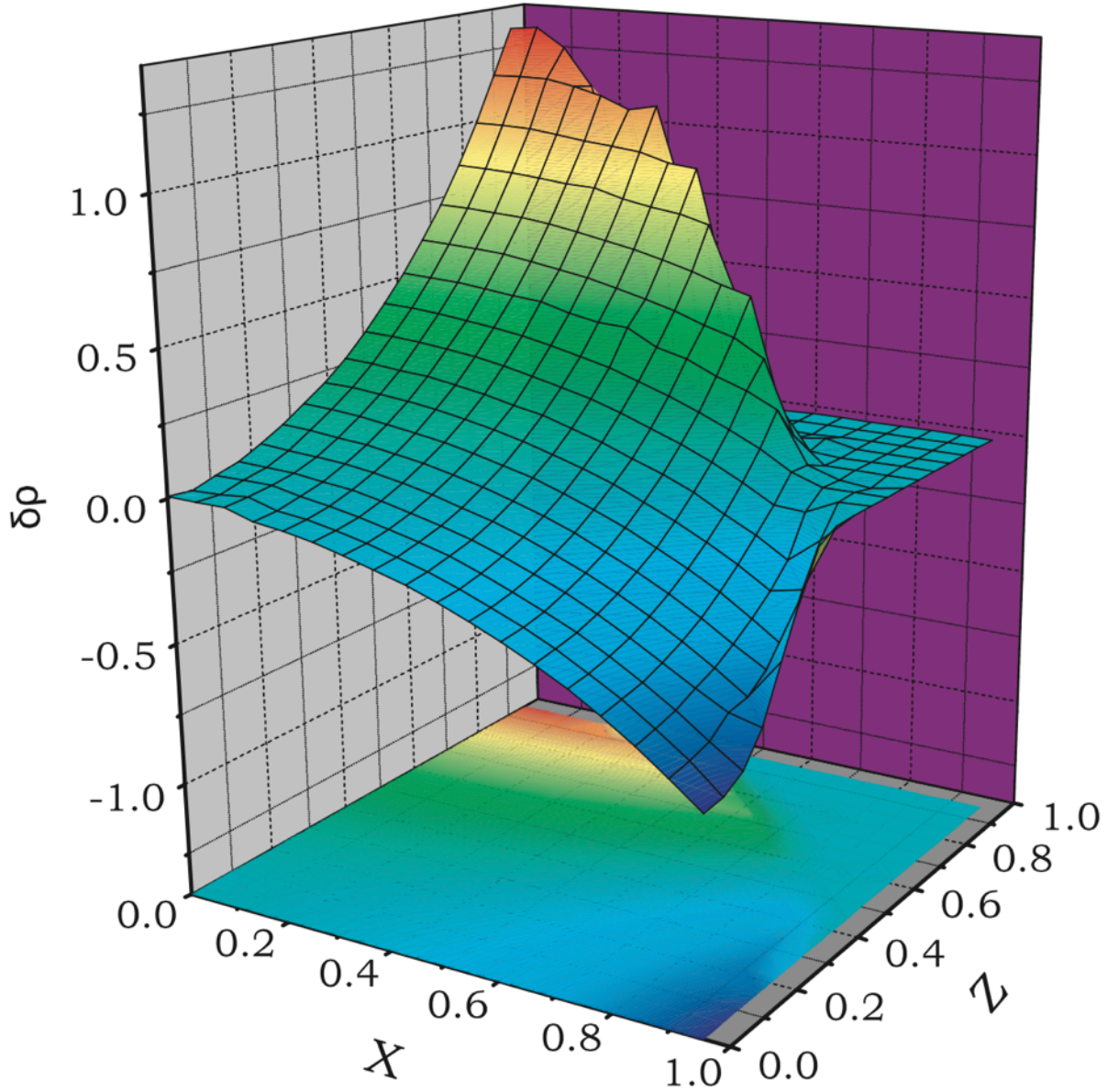

NS, Apostolatos & Font (2004)

Quadrupole Frequencies for Nonrotating Stars

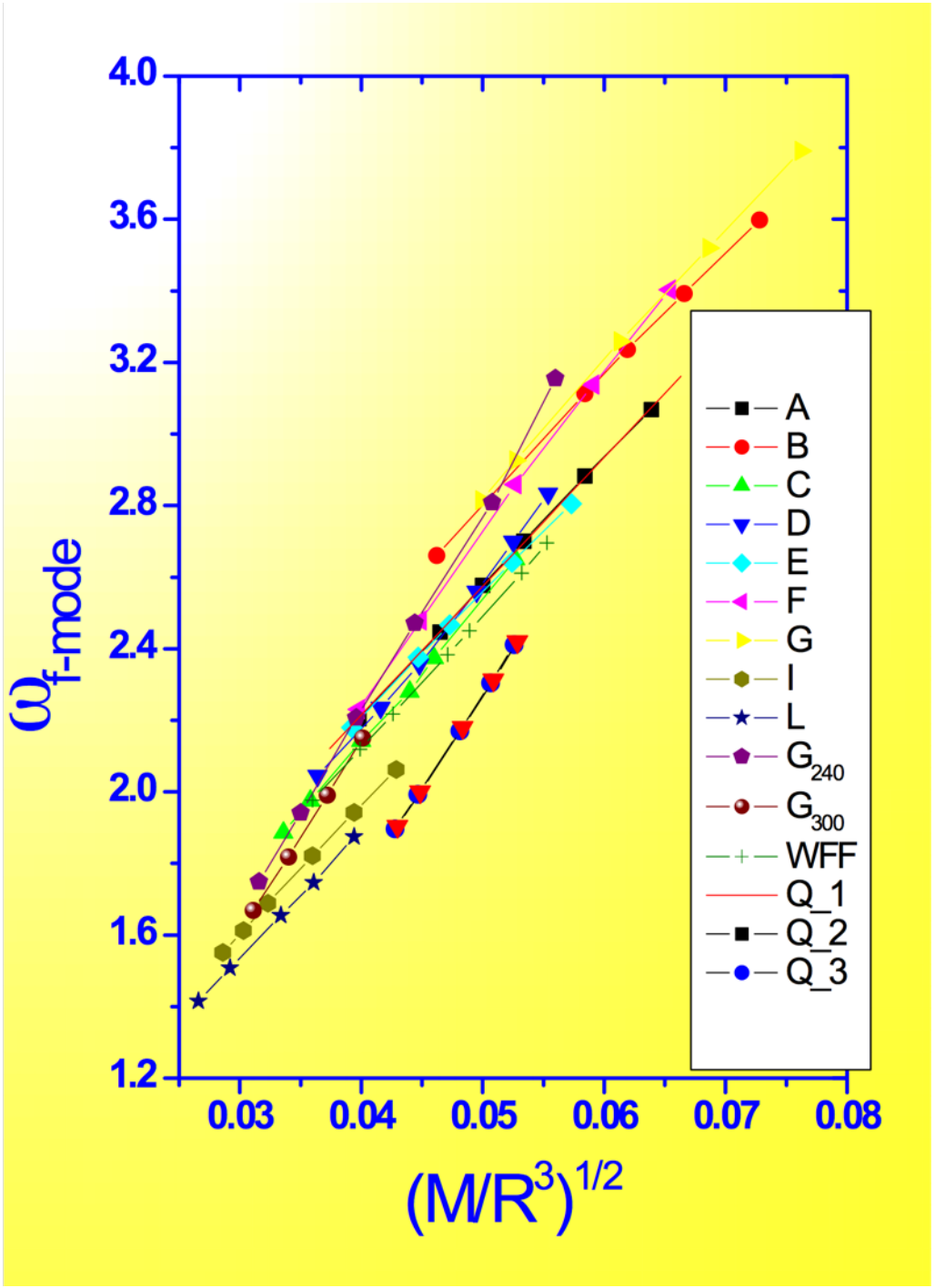

Empirical relations for GW asteroseismology:

$$\omega_f\,(kHz) \approx 0.78 + 1.637\left(\frac{M_{1.4}}{R_{10}^{\ 3}}\right)^{1/2}$$

Andersson & Kokkotas (1998)

GW emission

The luminosity in gravitational waves of the quadrupole mode is:

$$\left\langle \frac{dE}{dt} \right\rangle_{\mathrm{GW}} = -\frac{4\pi}{75}\sigma^6 \left(\int_0^R r^4 \delta\rho(r) dr \right)^2$$

GW emission

The luminosity in gravitational waves of the quadrupole mode is:

$$\left\langle \frac{dE}{dt} \right\rangle_{\rm GW} = -\frac{4\pi}{75}\sigma^6 \left(\int_0^R r^4 \delta\rho(r) dr \right)^2$$

The gravitational-wave damping timescale also satisfies an empirical relation:

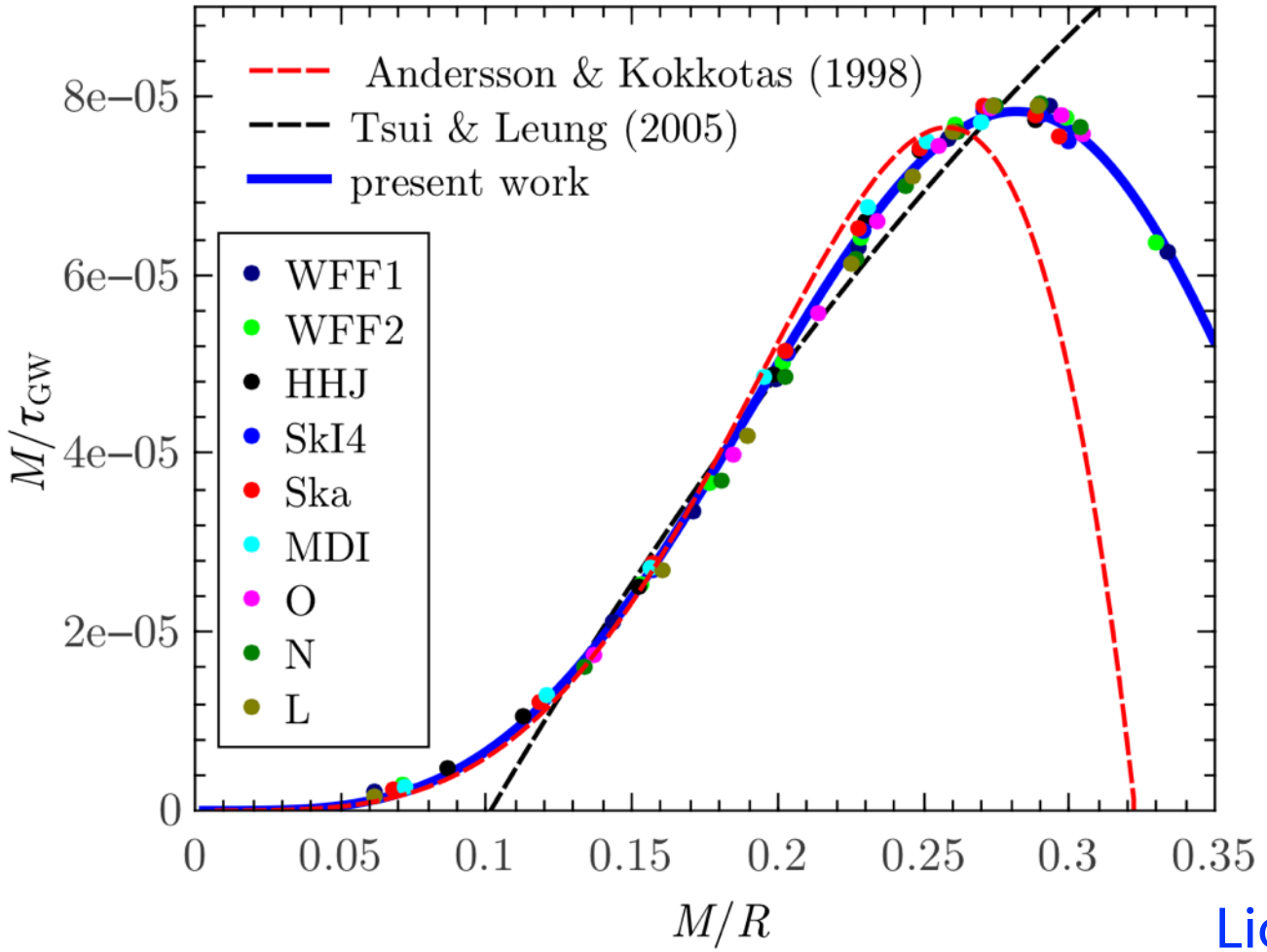

Lioutas & NS (2017)

Effects of Rotation on Axisymmetric Modes

In rotating stars, the mode eigenfunctions are distorted and acquire higher-order terms and axial terms:

$$P_l^{\rm rot} \sim \sum_{l'=0}^{\infty} (P_{l+2l'} + A_{l+2l'\pm1})$$

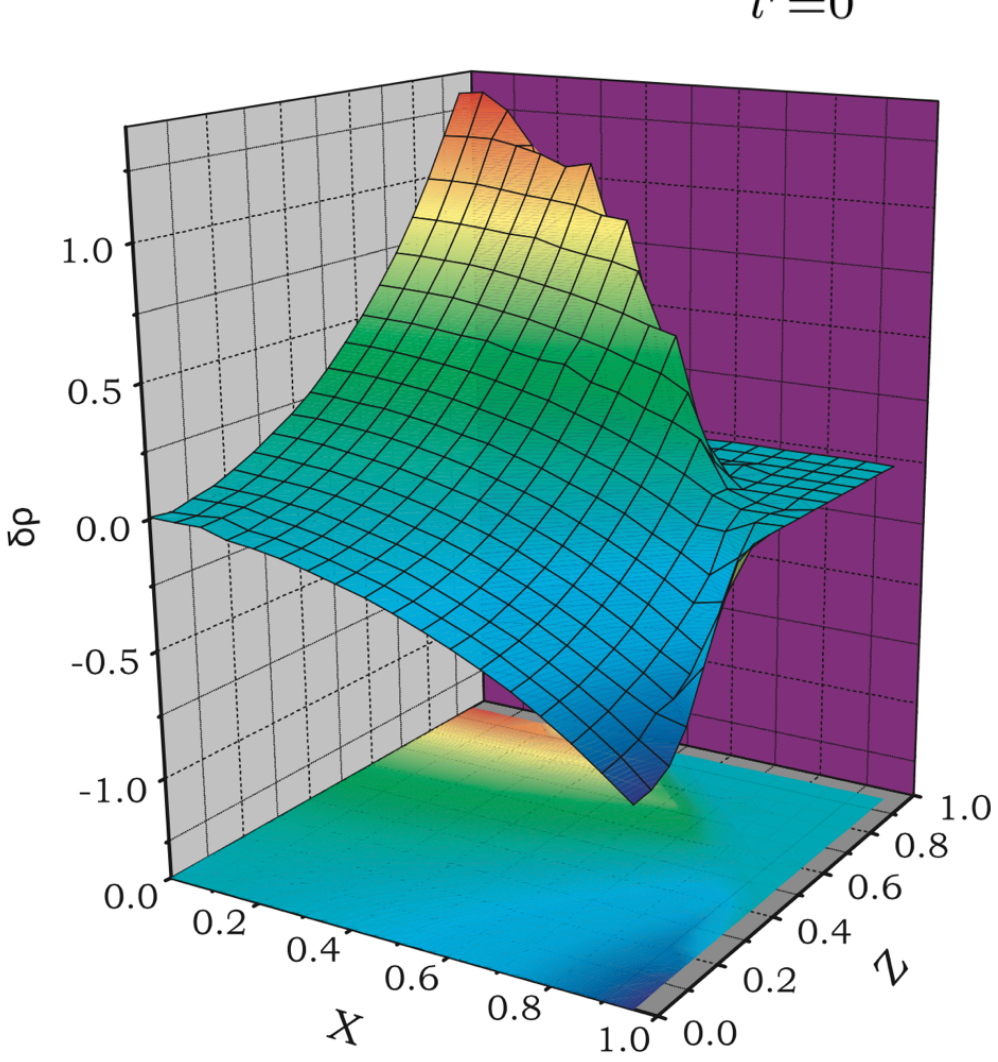

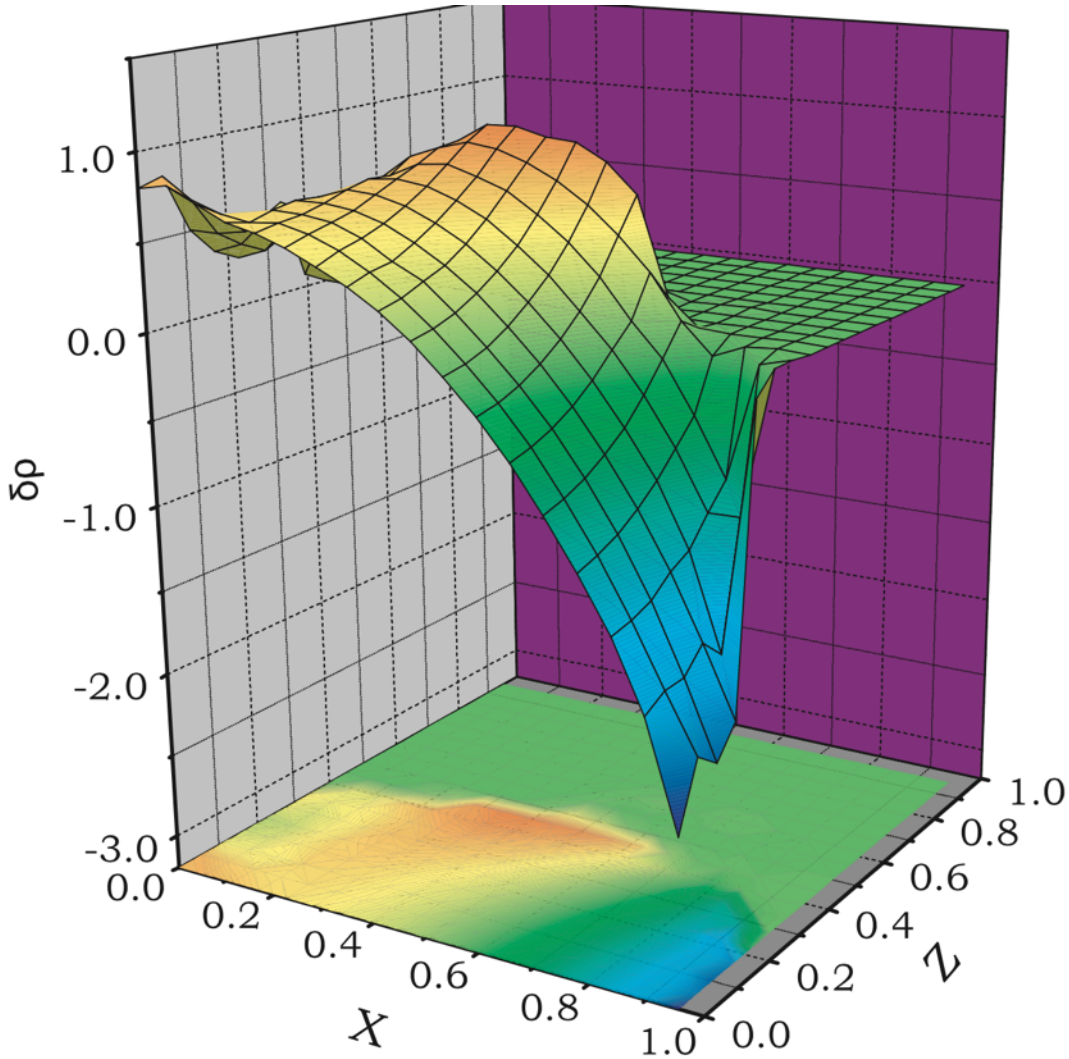

Effect of Rotation on Non-axisymmetric Modes

$l = m = +/- 2$ f-mode (in Cowling approximation),

Frequency splitting into *co-rotating* and *counter-rotating* branches.

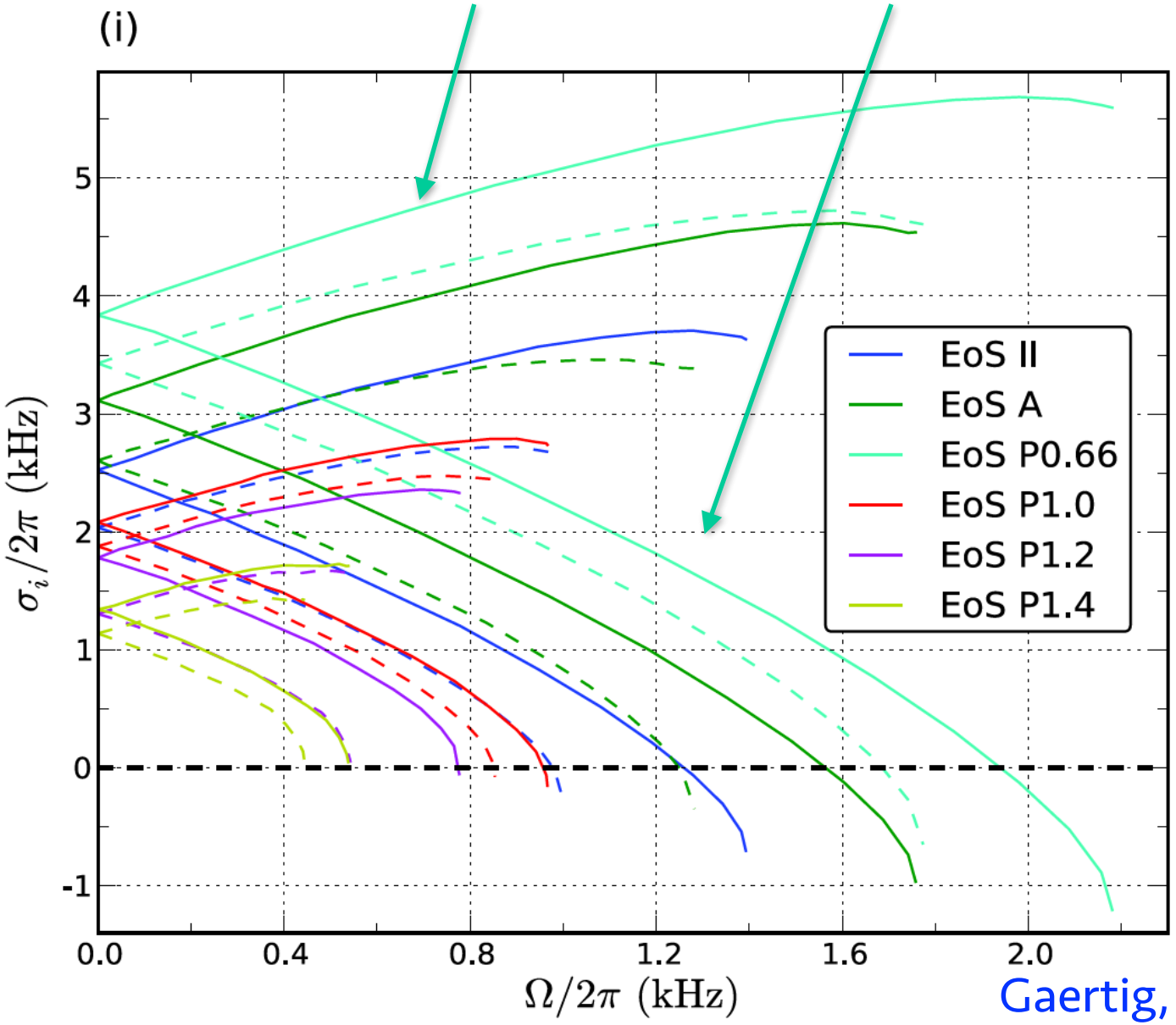

Gaertig, Kokkotas (2011)

Effect of Rotation on Non-axisymmetric Modes

The effect on rotation is universal (independent of EOS)!

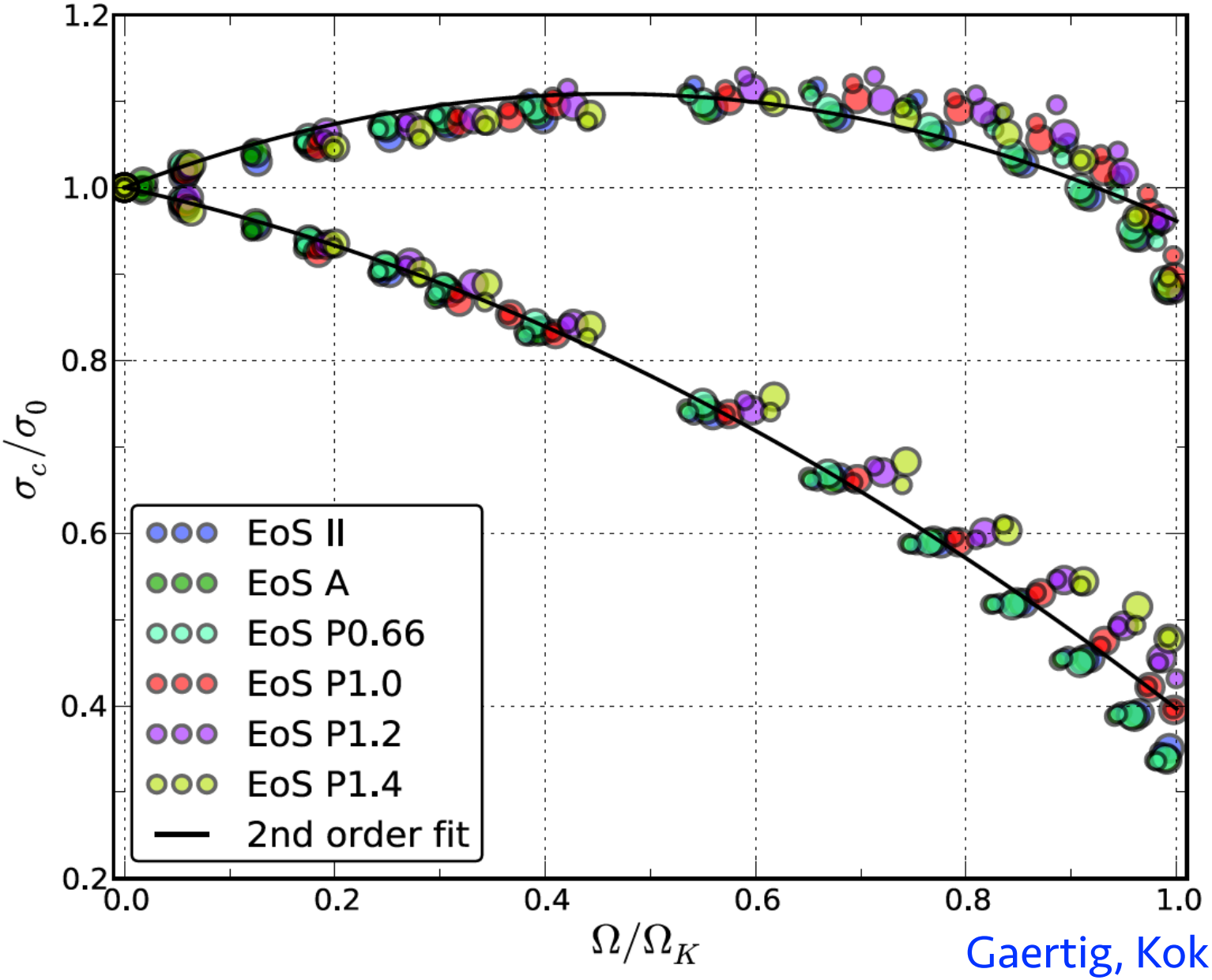

Gaertig, Kokkotas (2011)

Empirical Relations for Damping Timescale

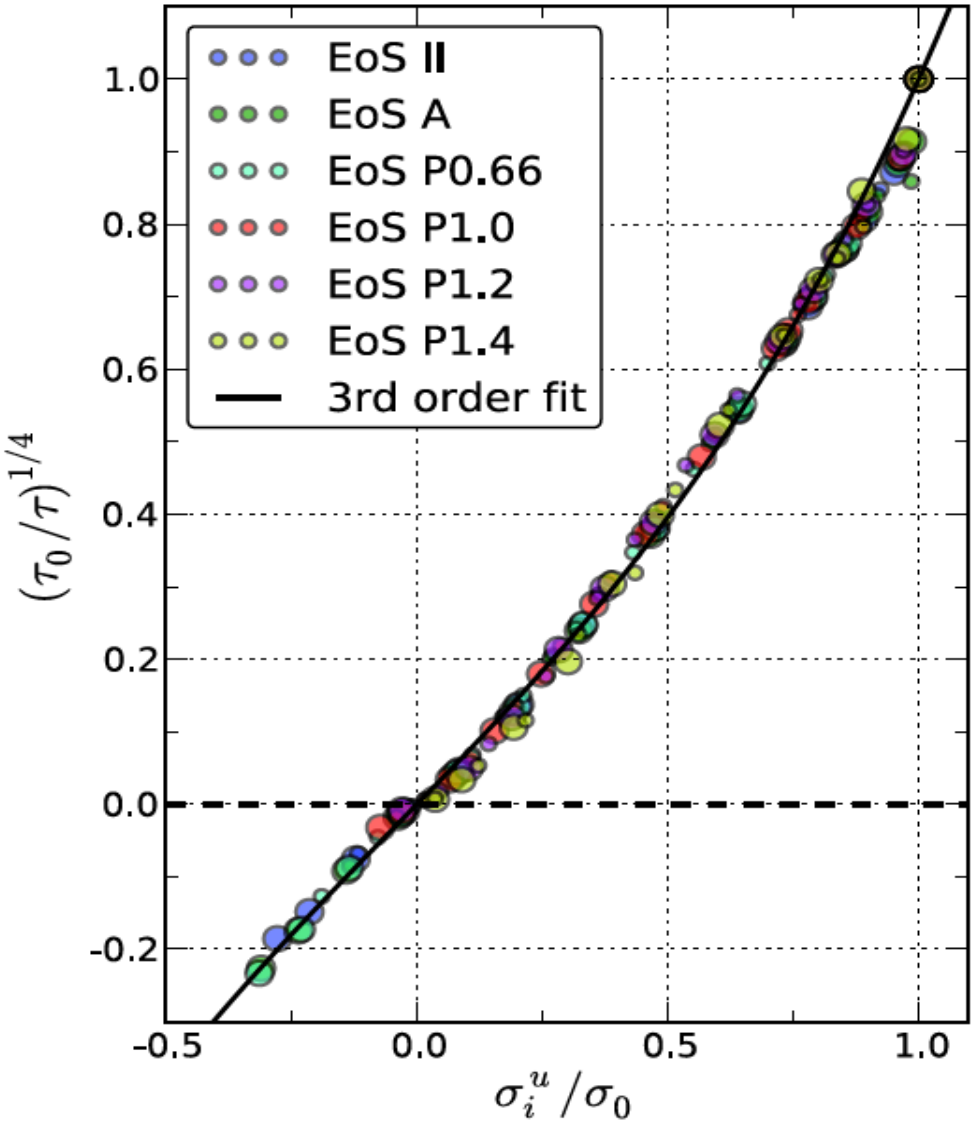

Counter-rotating (unstable) branch vs. *f* in *inertial* frame.

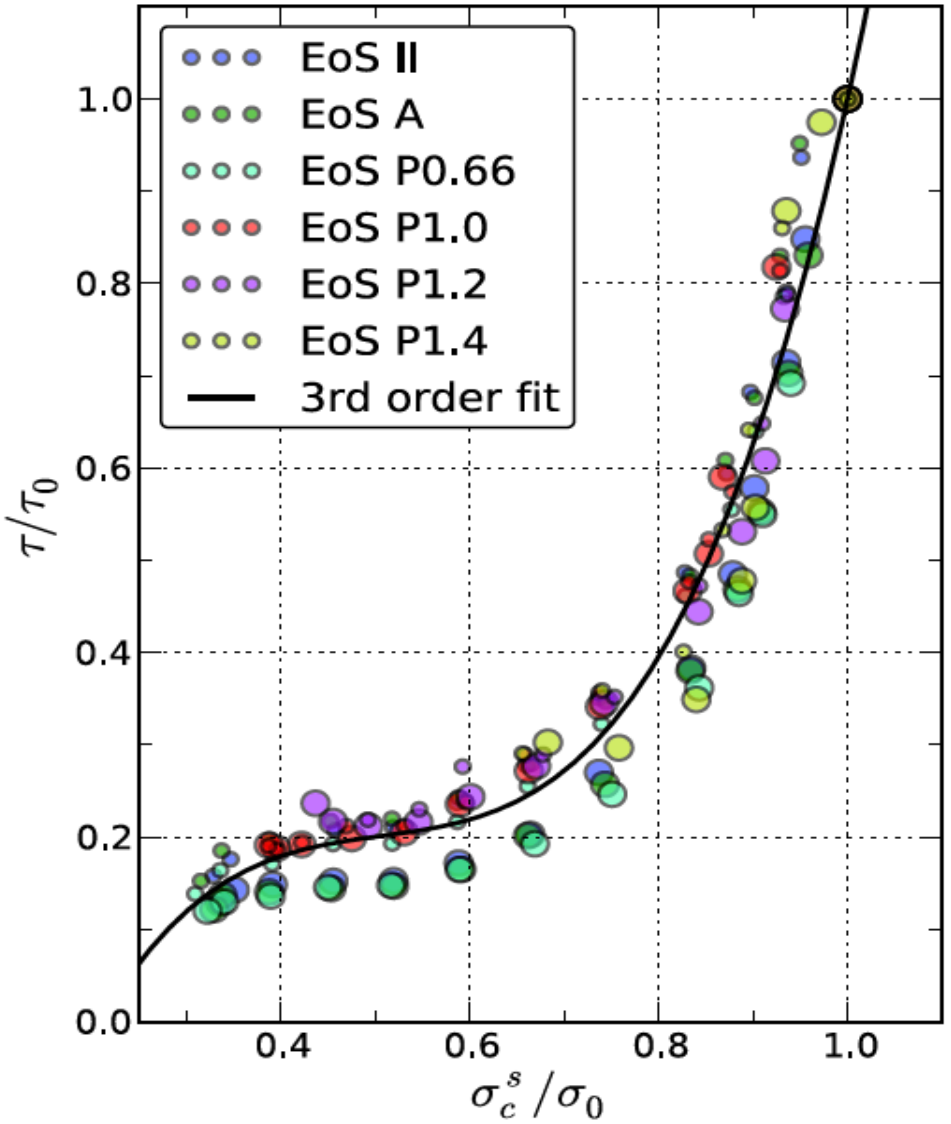

Corotating (stable) branch vs. *f* in *corotating* frame.

Gaertig, Kokkotas (2011)

Empirical Relations for Damping Timescale

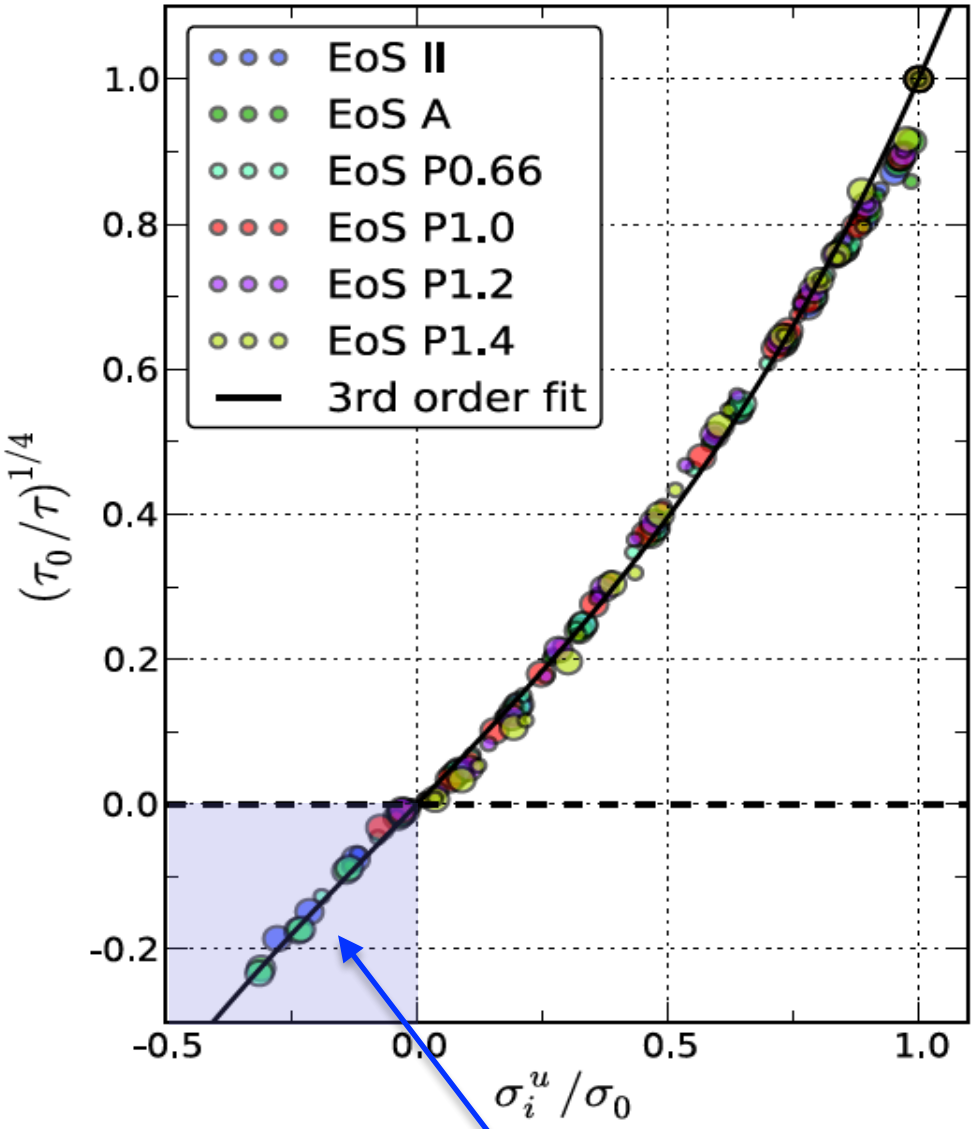

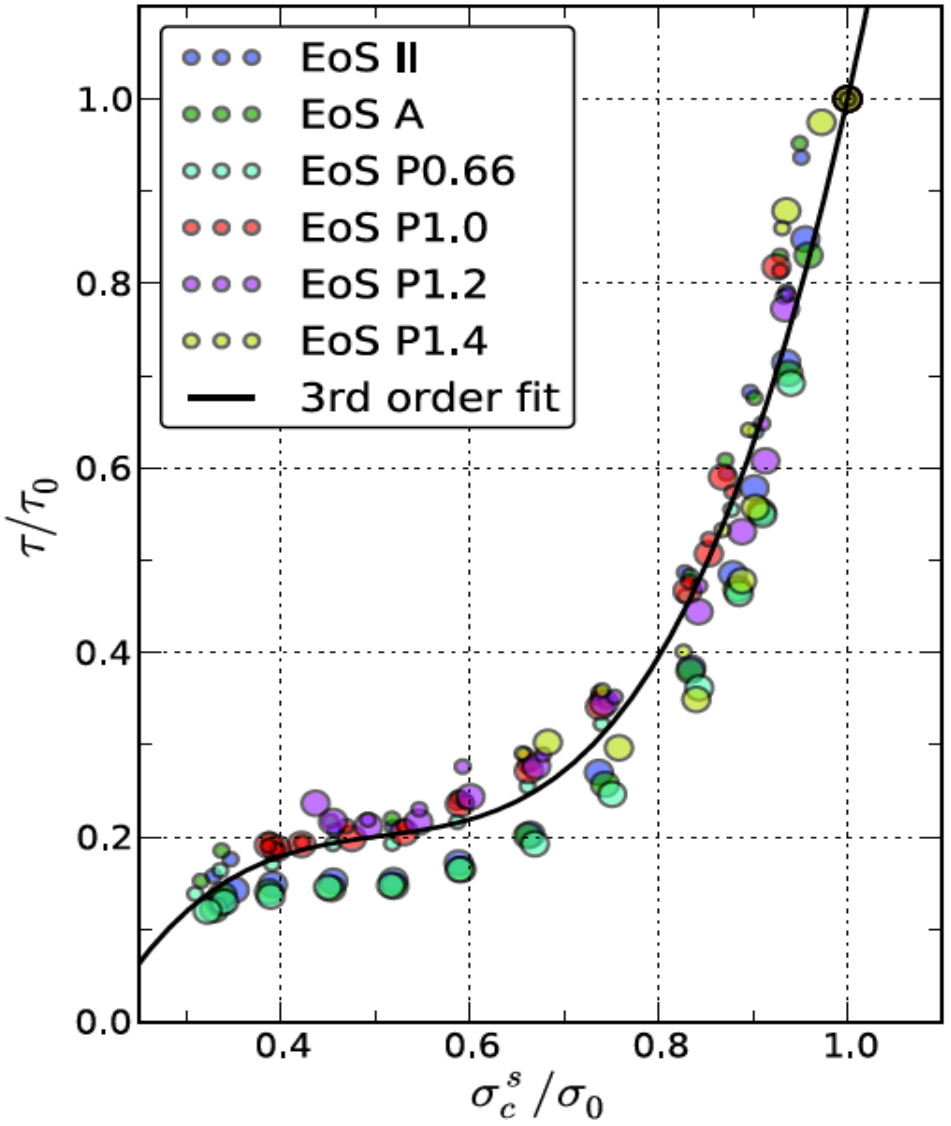

Counter-rotating (unstable) branch vs. *f* in *inertial* frame.

Corotating (stable) branch vs. *f* in *corotating* frame.

Chandrasekhar - Friedman - Schutz (CFS) instability

F-Mode Instability in Relativistic Stars

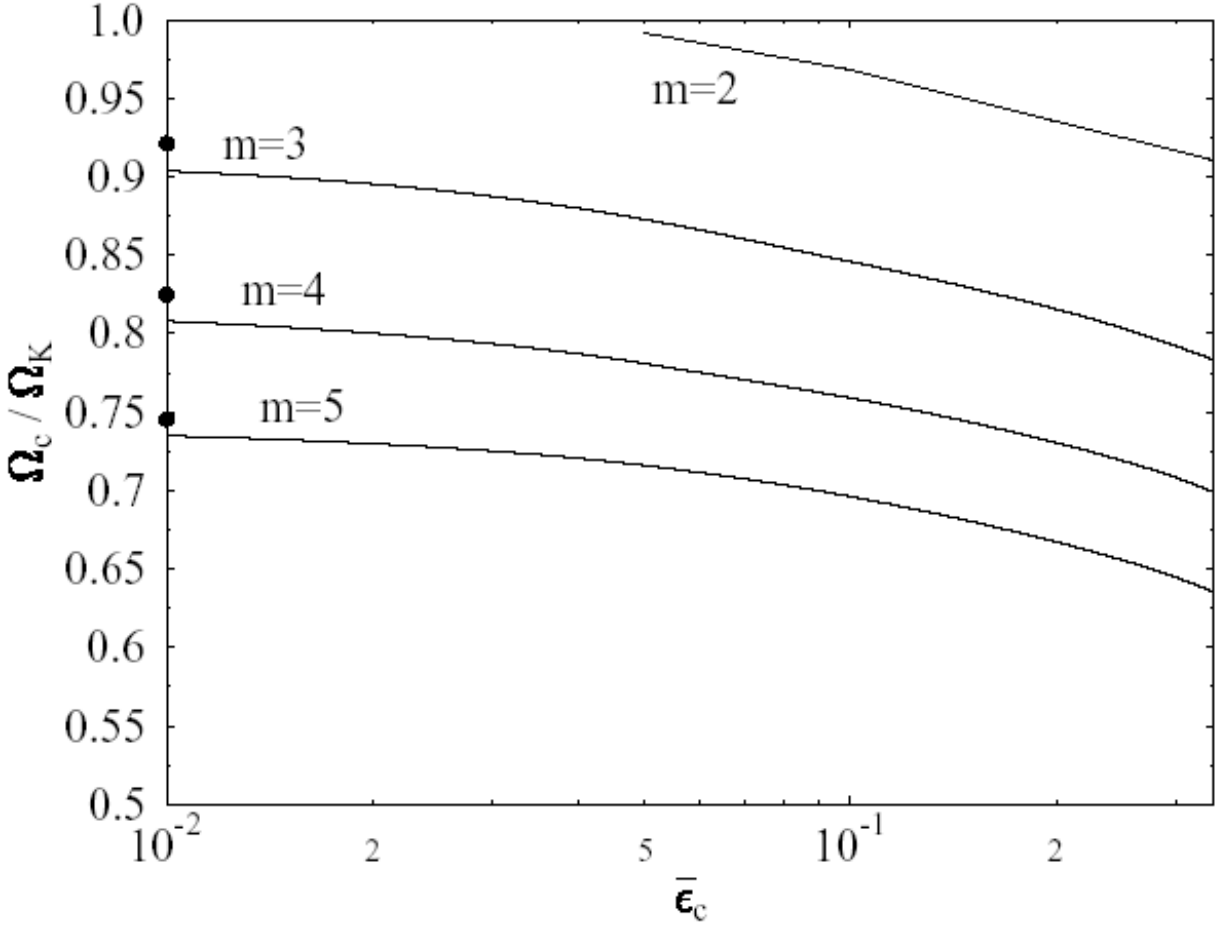

Onset of $l = m = 2$ instability for:

$\Omega > 0.85\,\Omega_K$	$\Omega > 0.95\,\Omega_K$
$T/W > 0.07$	$T/W > 0.14$
$N < 1.3$	$N < 0.81$
(Full GR)	(Newtonian)

(N.S & Friedman 1998)

Nonlinear Development of F-Mode Instability

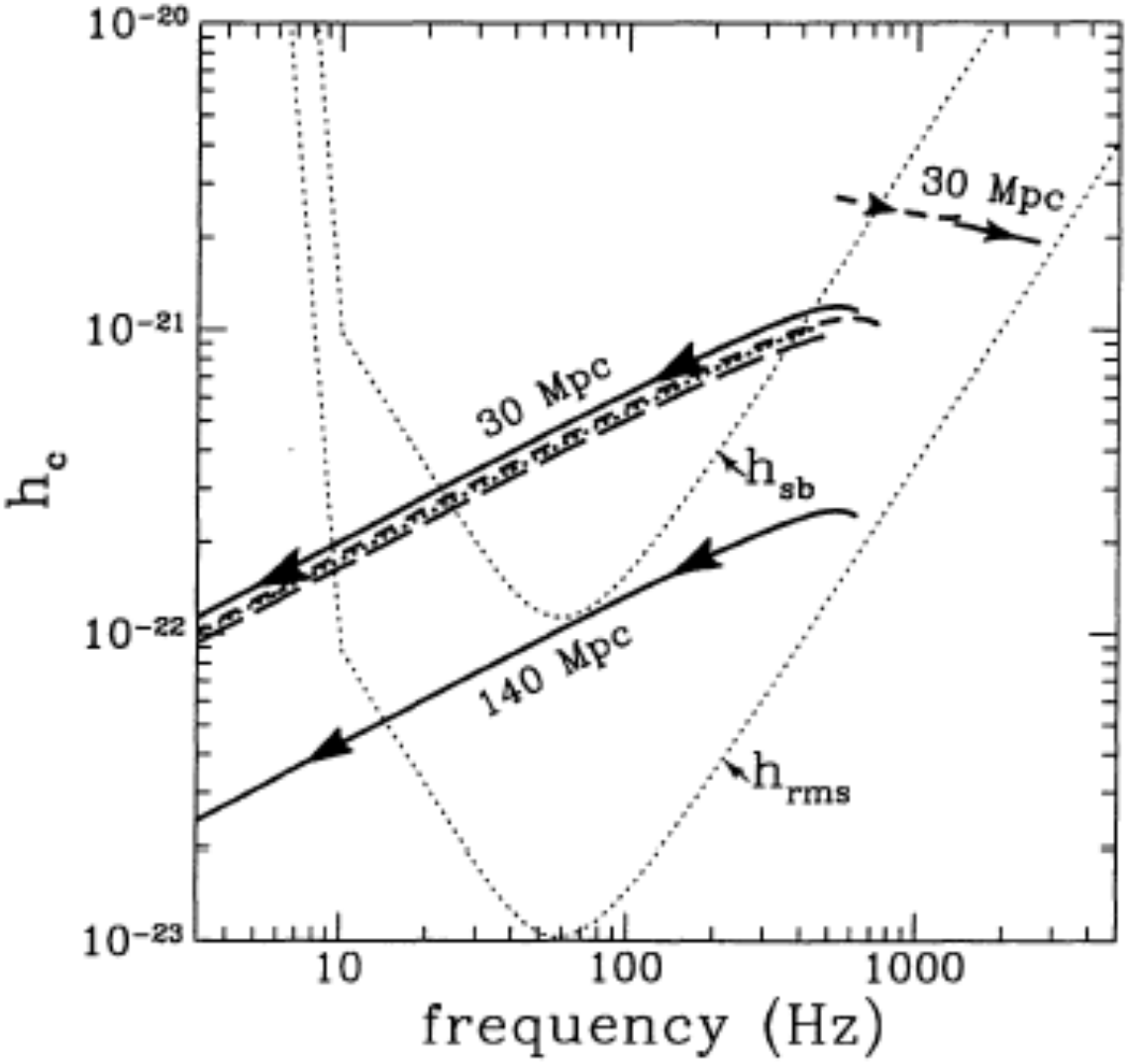

Lai & Shapiro, 1995

Main uncertainties:

1. Relativistic growth times
2. Nonlinear saturation
3. Initial rotation rates of protoneutron stars
4. Effect of magnetic fields

Nonlinear Saturation of l=m=2 f-Modes

At amplitude of a few times 10^{-2} the f-mode is saturated by wave-breaking at the surface.

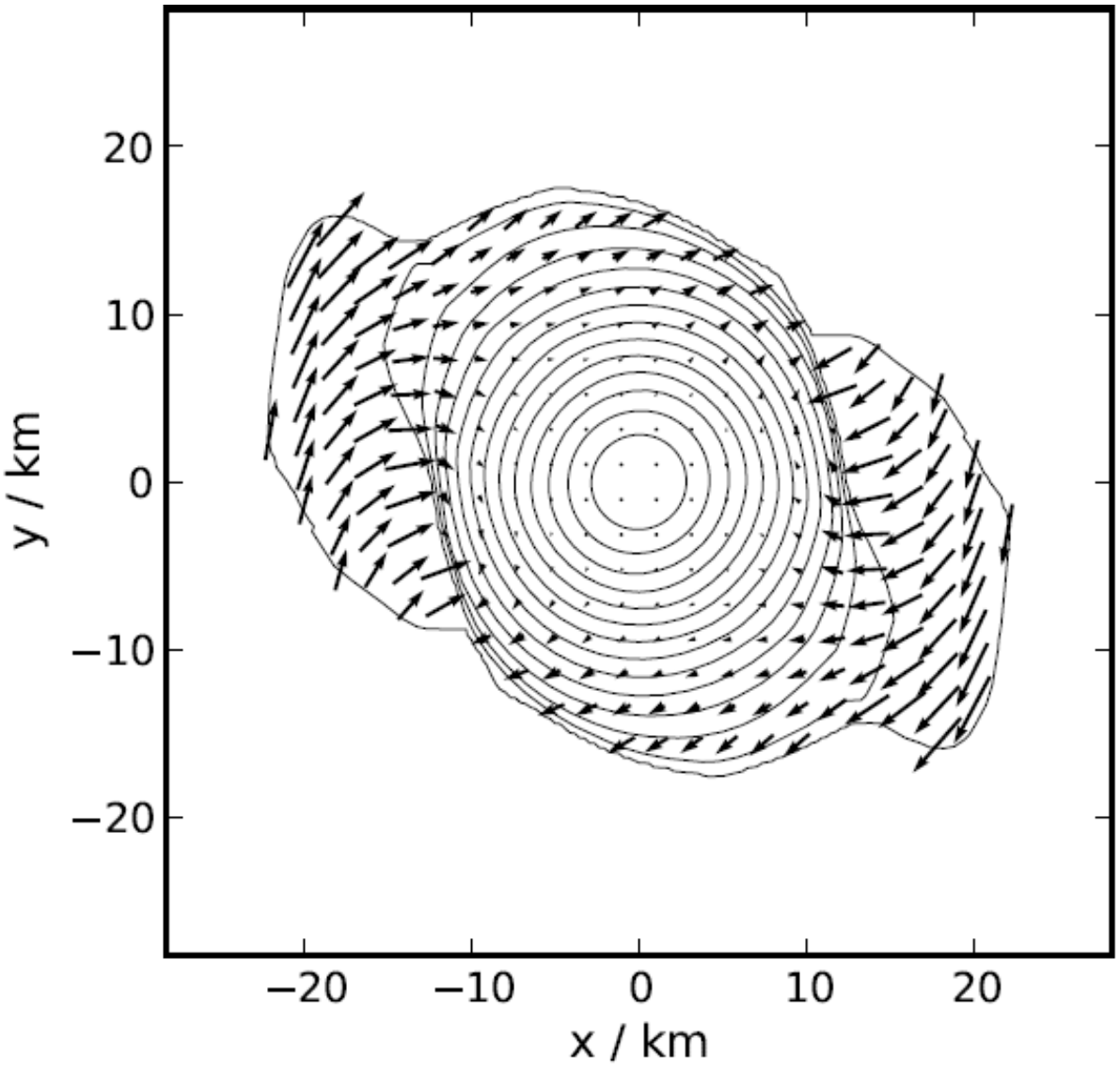

Kastaun, Willburger & Kokkotas (2010)

Quasi-linear Combination Frequencies

Linear sums and differences of linear mode frequencies:

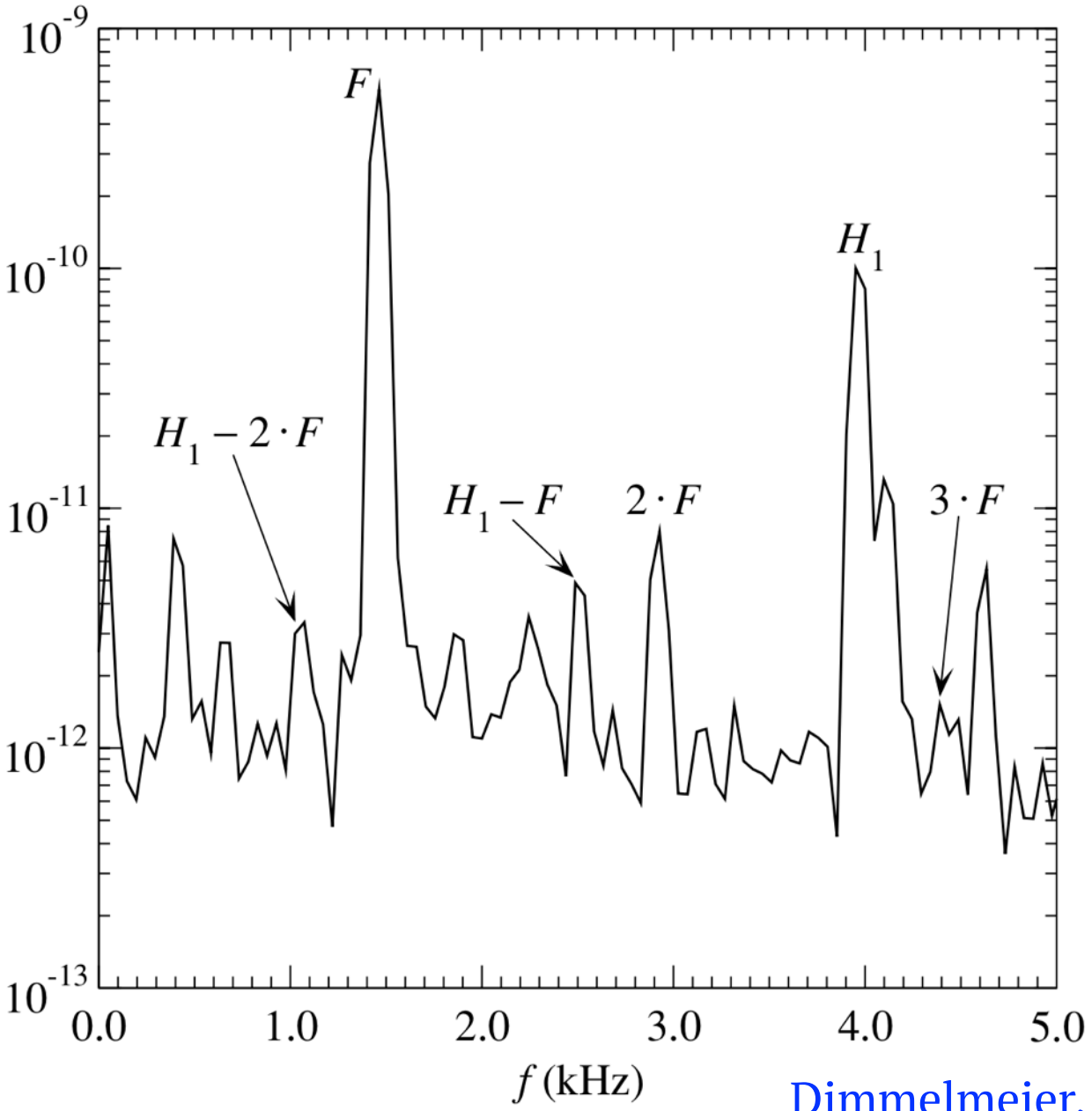

Dimmelmeier, NS & Font (2006)

Lattimer-Swesty 220 EOS 1.35+1.35

GRAVITATIONAL WAVE SPECTRUM

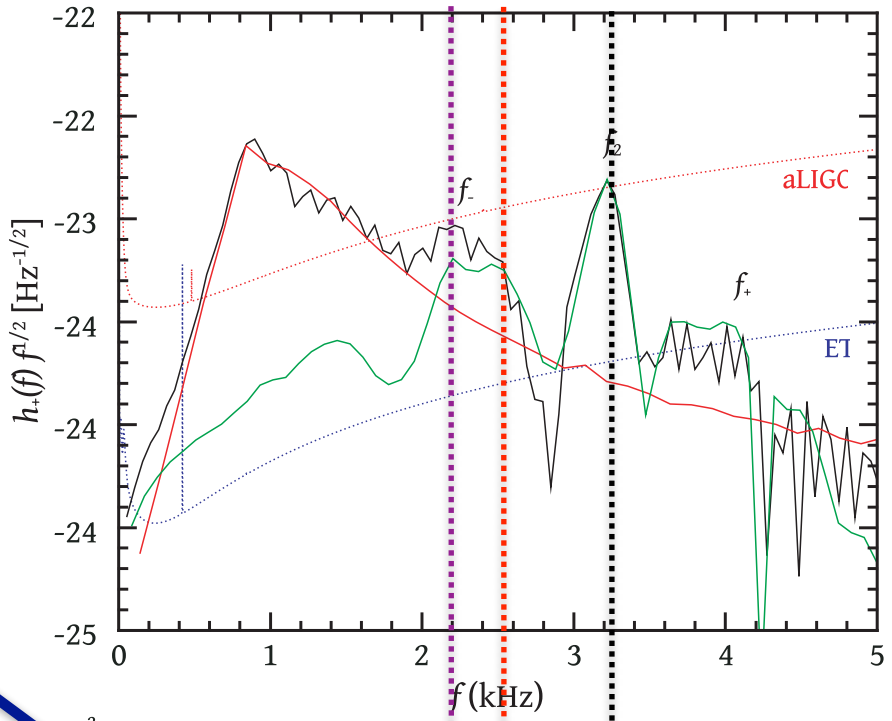

NS, Bauswein, Zagkouris & Janka (2011)

***l*=*m*=0 linear quasi-radial mode**

FFT OF HYDRODYNAMICS IN EQUATORIAL PLANE

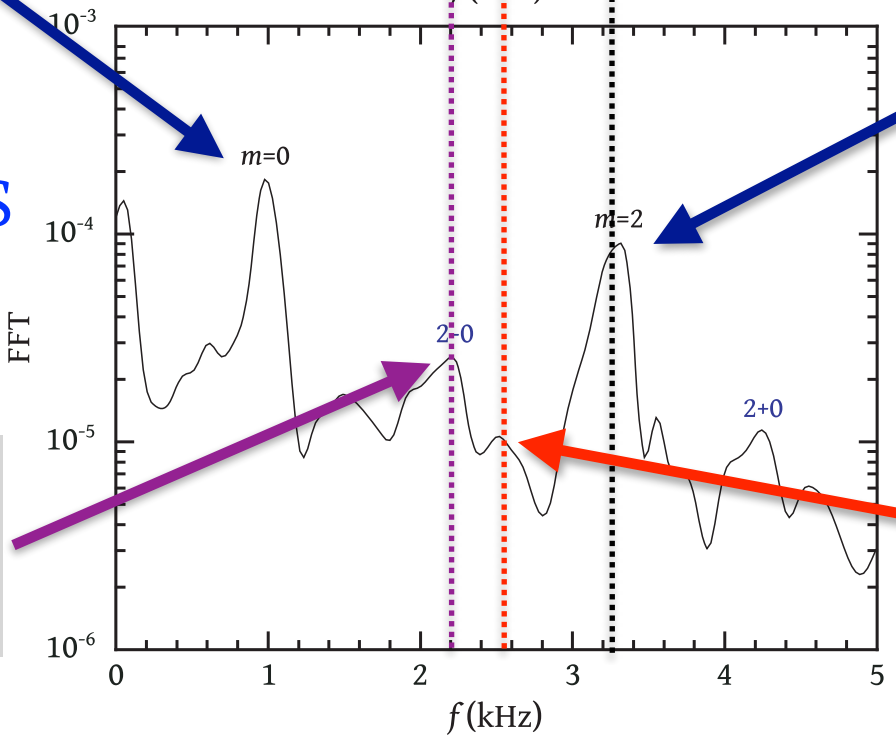

***l*=*m*=2 linear f-mode**

***"2-0" quasi-linear* combination frequency**

***nonlinear* spiral frequency**

Spiral Deformation

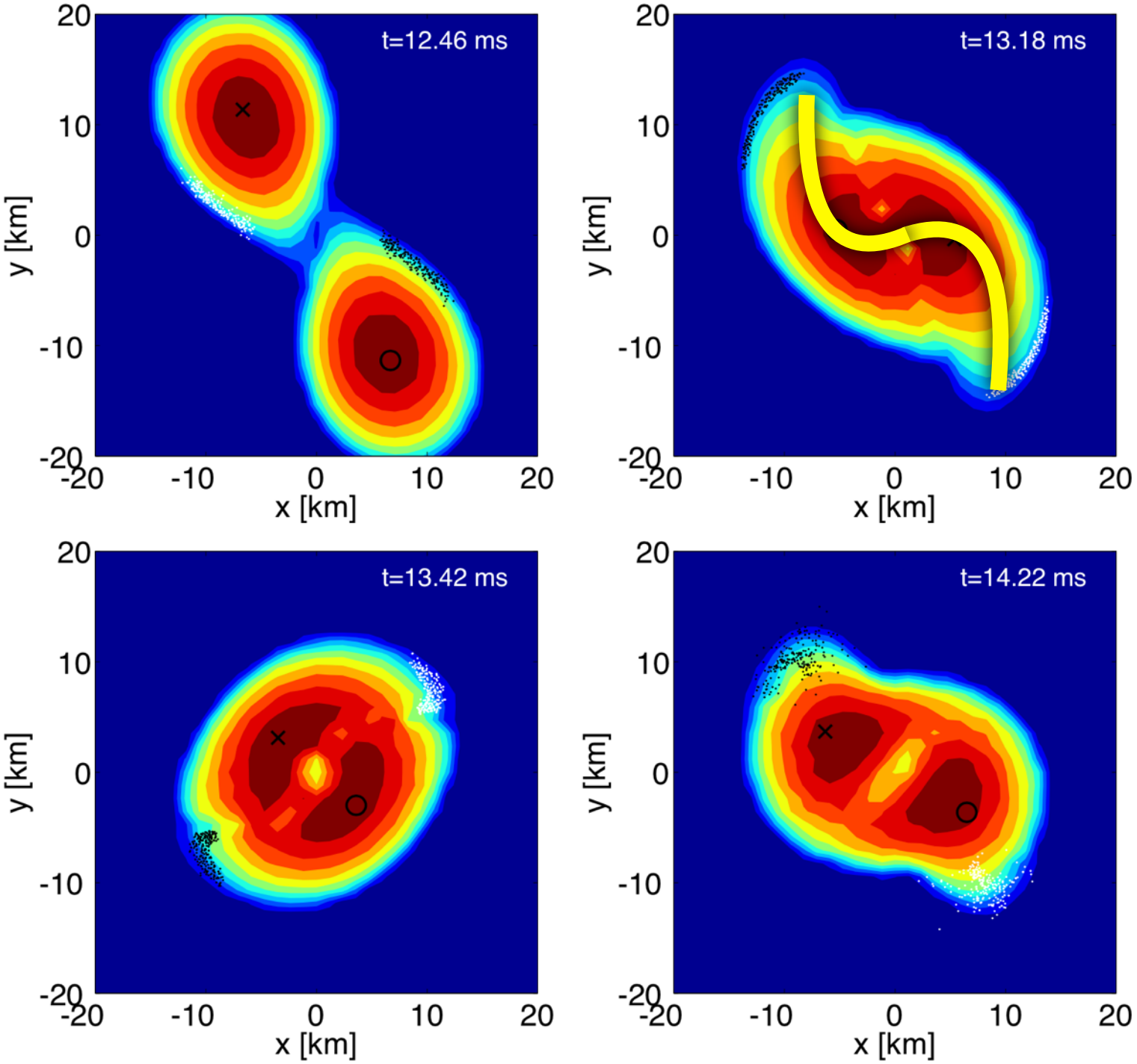

Bauswein & NS (2015)

Time-Frequency Analysis

Clark, Bauswein, NS &Shoemaker (2016)

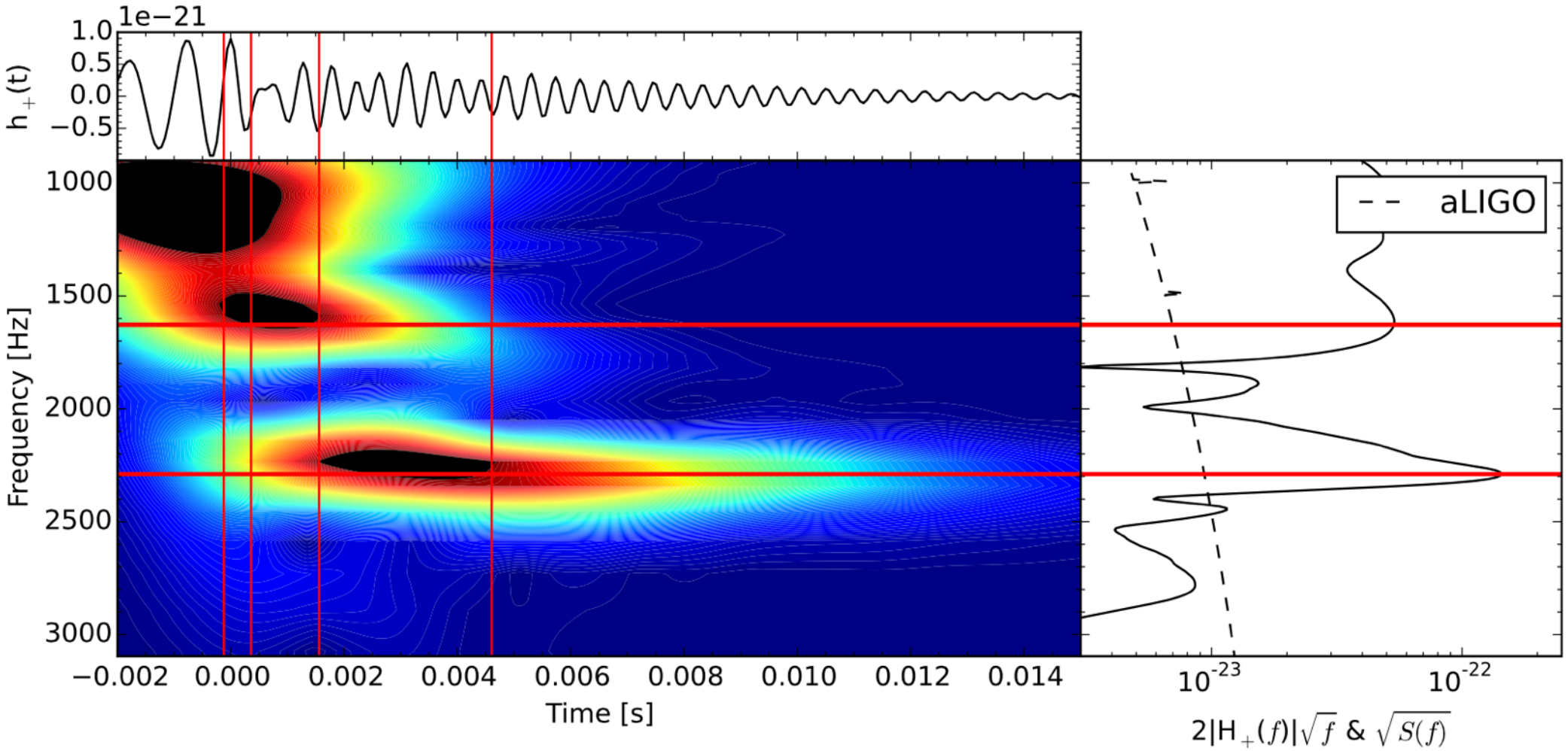

linear + quasi-linear + nonlinear

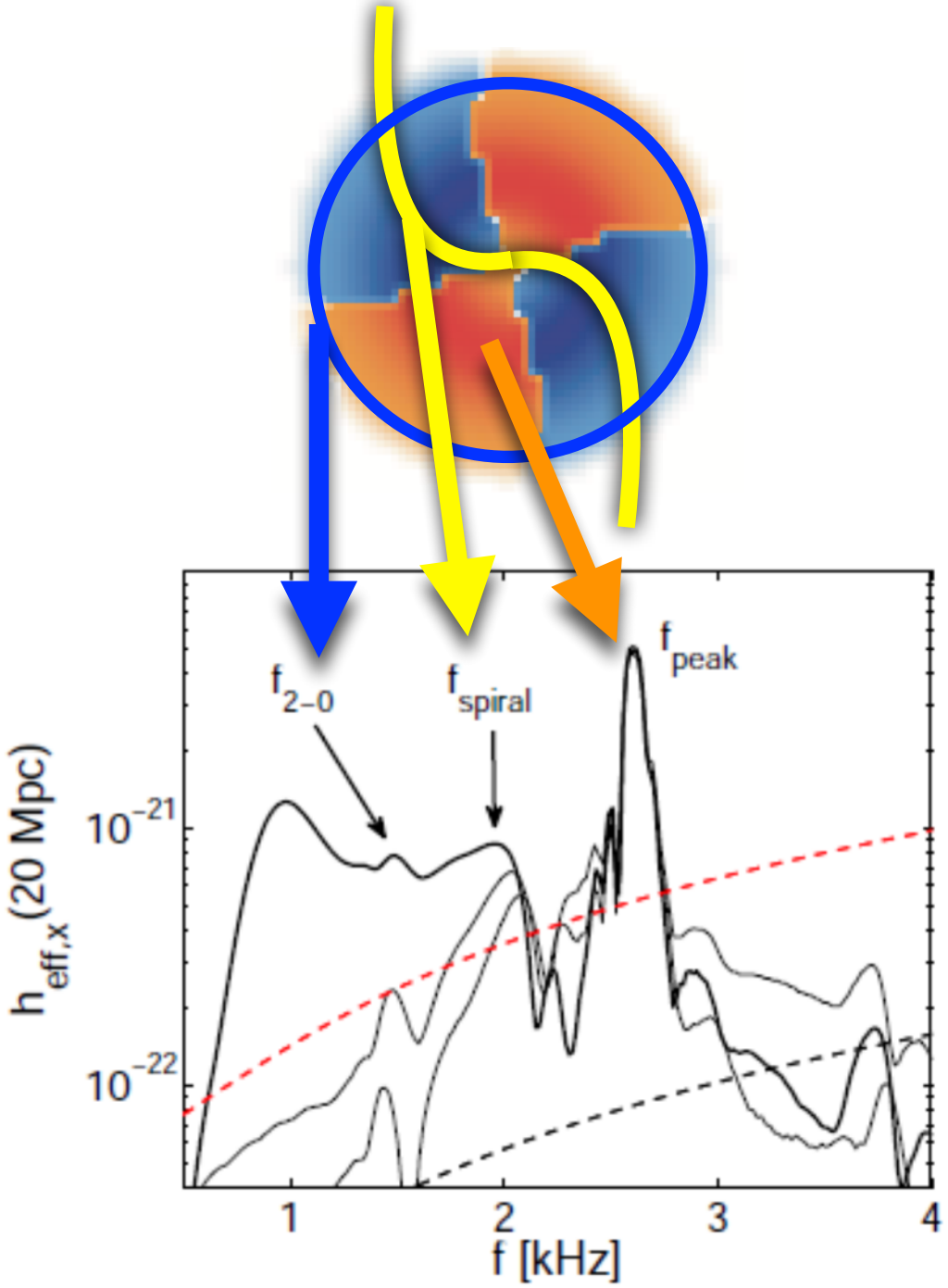

Three Types of Post-Merger Dynamics

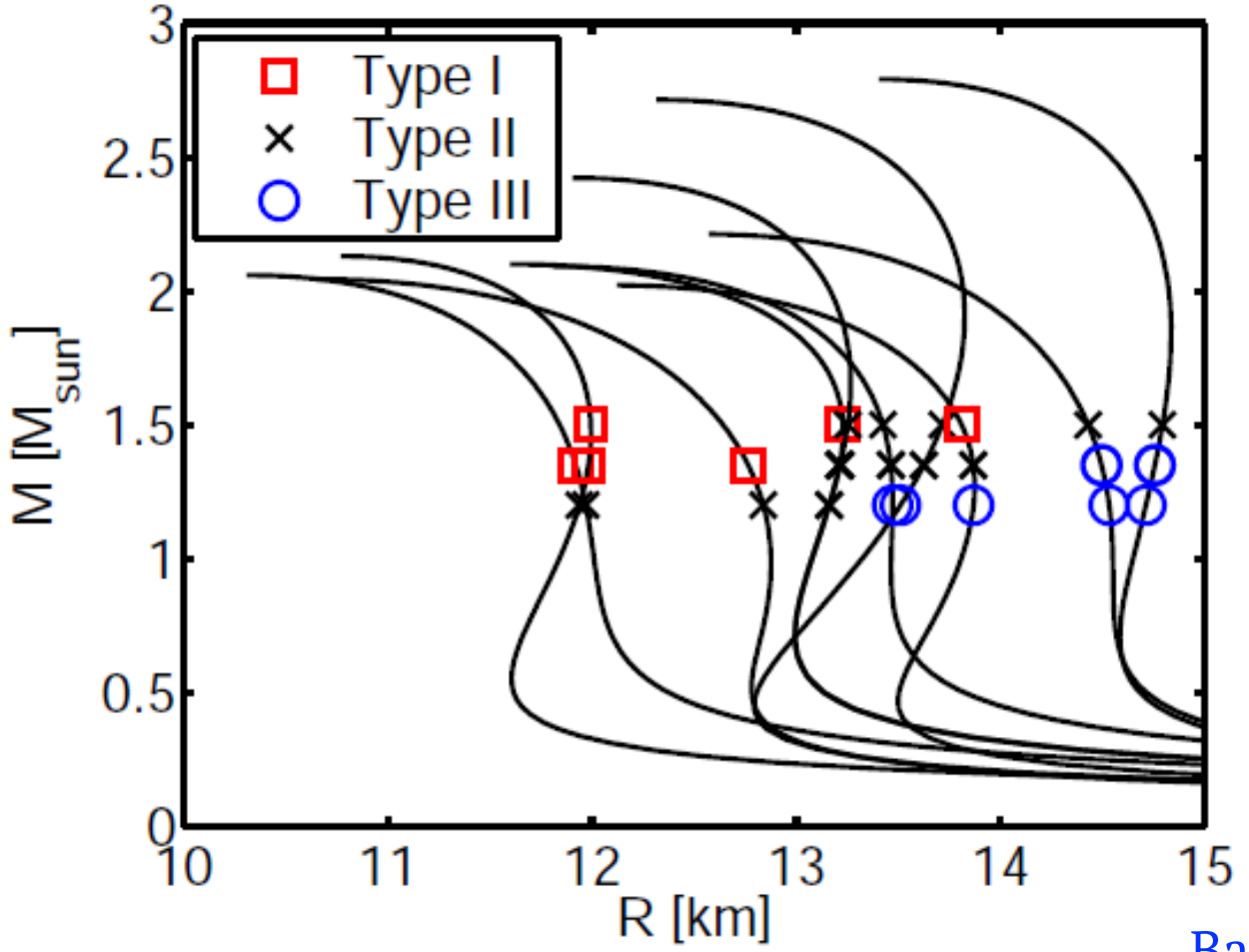

Bauswein, NS (2015)

Type I: the "2-0" combination frequency dominates

Type II: **both** the "2-0" and the $f_{\rm spiral}$ frequencies are present

Type III: the $f_{\rm spiral}$ frequency dominates

Radius Determination from Post-Merger Signal

Bauswein, Janka, Hebeler & Schwenk (2012)

f_{peak} correlates very well with the radius @ 1.6 Msun, if M_{tot} is known from inspiral.

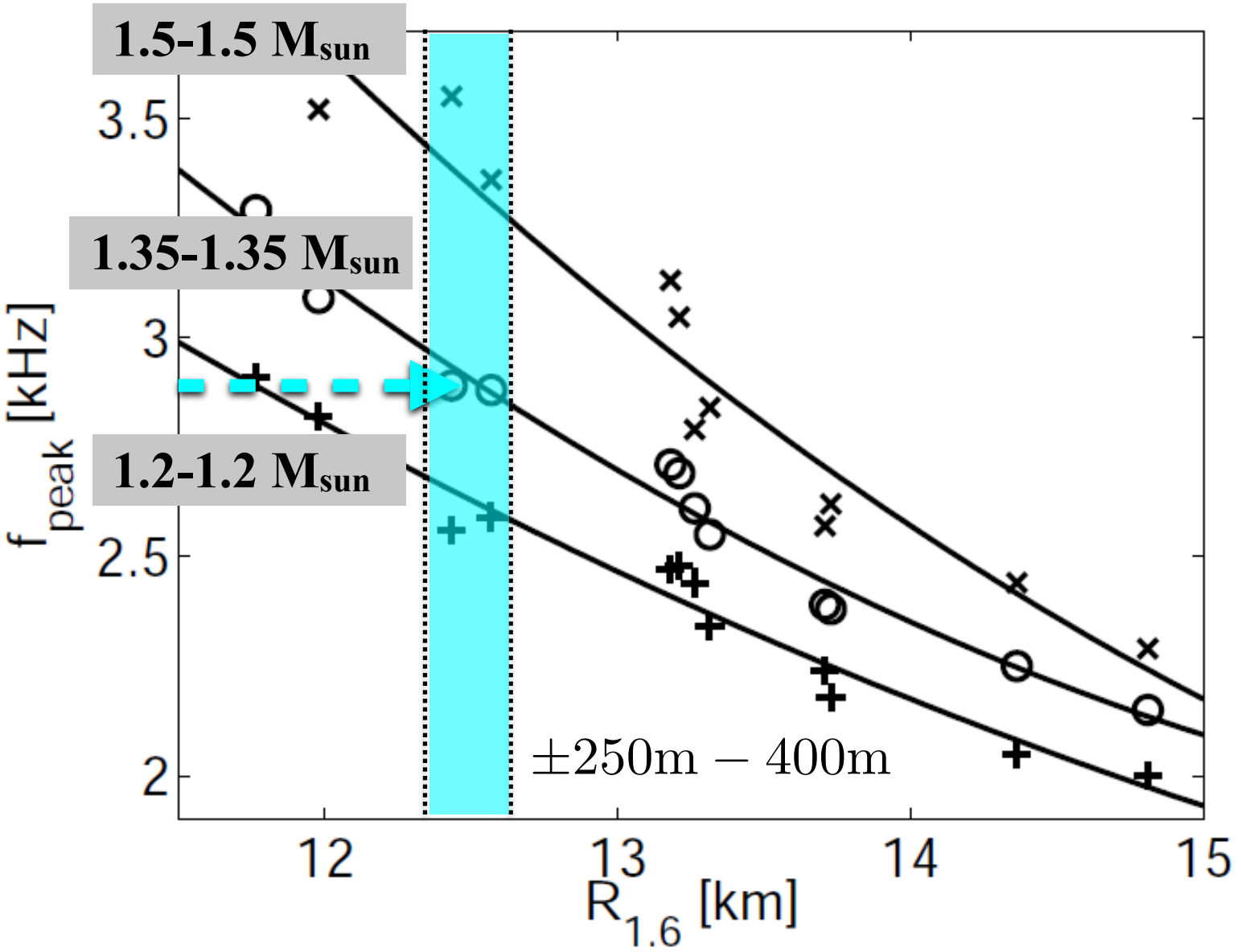

Revealing the EOS

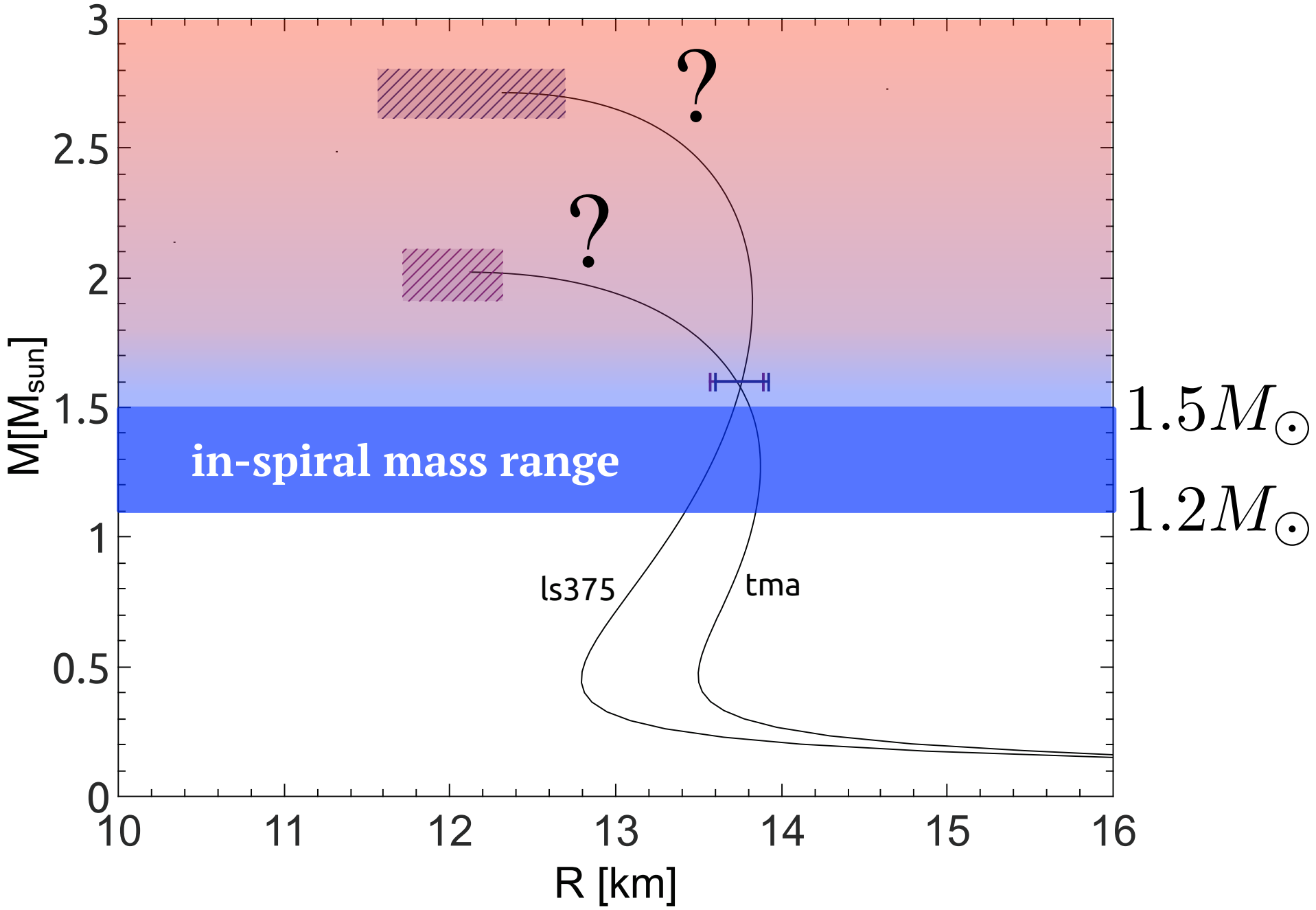

Extrapolating to Larger Masses

Bauswein, NS, Janka (2014)

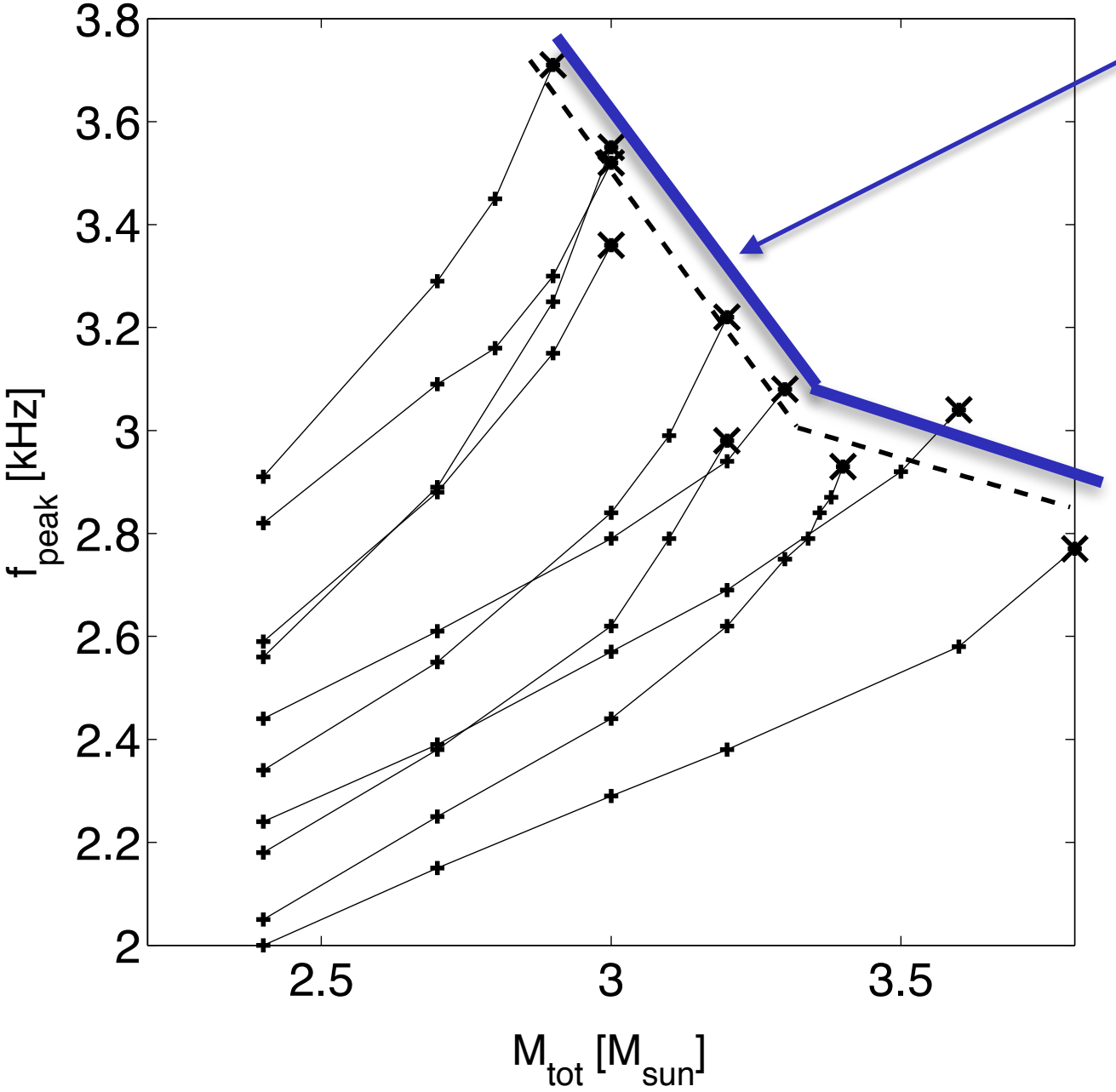

Extrapolating to Larger Masses

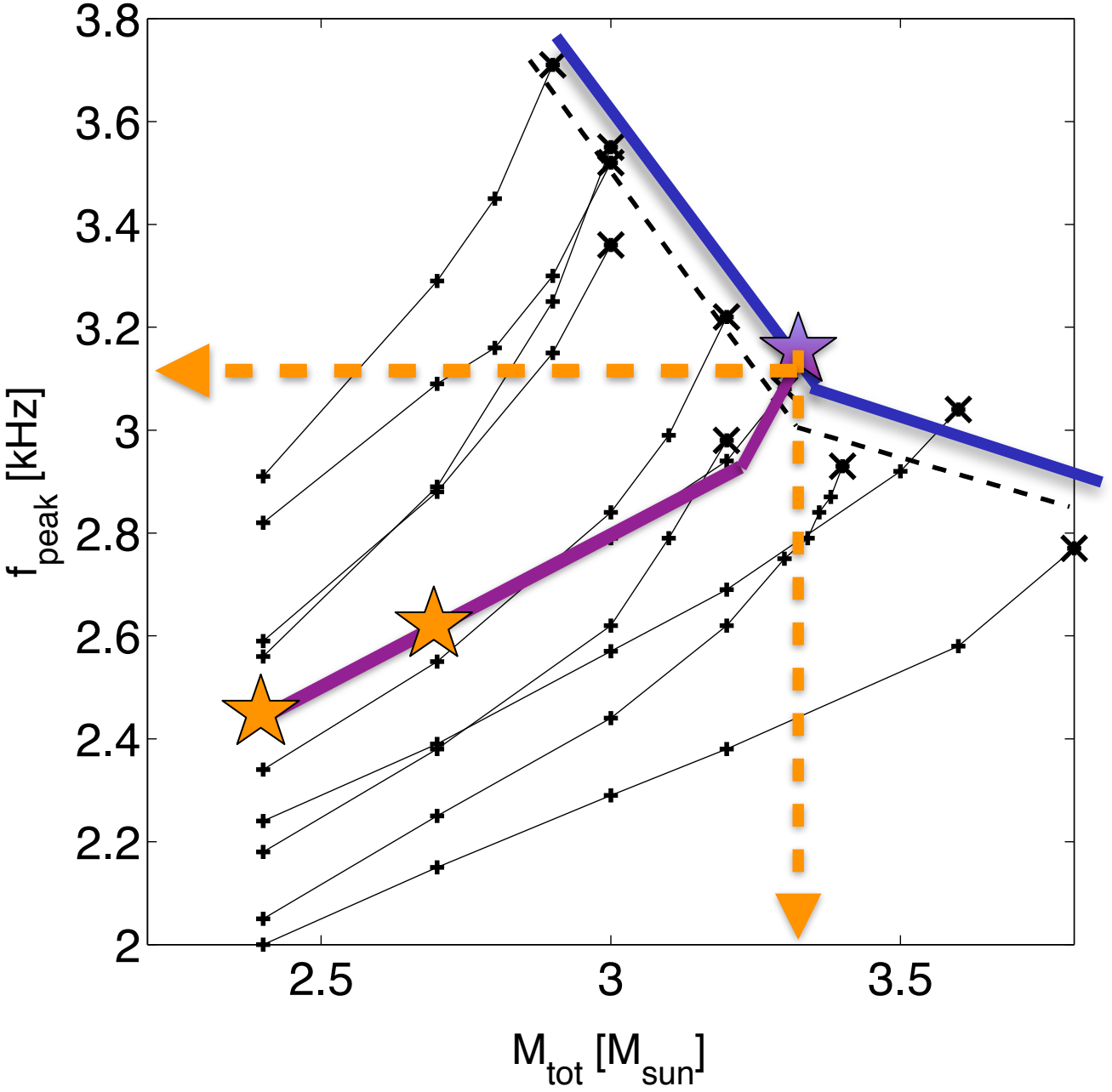

M_thres vs. M_max correlation

Bauswein, Baumgarte, Janka PRL (2013)

The threshold mass is related to the maximum TOV mass as

$$M_{\rm thres} = k \cdot M_{\rm max}$$

where *k* is dependent on the compactness.

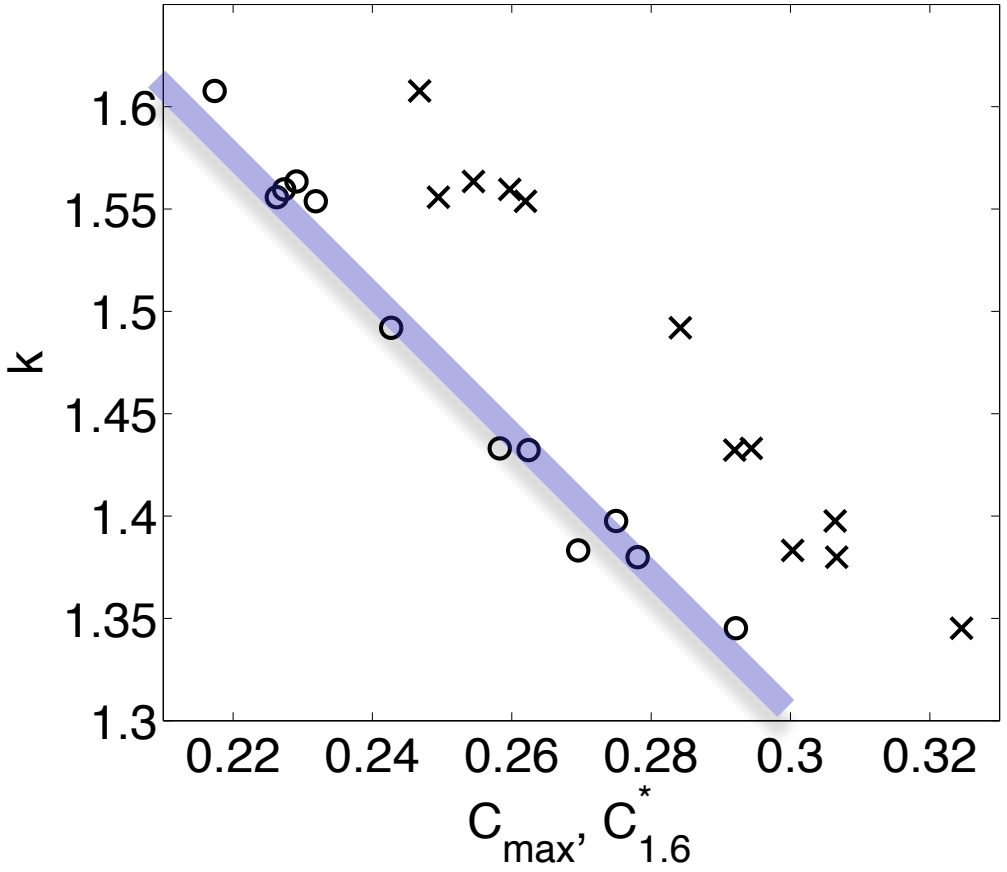

$$C_{\rm max} = (GM_{\rm max})/(c^2 R_{\rm max})$$

Breaking the EOS Degeneracy

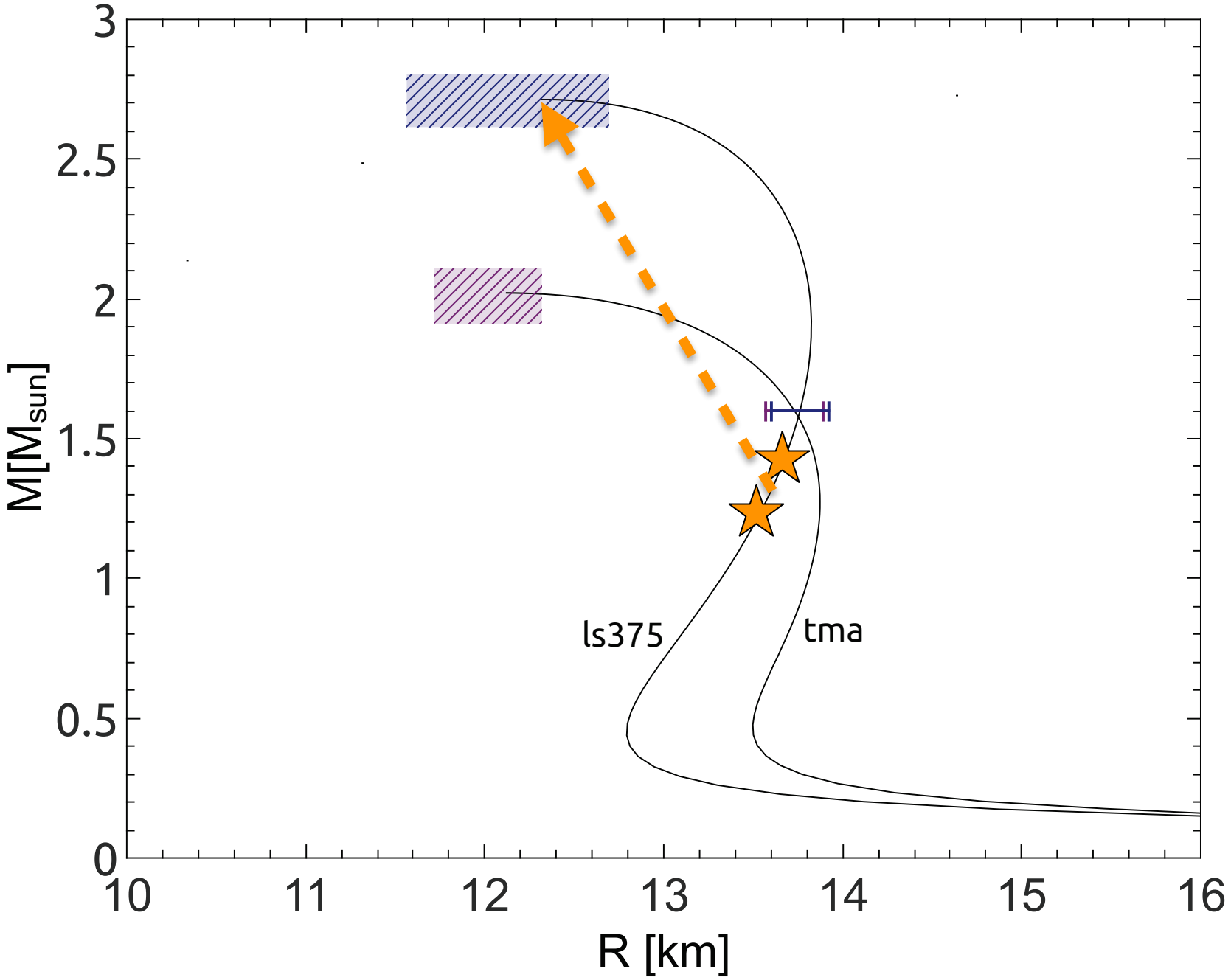

Principal Component Analysis (PCA)

Clark, Bauswein, NS, Shoemaker (2016)

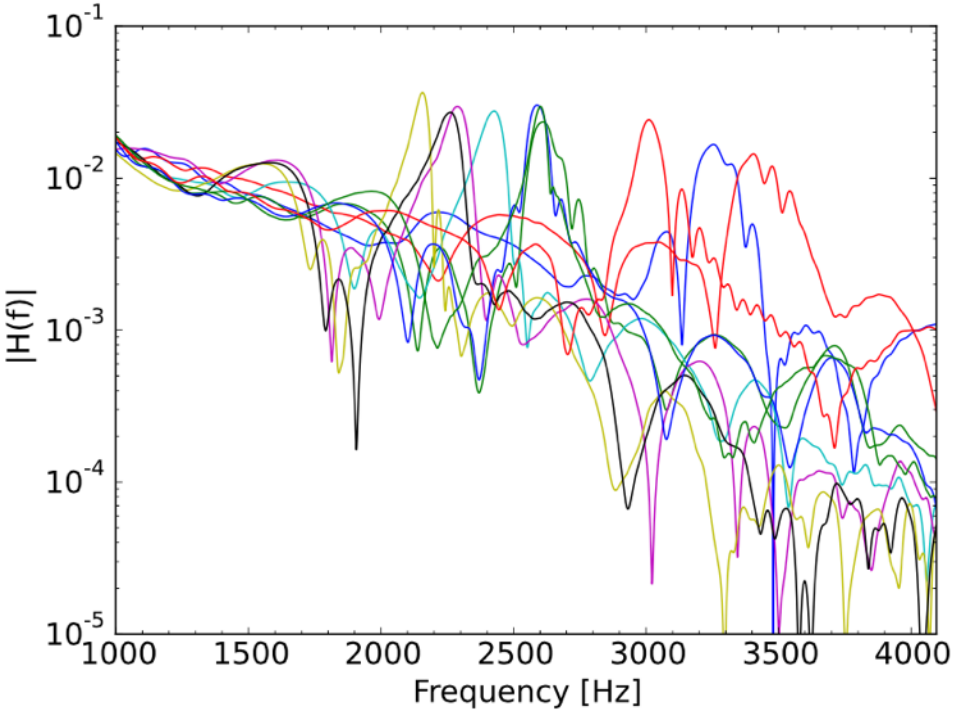

Actual fft's for different models.

Principal Component Analysis (PCA)

Clark, Bauswein, NS, Shoemaker (2016)

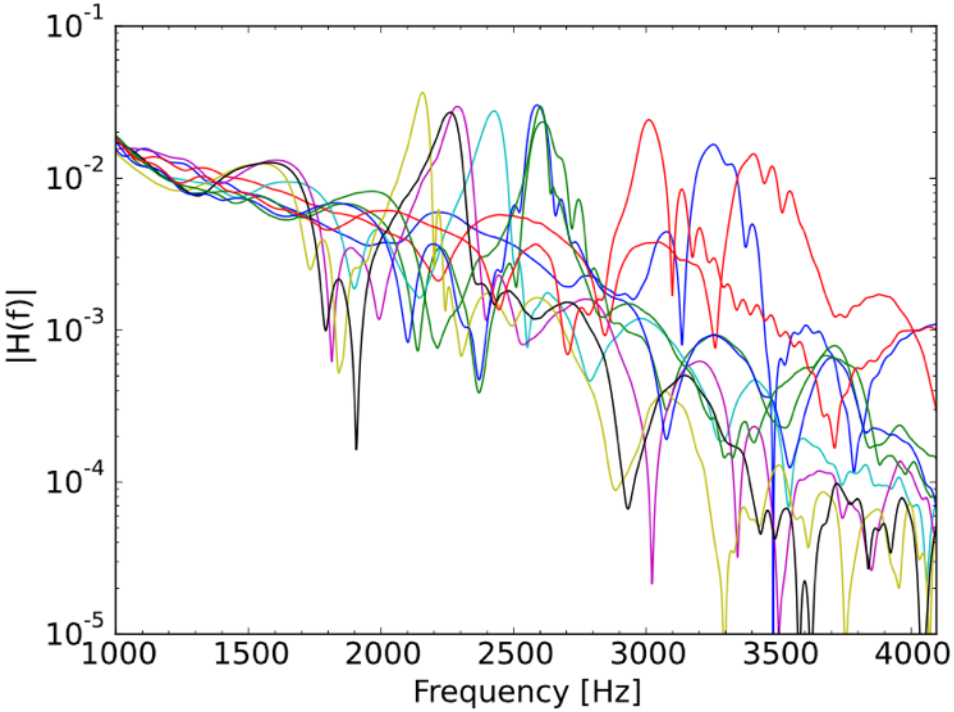

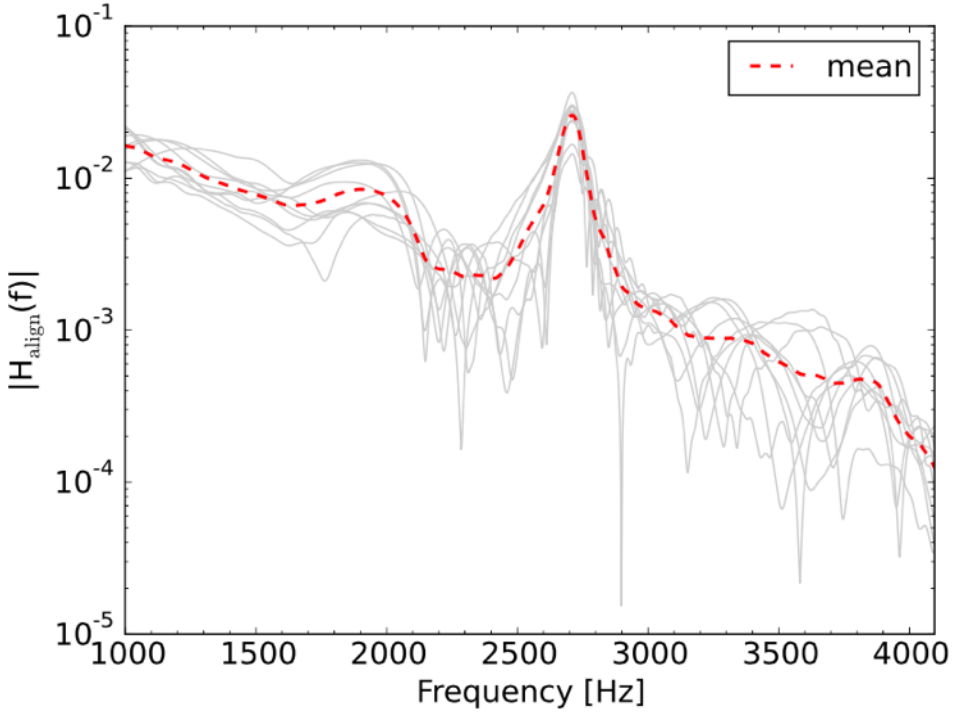

Actual fft's for different models.

Rescaled to common reference model.

Principal Component Analysis (PCA)

Clark, Bauswein, NS, Shoemaker (2016)

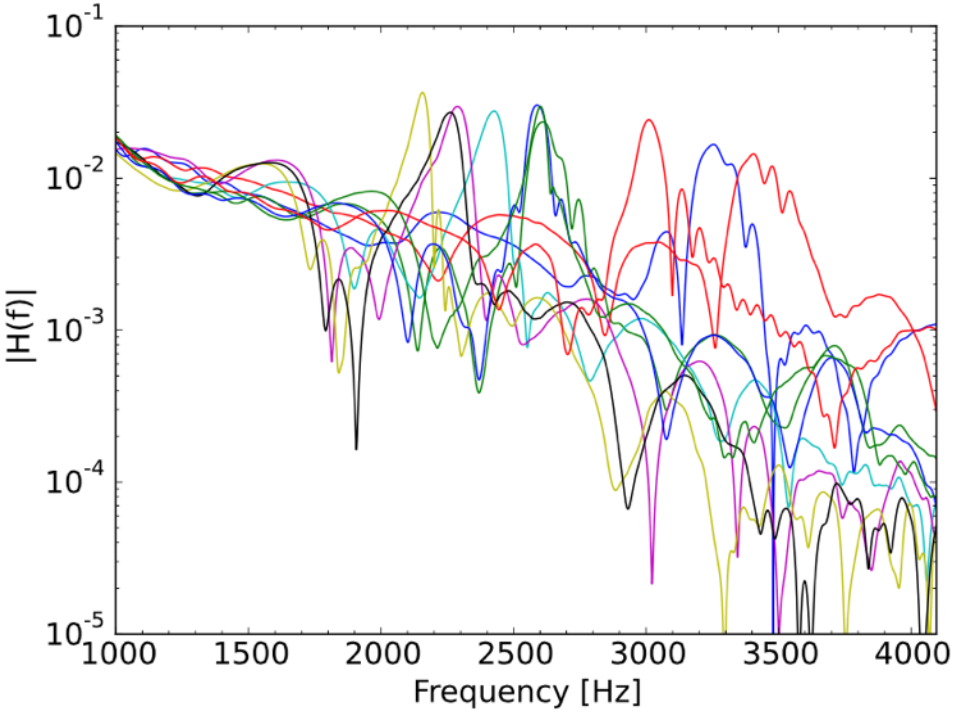

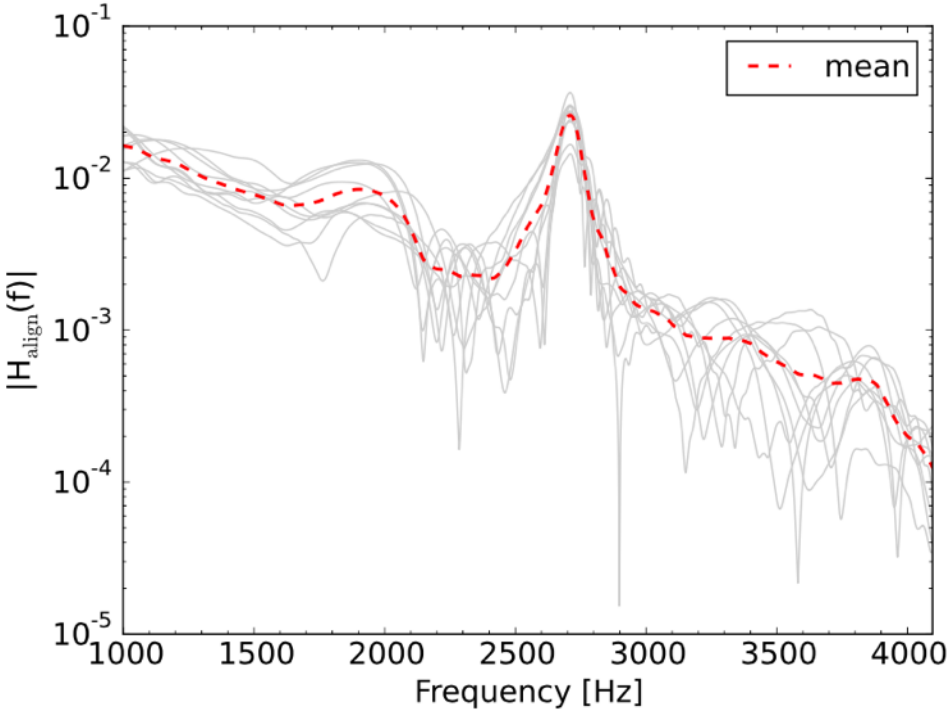

Actual fft's for different models.

Rescaled to common reference model.

Our PCA template extracts >90% of signal power compared to only 40% when using simple burst analysis.

PCA Reconstruction of signal

Clark, Bauswein, NS, Shoemaker (2016)

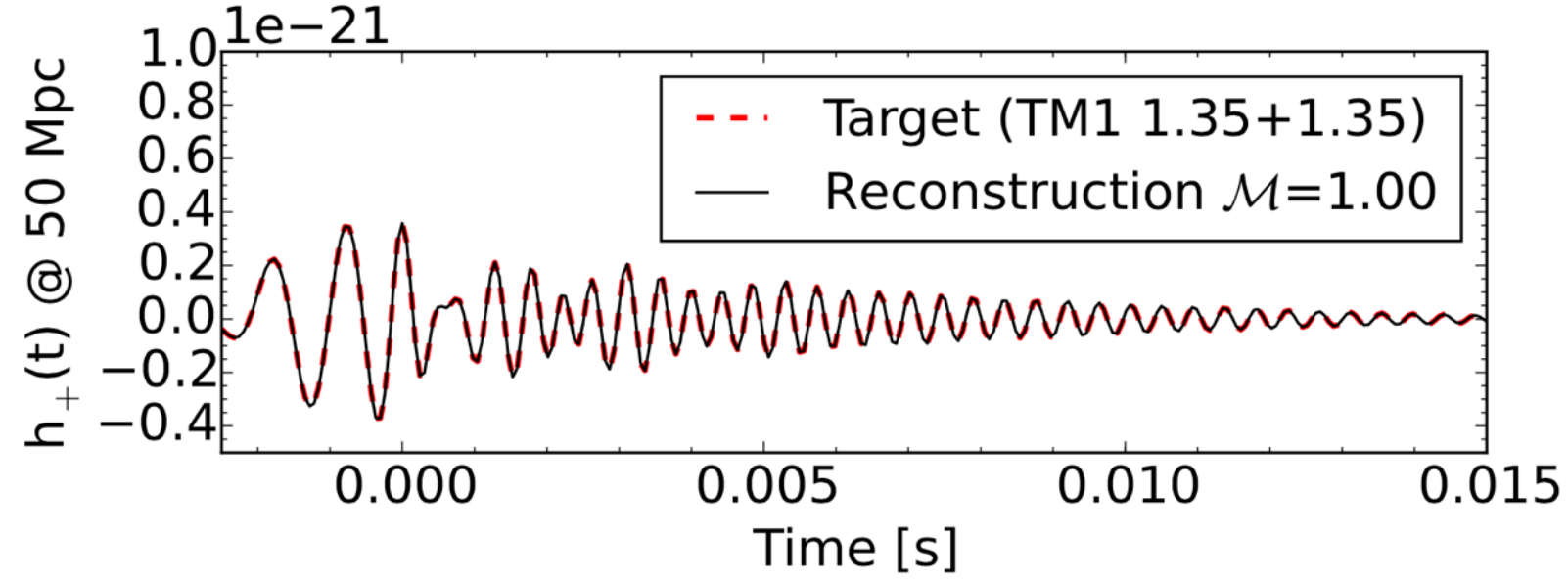

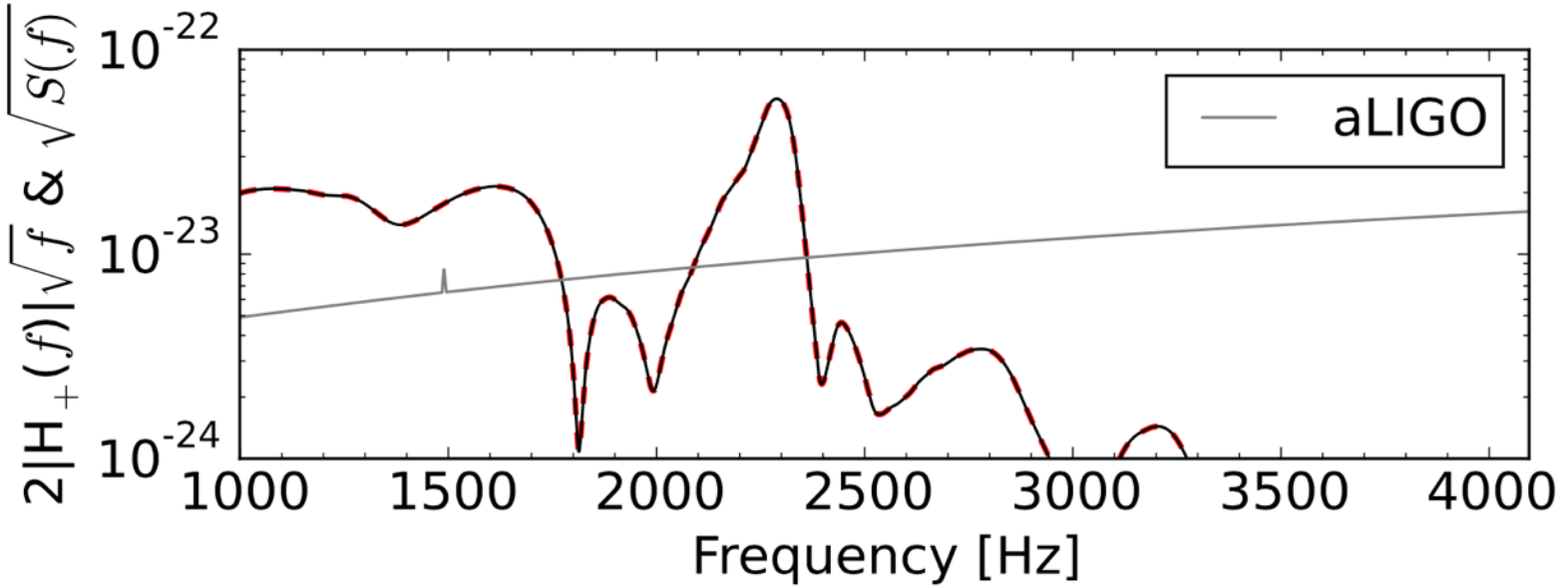

PLANNED UPGRADES AND NEW DETECTORS

Clark, Bauswein, NS, Shoemaker (2016)

LIGO A+ [74, 75] a set of upgrades to the existing LIGO facilities, including frequency-dependent squeezed light, improved mirror coatings and potentially increased laser beam sizes. Noise amplitude spectral sensitivity would be improved by a factor of $\sim$ 2.5-3 over 1–4 kHz. A+ could begin operation as early as 2017–18.

LIGO Voyager (LV) [75] a major upgrade to the existing LIGO facilities, including higher laser power, changes to materials used for suspensions and mirror substrates and, possibly, low temperature operation. LV would become operational around 2027–28 and offer noise amplitude spectral sensitivity improvements of $\sim$ 4.5-5 over 1–4 kHz.

LIGO Cosmic Explorer (CE) [75] a new LIGO facility rather than an upgrade, with operation envisioned to commence after 2035, probably as part of a network with LIGO Voyager. In its simplest incarnation, Cosmic Explorer would be a straightforward extrapolation of A+ technology to a much longer arm length of 40 km, referred to as CE1 which would be $\sim 14\times$ more sensitive than aLIGO over 1–4 kHz. An alternative extrapolation is that of Voyager technology to the 40 km arm length, referred to as CE2. CE2 is only $\sim 8\times$ more sensitive than aLIGO for the frequency range of interest in this study. For simplicity, we consider only CE1.

Einstein Telescope (ET-D) [76, 77] the European third-generation GW detector. In this work, we consider the ET-D configuration which is comprised of two individual inteferometers where one targets low frequency sensitivity and the other high frequency sensitivity. Both interferometers will be of 10 km arm length and housed in an underground facility. Furthermore, the full observatory will consist of three such detectors in a triangle arrangement. ET-D is $\sim 8\times$ more sensitive than aLIGO over 1–4 kHz. Due to the network configuration (i.e., the alignment of the component instruments) the effective sensitivity of ET-D is $\sim 18\%$ higher than that for a single ET-D detector.

Detectability

Clark, Bauswein, NS, Shoemaker (2016)

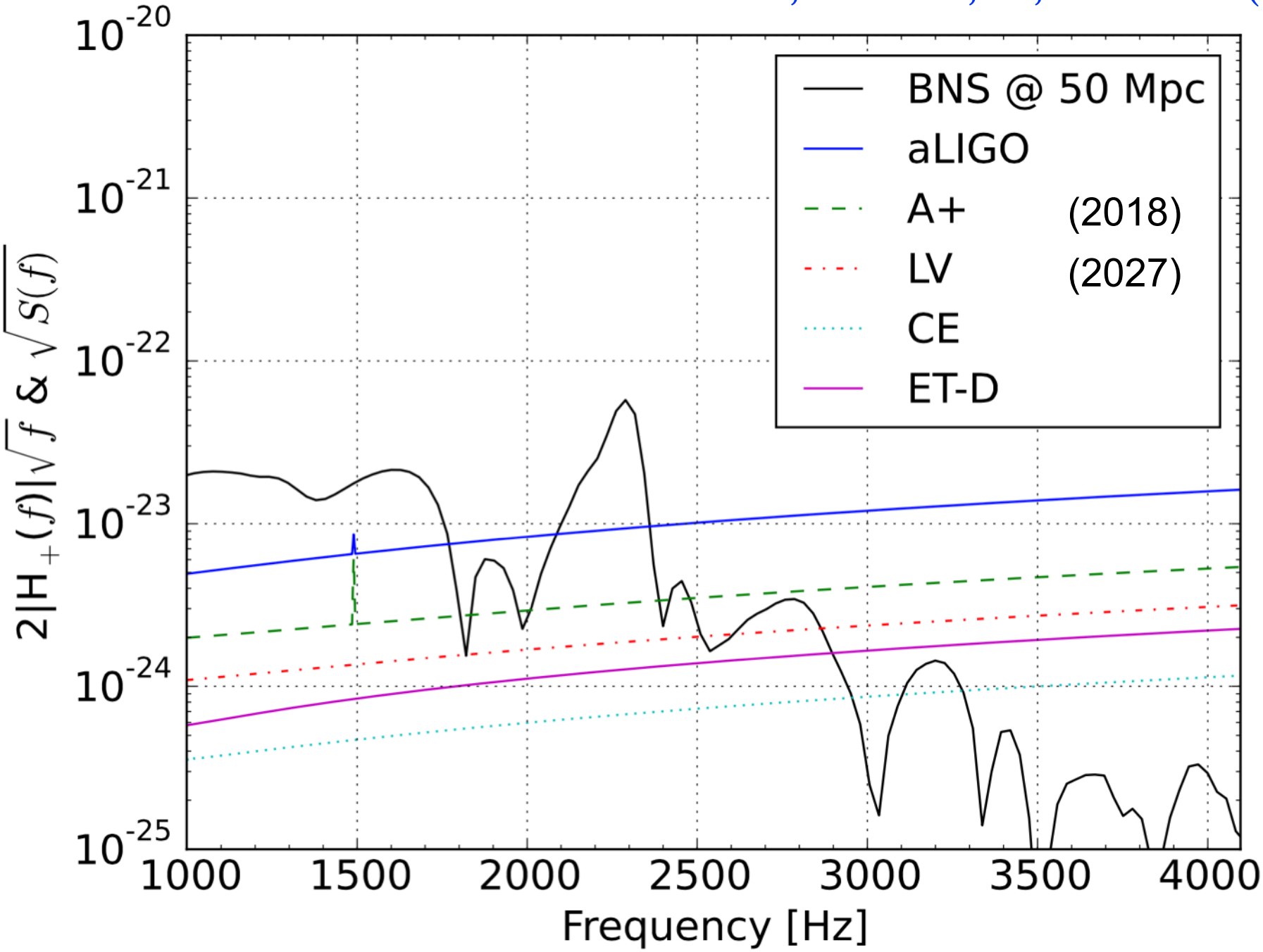

Coherent Wave Burst Analysis

Clark, Bauswein, NS, Shoemaker (2016)

Instrument	$\mathrm{SNR}_{\mathrm{full}}$	$\mathrm{SNR}_{\mathrm{post}}$	D_{hor} [Mpc]	$\dot{\mathcal{N}}_{\mathrm{det}}$ [year^{-1}]
aLIGO	$2.99^{3.86}_{2.37}$	$1.48^{1.86}_{1.13}$	$29.89^{38.57}_{23.76}$	$0.01^{0.03}_{0.01}$
A+	$7.89^{10.16}_{6.25}$	$4.19^{5.35}_{3.26}$	$78.89^{101.67}_{62.52}$	$0.13^{0.20}_{0.10}$
LV	$14.06^{18.13}_{11.16}$	$7.28^{9.30}_{5.64}$	$140.56^{181.29}_{111.60}$	$0.41^{0.88}_{0.21}$
ET-D	$26.65^{34.28}_{20.81}$	$12.16^{15.31}_{9.34}$	$266.52^{342.80}_{208.06}$	$2.81^{5.98}_{1.33}$
CE	$41.50^{53.52}_{32.99}$	$20.52^{25.83}_{15.72}$	$414.62^{535.221}_{329.88}$	$10.59^{22.78}_{5.33}$

Coherent Wave Burst Analysis

Clark, Bauswein, NS, Shoemaker (2016)

Instrument	$\mathrm{SNR}_{\mathrm{full}}$	$\mathrm{SNR}_{\mathrm{post}}$	D_{hor} [Mpc]	$\dot{\mathcal{N}}_{\mathrm{det}}$ [year^{-1}]
aLIGO	$2.99^{3.86}_{2.37}$	$1.48^{1.86}_{1.13}$	$29.89^{38.57}_{23.76}$	$0.01^{0.03}_{0.01}$
A+	$7.89^{10.16}_{6.25}$	$4.19^{5.35}_{3.26}$	$78.89^{101.67}_{62.52}$	$0.13^{0.20}_{0.10}$
LV	$14.06^{18.13}_{11.16}$	$7.28^{9.30}_{5.64}$	$140.56^{181.29}_{111.60}$	$0.41^{0.88}_{0.21}$
ET-D	$26.65^{34.28}_{20.81}$	$12.16^{15.31}_{9.34}$	$266.52^{342.80}_{208.06}$	$2.81^{5.98}_{1.33}$
CE	$41.50^{53.52}_{32.99}$	$20.52^{25.83}_{15.72}$	$414.62^{535.221}_{329.88}$	$10.59^{22.78}_{5.33}$

EOS from Inspiral Signal

Read et al. (2013)

The last part of the inspiral signal carries the imprint of the quadrupole *tidal deformability* $\lambda := -Q_{ij}/E_{ij} = 2/3\, k_2\, R^5$.

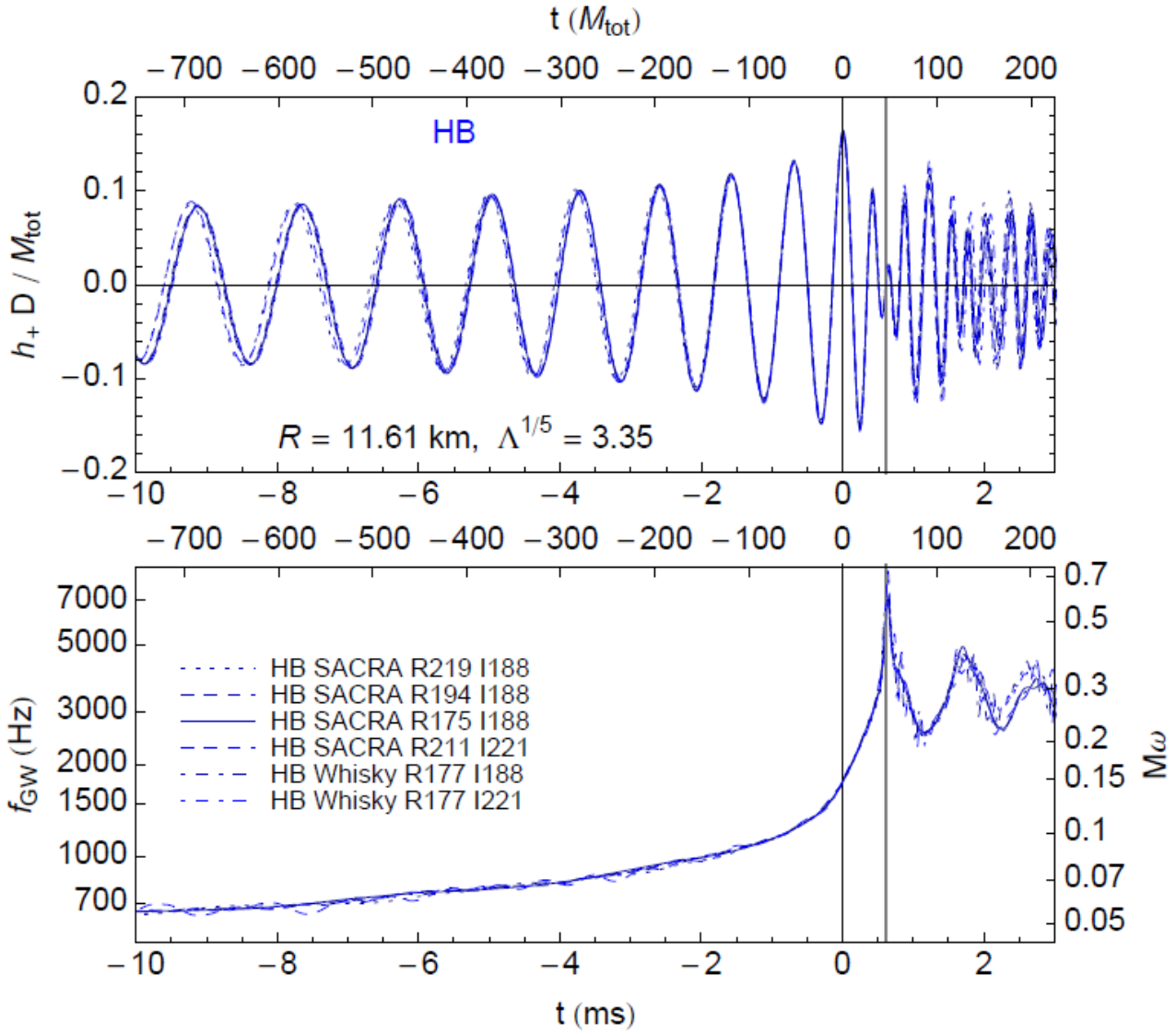

k_2 = tidal Love number

Dimensionless tidal deformability:

$$\Lambda \equiv \frac{2}{3} k_2 \left(\frac{R}{M}\right)^5$$

With an aLIGO class detector:

$\Delta R/R \sim 10\ \%$

@100 Mpc

Summary

- Post-merger GW asteroseismology is a viable method for constraining the EOS
- Neutron star radii can be measured to 400m (~3%) maximum uncertainty
- Principal Component Analysis (PCA) sufficient to reach >90% of optimal signal
- Realistic detection rates possible with upgraded LIGO Voyager by 2027.